

CHAPLIN AMYLOID FIBER FORMATION AND THE ROLE OF THE CHAPLINS
IN THE AERIAL DEVELOPMENT OF *STREPTOMYCES COELICOLOR*

CHAPLIN AMYLOID FIBER FORMATION AND THE ROLE OF THE CHAPLINS
IN THE AERIAL DEVELOPMENT OF *STREPTOMYCES COELICOLOR*

By

DAVID STUART CAPSTICK, B.Sc., M.Sc.

A Thesis

Submitted to the School of Graduate Studies

in Partial Fulfillment of the Requirements

for the Degree

Doctor of Philosophy

DOCTOR OF PHILOSOPHY (2011)

McMaster University

(Biology)

Hamilton, Ontario

TITLE: Chaplin amyloid fiber formation and the role of the chaplins in the aerial development of *Streptomyces coelicolor*

AUTHOR: David Stuart Capstick, B.Sc., M.Sc. (University of Waterloo)

SUPERVISOR: Dr. Marie A. Elliot

NUMBER OF PAGES: xi, 87

ABSTRACT

The chaplin proteins are functional amyloids that are produced by filamentous *Streptomyces* bacteria. The chaplins are essential for the morphological development of *S. coelicolor*, and are important for altering the surface ultrastructure of aerial hyphae and spores. Although it is well established that the chaplins play an important role in *S. coelicolor* aerial development, there is still much that remains unknown regarding their activity; in particular, how each of the chaplins contribute to promoting aerial development, and the importance that chaplin amyloidogenesis has in this process.

Previous work has revealed that only three of the eight chaplins (ChpE, ChpC, and ChpH) are necessary for promoting aerial development, and that ChpH plays a significant role in this process. For this reason, ChpH was used as the ‘model chaplin’ to examine the primary sequence determinants governing chaplin amyloidogenesis, and to explore the relationship between ChpH amyloid fiber formation and ChpH-dependent aerial development. This analysis revealed that ChpH contains two amyloidogenic regions, at the N- and C-termini, both of which are necessary for promoting aerial development, while the N-terminal domain is dispensable for surface fiber assembly.

A separate study focused on the role of the short chaplin ChpE. One of the surprising findings of this work is that, unlike the other chaplins, ChpE is essential for maintaining cell viability. The relationship between ChpE cell surface localization and the presence of the long chaplins was also examined. This work showed that the long chaplins are not required for the surface attachment of ChpE (nor the other short chaplins), but do function to enhance the activity of the short chaplins in promoting aerial development, in addition to being necessary for the organization and assembly of surface fibers.

ACKNOWLEDGEMENTS

First and foremost, I want to thank Dr. Marie Elliot for giving me the opportunity to work in her lab. I will always carry with me the proud distinction of being the very first graduate student in the Elliot lab. Dr. Elliot always pushed me to do my best work, and never gave up on me, even when I did.

I would like to thank the members of my supervisory committee, Dr. Justin Nodwell and Dr. Jianping Xu, for providing helpful and honest input regarding my work, and for always making sure that my research was heading in the most productive direction. Many thanks go to our collaborators, Dr. Joaquin Ortega and Ahmad Jomaa, for being tremendously generous with their time and expertise, and for their invaluable contribution to this work. I would also like to thank Dr. Douglas Davidson for our numerous scientific discussions, and for always treating me like an intellectual equal.

Just as important to me as my research accomplishments have been the friendships that I have made. I've had the pleasure of working with a great group of people, past and present, which made this experience that much more special to me. In particular, I would like to thank: Andrew Duong, for showing me how to live life '*Duong-style*'; Chan Gao, for having the uncanny ability to redirect any conversation toward the topic of her cat (*Meowoo!*); Henry Haiser, for instilling in me the importance of black socks, and for being my equal in knowing obscure Seinfeld references; Hindra, for always showing a level of patience and focus that I wish I had; Matt Moody, for having a shared appreciation for low-brow humour; Julia Świercz, for being the '*baby*' sister I never had; Mary Yousef, for always being honestly caring and concerned about others.

Finally, I would like to thank my parents, for all their love and support, and for always allowing me to follow my own path in life.

TABLE OF CONTENTS

Title page	i
Descriptive note	ii
Abstract	iii
Acknowledgements	iv
Table of Contents	v
List of Figures	viii
List of Tables	ix
List of Abbreviations	x

Chapter 1: General Introduction

1.1 The Actinomycetes	1
1.2 The Genus <i>Streptomyces</i>	1
1.3 The Model Streptomycete: <i>Streptomyces coelicolor</i> A3(2).....	1
1.4 <i>S. coelicolor</i> Aerial Development.....	2
1.4.1 Regulation of the Early Stages of Aerial development	
1.4.2 Regulation of the Later Stages of Development and Sporulation	
1.5 Morphogenetic Proteins Involved in Aerial Development	6
1.5.1 SapB	
1.5.2 The Chaplins	
1.5.2.1 The Chaplins and the Fungal Hydrophobins	
1.6 Amyloid Proteins	9
1.6.1 Functional Amyloids	
1.7 Aims of this Thesis	11
1.8 Figures.....	12

Chapter 2: Materials and Methods

2.1 Bacterial culturing and microbiological techniques	15
2.1.1 Bacterial growth media	
2.1.2 Bacterial strains and plasmids	
2.2 Bacterial genetic and molecular biology techniques	16
2.2.1 <i>Streptomyces</i> conjugation	
2.2.2 Protoplast transformation	
2.2.3 Preparing and transforming competent <i>E. coli</i> cells	
2.2.4 Bacterial two-hybrid assay	
2.2.5 DNA isolation	
2.2.5.1 Isolation of genomic DNA from <i>Streptomyces</i>	
2.2.5.2 Plasmid and cosmid DNA isolation from <i>E. coli</i>	
2.2.6 Agarose gel electrophoresis	

2.2.7	Restriction digestion of DNA	
2.2.8	Phosphorylation and dephosphorylation of DNA	
2.2.9	DNA ligations	
2.2.10	DNA amplification by PCR	
2.2.11	Creating gene knockouts in <i>S. coelicolor</i>	
2.2.12	Generating substitution mutations via PCR	
2.2.13	Creating gene deletions via PCR	
2.2.14	Construction of <i>chpH/chpH*</i> expression constructions	
2.3	Protein biochemical techniques	22
2.3.1	Purification and mass spectrometry analysis of chaplin proteins	
2.3.2	Synthetic peptide and amyloid ‘seed’ preparation	
2.3.3	Measuring amyloidogenesis with thioflavin T	
2.3.4	Circular dichroism secondary structure analysis	
2.3.5	Protease-resistance assay	
2.4	Microscopy techniques	24
2.4.1	Scanning electron microscopy (SEM)	
2.4.2	Transmission electron microscopy (TEM)	

Chapter 3: Chaplin Amyloidogenesis and Its Role in Aerial Development

3.1	Introduction	32
3.2	Results	33
3.2.1	<i>In vitro</i> characterization of ChpH amyloidogenesis	
3.2.2	Nucleation-dependence of ChpH polymerization	
3.2.3	The C-terminus of ChpH is amyloidogenic	
3.2.4	<i>In vitro</i> characterization of C-terminal ChpH mutants	
3.2.5	ChpH amyloidogenesis is required for promoting aerial development	
3.2.6	The ChpH N-terminus is amyloidogenic and important for aerial development	
3.2.7	ChpH mutations do not cause a dominant-negative phenotype	
3.2.8	Interactions between ChpH and the rodlin proteins	
3.3	Discussion	41
3.4	Figures and tables	45

Chapter 4: Characterization of the Unique Short Chaplin ChpE

4.1	Introduction	59
4.2	Results	59
4.2.1	Generating a <i>chpE</i> knockout mutant	
4.2.2	Examining the importance of the lack of Cys residues in ChpE	
4.2.3	<i>In vivo</i> ChpE polymerization	
4.2.4	Dependence of ChpE localization on the long chaplins	
4.3	Discussion	62

4.3.1 ChpE is essential for cell viability	
4.3.2 The role of Cys in the activity of the chaplins	
4.3.3 The role of the long chaplins	
4.4 Figures.....	67
<u>Chapter 5: Summary and Future Directions</u>	
5.1 Summary of research	69
5.2 A revised model for chaplin assembly.....	70
5.3 Future directions	71
5.3.1 Regulation of chaplin activity	
5.3.2 Surface localization of the chaplins	
5.3.3 Towards understanding the essential function of ChpE	
<u>References</u>	74

LIST OF FIGURES

- Figure 1.1** The life cycle of *S. coelicolor*
Figure 1.2 Overview of the chaplins
Figure 1.3 Rodlet surface ultrastructure
Figure 3.1 Overview of ChpH analysis
Figure 3.2 *In vitro* polymerization of the full-length ChpH peptide
Figure 3.3 Time course of negatively stained electron micrographs of ChpH peptides
Figure 3.4 Protease-resistance assay
Figure 3.5 *In vitro* polymerization of the C-terminal ChpH peptide
Figure 3.6 Analysis of the C-terminal mutant peptides
Figure 3.7 Developmental phenotypes of plate-grown ChpH mutants
Figure 3.8 SEM micrographs of ChpH mutant spore abundance
Figure 3.9 MALDI-ToF mass spectrometry of ChpH mutant cell wall extracts
Figure 3.10 SEM micrographs of the surface ultrastructure of ChpH mutants
Figure 3.11 *In vitro* polymerization of the N-terminal ChpH peptide
Figure 3.12 Hydropathy profile of ChpH
Figure 3.13 Developmental phenotype of a ChpH(S61D) mutant
Figure 4.1 Surface ultrastructure and plate phenotype of a *chpEC*-expressing strain
Figure 4.2 Analysis of a long chaplin mutant ($\Delta chpABC$)

LIST OF TABLES

Table 2.1	Strains and plasmids used in this work
Table 2.2	Oligonucleotides used in this work
Table 3.1	Hydrophobicity scores of ChpH mutants

LIST OF ABBREVIATIONS

A	adenine
aa	amino acid
Ala	alanine
Asp	aspartic acid
bp	base pair
C	cytosine <i>or</i>
C	carboxyl <i>or</i>
C	Celsius
CD	circular dichroism
CDA	calcium-dependent antibiotic
Cys	cysteine
dH ₂ O	distilled water
DMSO	dimethyl sulfoxide
DNA	deoxyribonucleic acid <i>or</i>
DNA	Difco nutrient agar
dNTP	deoxyribonucleotide
DTT	dithiothreitol
EDTA	ethylenediaminetetraacetic acid
Fwd	forward
G	guanine
g	grams <i>or</i>
g	gravity
Gly	glycine
HFIP	hexafluoro-2-isopropanol
hrs	hours
IPTG	isopropyl β -D-1-thiogalactopyranoside
kPa	kilopascal
kV	kilovolt
L	liter
LB	Luria Bertani
M	Molar
MALDI-ToF	Matrix-assisted laser desorption/ionization time-of-flight
mg	milligram
min	minute
ml	milliliter
mm	millimeter
mM	millimolar
MS	mannitol soy flour agar
N	amino
ng	nanogram
nm	nanometer
nt	nucleotide

OD	optical density
PCR	polymerase chain reaction
PEG	polyethylene glycol
PTA	phosphotungstic acid
Rev	reverse
rpm	rotations per minute
s	seconds
SDS	sodium dodecyl sulfate
SEM	scanning electron microscopy
Ser	serine
T	thymine
Tat	twin-arginine transport
TEM	transmission electron microscopy
TFA	trifluoroacetic acid
ThT	thioflavin T
Tris	Tris(hydroxymethyl)aminomethane
TSB	tryptone soya broth
U	units
Val	valine
VKOR	vitamin K epoxide reductase
w/w	weight per weight
WT	wild type
X-gal	5-bromo-4-chloro-3-indolyl- β -D-galactopyranoside
YEME	yeast extract-malt extract
YT	yeast tryptone broth
μ g	microgram
μ l	microliter

CHAPTER 1

General Introduction

1.1 The Actinomycetes

In 1877, the German botanist Carl Harz described the first actinomycete (*Actinomyces bovis*) isolated from infected cattle afflicted with ‘lump jaw’ (Harz, 1877). These filamentous organisms were originally believed to be fungi, and were named ‘actinomycetes’, from the Greek words ‘*aktis*’ (ray) and ‘*mykes*’ (fungus). It was not until the 1950’s that the actinomycetes were no longer regarded as a fungal-bacterial intermediary, but instead were recognized as true prokaryotic, Gram-positive bacteria (Waksman, 1950). Actinomycetes represent a large proportion of the microbial population in soil ($>10^6$ colony forming units per gram), but can also be found in both freshwater and marine environments (Goodfellow & Williams, 1983). Most actinomycetes are saprophytes, although there are some that are capable of adopting a pathogenic lifestyle, such as *Mycobacterium tuberculosis*, *M. leprae*, and *Corynebacterium diphtheriae*, the causative agents of tuberculosis, leprosy, and diphtheria, respectively (Stackebrandt & Woese, 1981).

1.2 The Genus *Streptomyces*

A prominent member of the actinomycetes is *Streptomyces*. Ecologically, streptomycetes are vital for their ability to degrade complex mixtures of dead organic material, and breakdown recalcitrant polymers, such as lignocellulose and chitin (Goodfellow & Williams, 1983, McCarthy, 1987, McCarthy & Williams, 1992, Crawford, 1978), playing a key role in carbon recycling within the soil environment. Most significantly, the streptomycetes represent a tremendous natural source of bioactive compounds. It is estimated that, collectively, the actinomycetes produce over 10,000 bioactive compounds (45% of all known bioactive microbial metabolites), 7,600 of which are produced by streptomycetes (Berdy, 2005). These molecules include fungicides, immune-suppressants, and over half of the antibiotics used medically worldwide (Kieser *et al.*, 2000, Hopwood, 2007). Since the discovery of the first clinically-relevant antibiotic (streptomycin) isolated from *Streptomyces griseus* in the 1940s (Jones *et al.*, 1944), the streptomycetes have been studied intensely for their immense pharmaceutical and biotechnological importance.

1.3 The Model Streptomycete: *Streptomyces coelicolor* A3(2)

Among the streptomycetes, the genetically best-studied species is *Streptomyces coelicolor* A3(2) (Hopwood, 1999). *S. coelicolor* produces at least four antibiotics: actinorhodin, undecylprodigiosin, methylenomycin, and calcium-dependent lipopeptide antibiotic (CDA). Undecylprodigiosin has shown potential pharmaceutical value, due to

its anti-cancer activity (Ho *et al.*, 2007), while CDA has anti-microbial activity against a range of Gram-positive bacteria (Lakey *et al.*, 1983) and is closely related to daptomycin, which has recently been approved as an antibiotic for clinical use (Enoch *et al.*, 2007). In 2002, a major breakthrough in *Streptomyces* research came with the sequencing of the *S. coelicolor* genome (Bentley *et al.*, 2002). The genome of *S. coelicolor* has a relatively high G+C content (over 70%) and consists of a linear chromosome (8.7 Mb), two plasmids (SCP1, linear, 365 kb; SCP2, circular, 31 kb) (Bentley *et al.*, 2002, Bibb *et al.*, 1977), and a third plasmid (SLP1, 17 kb) that is integrated into the chromosome (Bibb *et al.*, 1981, Omer *et al.*, 1988). The *S. coelicolor* chromosome encodes a predicted 7,825 genes, of which, 965 (12.3%) are predicted to be involved in regulation (Bentley *et al.*, 2002), possibly reflecting the complex lifestyle of *Streptomyces* and a need for an equally complex regulatory network. In addition, the genome putatively encodes 819 secreted proteins (10.5%) and 614 proteins (7.8%) with domains suggesting a role in transport (Bentley *et al.*, 2002); collectively, these gene products would allow *S. coelicolor* to utilize a variety of different nutrients from the soil environment. The genome also codes for complete Sec and Tat (twin arginine translocation) protein transport systems (Bentley *et al.*, 2002), responsible for the translocation of unfolded and pre-folded proteins, respectively (Fekkes & Driessen, 1999, Berks *et al.*, 2000).

1.4 *S. coelicolor* Aerial Development

The *S. coelicolor* life cycle (Figure 1.1) begins with a germinating spore, from which one or more germ tubes emerge and grow by hyphal tip extension, eventually forming a multi-genomic branching network of vegetative (substrate) mycelia. During the early stages of development, a physiological cue (possibly nutrient limitation) signals the production of aerial hyphae, which extend upward from the colony surface. The vegetative mycelium is partially cannibalized to provide a source of nutrients for the growing aerial hyphae (Mendez *et al.*, 1985). In the laboratory, aerial hyphae production causes the surface of colonies to appear white and fuzzy, instead of smooth and translucent, as they do during vegetative growth. Concurrent with the raising of aerial hyphae is the production of secondary metabolites, including the pigmented antibiotics actinorhodin (blue) and undecylprodigiosin (red). The upward growth of aerial hyphae eventually ceases, and is followed by a synchronous round of cell division that subdivides the multi-genomic aerial hypha into chains of unigenomic spores. Colonies at this stage in development appear grey due to the synthesis of a grey polyketide pigment that is present on the surface of the mature spores (Elliot *et al.*, 2007).

1.4.1 Regulation of the Early Stages of Aerial Development

There is much that remains to be uncovered about how *S. coelicolor* makes the morphological leap from growing vegetatively to producing aerial hyphae, which ultimately metamorphose into chains of reproductive spores. A crucial turning point in *Streptomyces* developmental research came in the 1960s and 70s with the isolation and genetic mapping of *S. coelicolor* mutants that were developmentally arrested, unable to

produce aerial hyphae (the so-called ‘bald’ phenotype) (Hopwood, 1967, Merrick, 1976). To date, 12 ‘classical’ **bald** genes (*bld*) genes have been annotated (*bldA, B, C, D, G, H, I, J, K, L, M, N*), and new mutations that prevent aerial development continue to be isolated (Elliot *et al.*, 2007). In addition, some *bld* mutations also impact antibiotic production and cause defects in carbon utilization (Champness, 1988, Champness & Chater, 1994, Pope *et al.*, 1996), revealing a strong regulatory link between primary and secondary metabolism and aerial development. It is therefore not surprising that most *bld* genes encode regulatory proteins, and for many, the targets of their regulation are not limited solely to aerial development-related genes. Undoubtedly, the best example of such a global regulator is BldD (Elliot *et al.*, 1998, Elliot *et al.*, 2001, Elliot & Leskiw, 1999, den Hengst *et al.*, 2010). BldD is a DNA-binding protein that is most abundant during vegetative growth, when it is believed to function as a global repressor of genes involved in aerial development and antibiotic biosynthesis (den Hengst *et al.*, 2010, Elliot *et al.*, 2001). In total, BldD controls the expression of ~167 genes, many of which (~25%) encode other regulatory proteins (den Hengst *et al.*, 2010), emphasizing the impact BldD has on global transcription levels in *S. coelicolor*. The direct target genes of BldD are very diverse: from those involved in aerial development (e.g. *chpH, ftsZ, whiG*), to antibiotic biosynthesis (e.g. *nsdA*), stress response (e.g. *sigH*), and primary metabolism (e.g. *glgBII, pepA*), among others (Elliot *et al.*, 2001, den Hengst *et al.*, 2010, Kelemen *et al.*, 2001). In addition, BldD also directly regulates the activity of other *bld* genes, including *bldA* (leucyl tRNA), *bldC* (MerR-type transcriptional activator), and *bldN* (extracytoplasmic function sigma factor) (Bibb *et al.*, 2000, Hunt *et al.*, 2005, Lawlor *et al.*, 1987), revealing that there is a large degree of regulatory overlap between the *bld* genes. Interestingly, BldD is not predicted to bind within the promoter region of *bldA*, but instead binds within the sequence representing the primary transcript of *bldA*. The ‘BldD box’ is found immediately downstream of the site in the *bldA* transcript where it would be processed to generate the mature 3’ end of the leucyl tRNA, suggesting that BldD may regulate the post-transcriptional processing of the *bldA* transcript (den Hengst *et al.*, 2010). The leucyl tRNA encoded by *bldA* allows for the efficient translation of the UUA codon, which occurs relatively rarely within the G+C-rich *S. coelicolor* genome (Lawlor *et al.*, 1987, Leskiw *et al.*, 1991). There are a total of 145 genes encoded by the *S. coelicolor* genome (~2% of genes) that contain one or more TTA codons (Bentley *et al.*, 2002, Chandra & Chater, 2008); notably, the TTA codon occurs within the activators of the undecylprodigiosin and actinorhodin biosynthesis pathways, which is why *bldA* mutants fail to produce these pigmented antibiotics (Fernandez-Moreno *et al.*, 1991, White & Bibb, 1997). In addition, the inability of *bldA* mutants to raise aerial hyphae is at least partially due to a TTA codon found in *bldH* (*adpA*) (Takano *et al.*, 2003).

Work by Willey *et al.* (1993) has shown that certain pairs of *bld* mutants, when grown adjacent to each other on rich media, can extracellularly complement their bald phenotype, forming aerial hyphae at the junction of growth. By examining combinations of *bld* mutants, differences were found in their ability to complement other *bld* mutants, and from this, a complementation hierarchy was established (Willey *et al.*, 1993, Nodwell *et al.*, 1996) (shown below).

$$[bldJ] < [bldK, bldL] < [bldA, bldH] < [bldG] < [bldC] < [bldD, bldM]$$

This revealed that all the *bld* mutants in the hierarchy could complement *bldJ*, while none of them could complement *bldD* or *bldM*. *bldB*, *bldI*, and *bldN* did not fit into the complementation hierarchy. This hierarchy is thought to represent a *bld* gene-dependent signaling cascade that involves at least five extracellular signals that are required for the formation of aerial hyphae (Willey *et al.*, 1993, Nodwell *et al.*, 1996). It has been proposed that such a cascade would allow *Streptomyces* to integrate different environmental signals that influence the development of aerial hyphae (Chater, 2001, Pope *et al.*, 1996, Kelemen & Buttner, 1998). Evidence for one of these putative extracellular signaling factors was uncovered by Nodwell *et al.* (1996), where it was shown that the *bldK* locus encodes an oligopeptide permease that imports a *bldJ*-dependent extracellular factor (Nodwell & Losick, 1998). It is, however, unlikely that the regulatory cascade leading to the commencement of aerial development progresses in such a simple and linear fashion. Despite this, these observations provide evidence to support an important role for extracellular factors in the promotion of *S. coelicolor* aerial development.

1.4.2 Regulation of the Later Stages of Aerial Development and Sporulation

The morphological transition that aerial hyphae undergo to form chains of reproductive spores is a highly complex, multi-staged process (Chater, 2001). Aerial hyphae first undergo a round of synchronous cell division, forming septa that divide the hyphae into pre-spore compartments. At the same time, multiple copies of the chromosome (50-60 copies per aerial hyphae) are segregated such that each pre-spore compartment receives a single copy of the chromosome. The pre-spore wall thickens and spore maturation concludes with a grey polyketide pigment being deposited on the surface of the rounded, mature spores. The different stages of sporulation are controlled by a host of regulatory factors encoded by the *whi* genes. Mutations in the *whi* genes cause colonies to appear morphologically **white** due to an absence of the grey spore-associated pigment. Thus far, there are 12 *whi* genes that have been identified, and these are grouped into two categories according to the stage of sporulation that is affected. The ‘early’ *whi* genes include *whiA*, *B*, *G*, *H*, *I*, and *J* and mutations in these genes result in defects in the initial stages of aerial hyphal differentiation and septation. In contrast, mutations in *whiD*, *E*, *F*, *L*, *M*, and *O* (the ‘late’ *whi* genes) affect the final stages of spore maturation (Chater, 2001, Elliot *et al.*, 2007). *whiG* encodes an alternative sigma factor (σ^{WhiG}) that is critical for the initiation of aerial hyphae differentiation (Chater, 2001, Chater *et al.*, 1989). *whiG* mutants exhibit long aerial hyphae that do not coil or go on to form septa (Chater, 1972, Chater, 1975, Wildermuth & Hopwood, 1970). σ^{WhiG} directs the transcription of two other early *whi* genes, *whiH* and *whiI*. Both WhiH and WhiI are regulatory proteins that contain a DNA-binding domain and a signal-sensing domain (Ryding *et al.*, 1998, Ainsa *et al.*, 1999). Mutants of *whiH* or *whiI* form aerial hyphae that are loosely coiled, but do not sporulate. WhiB and WhiD represent a class of actinomycete-specific proteins known as ‘Wbl proteins’ (**WhiB-like**) (Molle *et al.*, 2000, Soliveri *et al.*, 2000). Both WhiB and WhiD contain four highly conserved cysteine residues that bind an oxygen-sensitive [4Fe-4S] cluster, and are believed to be involved in

redox signaling through their disulfide reductase activity (Alam *et al.*, 2007, Jakimowicz *et al.*, 2005). The *whiE* locus represents two divergently transcribed units made up of seven genes that are responsible for the synthesis of the grey polyketide pigment, which is deposited on the surface of mature spores (Davis & Chater, 1990, Kelemen *et al.*, 1998).

In addition to the ‘classical’ *whi* genes, there have been a number of other proteins that have been discovered to be involved in sporulation. Among these, is the tubulin-like FtsZ protein, which plays an essential role during sporulation (McCormick *et al.*, 1994). In most bacteria, FtsZ is absolutely required for cell viability, as it designates the future site of cell division, forming a ring-like structure (the ‘Z-ring’) that helps recruit other proteins involved in septum formation (Adams & Errington, 2009). Due to the filamentous lifestyle of *S. coelicolor*, FtsZ is dispensable for vegetative growth, and is only required for septation during sporulation (McCormick *et al.*, 1994). FtsZ first forms a helical filament along the length of the aerial hyphae, which is then resolved to form a ‘ladder’ of regularly spaced Z-rings (Grantcharova *et al.*, 2005). Z-ring formation is believed to depend (directly/indirectly) on other proteins, as mutations in two other cell division genes (*ftsW* and *ftsI*), as well as in two *Streptomyces*-specific protein-coding genes (*ssgA* and *ssgB*) cause perturbations to Z-ring assembly (Bennett *et al.*, 2009, Mistry *et al.*, 2008, Willemse *et al.*, 2011). While it remains unclear whether FtsW and/or FtsI directly interacts with FtsZ in *S. coelicolor* [a direct interaction has been observed between FtsW and both FtsI and FtsZ in *M. tuberculosis* (Datta *et al.*, 2002, Datta *et al.*, 2006)], mutations in either *ftsW* or *ftsI* prevent the resolution of helical FtsZ filaments to Z-rings (Mistry *et al.*, 2008, Bennett *et al.*, 2009). The connection between SsgA/SsgB and FtsZ is better understood. Prior to Z-ring formation, SsgA localizes to the future site of septation, where it recruits SsgB, which directly interacts with FtsZ to promote Z-ring assembly (Willemse *et al.*, 2011). Interestingly, SsgA is not absolutely required for sporulation during growth on mannitol-containing media (van Wezel *et al.*, 2000), suggesting that some functional redundancy exists. This is perhaps, not unexpected, as the *S. coelicolor* genome encodes a total of seven SsgA-like proteins (SALPs), which have been shown to have roles in various stages of sporulation (Noens *et al.*, 2005).

An important aspect of sporulation is the faithful segregation of single copies of the linear chromosome into each spore compartment, a process mediated by the Par system and FtsK. The Par system includes an ATPase (ParA) and a DNA-binding protein (ParB) that specifically binds centromere-like sequences (*parS*) that flank the chromosomal origin of replication (*oriC*) (Thanbichler & Shapiro, 2008). ParA forms helical filaments that traverse the length of the aerial hyphae and interact with the ParB-*parS* nucleoprotein complex. This interaction is believed to provide the force necessary to segregate the chromosome. The Par system is not essential for viability, as vegetative and aerial growth is unaffected by mutations in the *par* genes; however, *par* mutants exhibit a significantly higher incidence of anucleate spores (Kim *et al.*, 2000). As the aerial hyphae septate, the DNA translocase FtsK functions as a DNA ‘pump’ to ensure that the arms of the linear chromosome are not trapped by the closing septa; in the absence of FtsK, large portions of the linear chromosome (>10%) can be lost (Wang *et al.*, 2007a).

As the spores mature during the final stages of sporulation, the protective spore wall thickens, and individual spores become more rounded in their shape. Spore wall assembly depends on two actin-like homologs, MreB and Mbl, which are believed to act as cytoskeletal scaffolds for the biosynthesis of peptidoglycan (Mazza *et al.*, 2006, Heichlinger *et al.*, 2011). Deletion of either *mreB* or *mbl* causes spores to germinate prematurely and to have uncharacteristically thin spore walls, leading to reduced stress resistance, including tolerance to heat stress (Mazza *et al.*, 2006, Heichlinger *et al.*, 2011). Remodeling of the spore wall has recently been shown to also depend on the activity of at least four peptidoglycan hydrolases: RpfA, SwlA, SwlB, and SwlC (Haiser *et al.*, 2009). Mutations in any of these four hydrolase-encoding genes causes the spore cell wall to be unusually thin, and the resulting spores to be more sensitive to heat stress (Haiser *et al.*, 2009). Mutants of *rpfA*, *swlB*, and *swlC* also exhibited defects in spore separation (Haiser *et al.*, 2009), indicating that these enzymes function at multiple stages in sporulation.

1.5 Morphogenetic Proteins Involved in Aerial Development

In *S. coelicolor*, the emergence of aerial hyphae depends on two morphogenetic protein families: SapB and the chaplins (Tillotson *et al.*, 1998, Willey *et al.*, 1991, Elliot *et al.*, 2003, Claessen *et al.*, 2003). Both SapB and the chaplins are highly surface active and are believed to lower the surface tension at the aqueous colony-air interface, allowing aerial hyphae to extend into the air; in their absence, colonies fail to produce aerial hyphae and appear bald. When *S. coelicolor* is grown on rich (glucose-containing) media, aerial development is mediated by the activity of both SapB and the chaplins. However, when cultured with less readily utilized carbon sources (e.g. mannitol or arabinose), *S. coelicolor* aerial development depends entirely on the chaplins (Capstick *et al.*, 2007), as mature SapB is not produced under these conditions (Willey *et al.*, 1991). Therefore, there exist two distinct pathways in *S. coelicolor* for raising aerial hyphae: one that is chaplin/SapB-dependent, and another that is solely chaplin-dependent (Capstick *et al.*, 2007).

1.5.1 SapB

SapB was first described by Guijarro *et al.* (1988), and is produced by the *ram* (rapid aerial mycelium) gene cluster. The *ram* locus consists of *ramC*, *ramS*, *ramA*, *ramB*, and the divergently transcribed *ramR* gene (Willey *et al.*, 2006). With the exception of BldM and BldN, expression of the *ram* genes is *bld* gene-dependent (Willey *et al.*, 1991, Willey *et al.*, 2006). Among the *ram* genes, *ramR* encodes a response regulator that controls the expression of the *ramCSAB* gene cluster, while *ramAB* encode components of an ABC transporter proposed to be responsible for transporting SapB out of the cell (Ma & Kendall, 1994). The *ramS* gene encodes a 42 amino acid peptide that is believed to be post-translationally modified by the dimeric, membrane-associated RamC protein (Hudson & Nodwell, 2004, Hudson *et al.*, 2002), converting RamS into the 21 amino acid lantibiotic-like peptide SapB (Kodani *et al.*, 2004). Lantibiotics are small peptides (19-38 amino acids) that are post-translationally modified through a complex,

multi-step process, typically involving a dehydration reaction, followed by the formation of intramolecular lanthionine rings, and finally proteolytic cleavage of the leader sequence (Willey & van der Donk, 2007). Lantibiotics are produced by Gram-positive bacteria and exhibit anti-microbial activity towards a broad range of Gram-positive bacteria, but only a few Gram-negative species (Willey & van der Donk, 2007, Bierbaum & Sahl, 2009); SapB, however, does not appear to have antibiotic activity (Kodani *et al.*, 2004). Deleting any of *ramC*, *ramS*, *ramR*, or *ramCSAB* causes a bald phenotype on rich media (Nguyen *et al.*, 2002, Capstick *et al.*, 2007, O'Connor *et al.*, 2002). However, when grown on minimal media (non-glucose-containing media), a *ram* mutant looks indistinguishable from the wild type (Capstick *et al.*, 2007).

The developmental *bld* gene-dependent signaling cascade that has been proposed (Section 1.4.1) is thought to conclude with the synthesis and secretion of SapB (and likely other morphogens), as most *bld* mutants are defective in SapB production (Willey *et al.*, 1993, Nodwell & Losick, 1998, Nodwell *et al.*, 1996, Nodwell *et al.*, 1999). The exogenous application of purified SapB to growing *bld* mutants can restore their ability to erect aerial hyphae (Tillotson *et al.*, 1998). As well, overexpression of *ramR* in *bld* mutants can also restore aerial hyphae formation (Nguyen *et al.*, 2002). In both cases, the aerial hyphae do not further differentiate into mature spores, implying that SapB serves a mechanistic role only, and that other signals are required for differentiation to proceed to completion.

1.5.2 The Chaplins

The chaplins (*coelicolor* hydrophobic aerial proteins) are a family of eight secreted proteins, ChpA-H, which are encoded by genes found primarily within the core region of the linear chromosome (Figure 1.2A). The chaplins are subdivided into two groups according to size: the ‘long chaplins’ (ChpA-C) are 210 – 230 amino acids in length and include two ‘chaplin domains’, while the ‘short chaplins’ (ChpD-H) are 50 – 60 amino acids in length and include only a single chaplin domain (Figure 1.2B) (Elliot *et al.*, 2003, Claessen *et al.*, 2003). Each chaplin domain, with the exception of ChpE and the second chaplin domain of ChpB, contains two highly conserved cysteine (Cys) residues (Figure 1.2C) that form intramolecular disulfide bonds (Elliot *et al.*, 2003). The N-terminus of each chaplin protein includes a signal peptide that targets them for secretion via the Sec translocation system (Elliot *et al.*, 2003, Claessen *et al.*, 2003). In addition, the long chaplins have a C-terminal sortase recognition motif (LAXTG) that is followed by a hydrophobic region and positively charged tail, presumably serving to target them for attachment to the cell wall through the activity of a sortase enzyme(s). Sortases are transpeptidases found in Gram-positive bacteria, which cleave surface proteins at the sortase recognition site and covalently link them to the growing peptidoglycan layer (Marraffini *et al.*, 2006).

Following secretion, the short chaplins are predicted to polymerize into fibers that are predicted to interact with the cell wall-anchored long chaplins (Elliot *et al.*, 2003, Claessen *et al.*, 2003). Chaplin fibers decorate aerial hyphae and spores, forming a characteristic paired-rod (‘rodlet’) ultrastructure (Figure 1.3). The organization of chaplin

fibers into rodlets appears to depend on a second group of proteins, the rodlin (Claessen *et al.*, 2004, Claessen *et al.*, 2002). The expression of the rodlin genes (*rdlA* and *rdlB*) is *bld* gene-dependent (Elliot *et al.*, 2003); however, the rodlin is not required for aerial development per se, as a rodlin mutant can still raise a robust aerial mycelium (Claessen *et al.*, 2002). The rodlin is also not conserved across all streptomycetes, and is absent from the genomes of *Streptomyces* species that do not produce rodlets on their surface (e.g. *S. avermitilis*). In *S. coelicolor*, deletion of one or both of the rodlin genes results in an absence of surface rodlets; instead, the cell surface appears relatively smooth (Claessen *et al.*, 2004). In addition to the rodlets of *S. coelicolor* and the smooth surface of *S. avermitilis*, the surfaces of streptomycetes can also be adorned with spike- or wart-like protrusions (e.g. *S. echinatus* and *S. steffisburgensis*, respectively), or have a ‘hairy’ appearance (e.g. *S. pactum*) (Dietz & Mathews, 1971). Although there is some evidence to suggest that the rodlet ultrastructure of *S. coelicolor* is important for attachment to solid surfaces (polystyrene) (Claessen *et al.*, 2002), it is not clear what role these different surface decorations play in streptomycete biology.

The intricate matrix of chaplin/rodlin fibers cover aerial hyphae and spores in a resilient hydrophobic coat, which likely protects against desiccation and provides stability to aerial structures. In addition to promoting aerial development and modifying the cell surface, the chaplins also form fimbriae that extend from the mycelial surface when *S. coelicolor* is grown in standing liquid culture; these fimbriae are important for attachment to solid surfaces (de Jong *et al.*, 2009b). Intriguingly, fibers produced by the chaplins have characteristics that are shared by amyloid proteins (very insoluble, heat-stable, β -rich secondary structure) and readily bind the amyloid-specific dyes Congo red and thioflavin T (Capstick *et al.*, 2011, Claessen *et al.*, 2003, de Jong *et al.*, 2009b, Sawyer *et al.*, 2011). Amyloids are well known for their cytotoxicity (Chiti & Dobson, 2006), so it is fascinating that amyloidogenic proteins such as the chaplins play such an essential role in *Streptomyces* morphological development.

The transcription of the *chp* genes is *bld* gene-dependent and *whi* gene-independent (Elliot *et al.*, 2003). Interestingly, the phenotypes of many *bld* mutants (with the exception of *bldB*, *bldM*, and *bldN*) can at least be partially rescued when grown on mannitol-containing media instead of glucose (‘conditional’ *bld* mutants) (Pope *et al.*, 1996, Willey *et al.*, 1991, Willey *et al.*, 1993, Bibb *et al.*, 2000, Molle & Buttner, 2000), suggesting that separate pathways are responsible for morphogenesis under nutrient-poor and nutrient-rich conditions. As SapB is not produced on mannitol-containing media (Willey *et al.*, 1991), the ability of conditional *bld* mutants to raise aerial hyphae under these conditions is therefore solely due to their production of chaplin proteins (Capstick *et al.*, 2007).

During development, the expression of *chpA*, *D*, *F*, and *G* is highest during late aerial hyphae formation and early sporulation, while *chpE* and *chpH* are expressed throughout all stages of development (Elliot *et al.*, 2003, Claessen *et al.*, 2003). Creating single or even double *chp* gene deletions causes no visible change in phenotype; however, making quadruple ($\Delta chpACDH$) or quintuple ($\Delta chpABCDH$) *chp* deletions causes a pronounced delay in aerial development (Elliot *et al.*, 2003). Under nutrient-poor conditions (where SapB is not produced), a complete 8 \times *chp* mutant ($\Delta chpABCDEFGH$)

is almost completely bald, producing only very sparse aerial hyphae and lacking surface hydrophobicity (Capstick *et al.*, 2007, Claessen *et al.*, 2004). The phenotype of a multiple *chp* mutant can be partially rescued by the exogenous application of purified chaplin proteins (Elliot *et al.*, 2003, Claessen *et al.*, 2003). In addition, application of purified SapB or over-expression of the regulator of the SapB-producing *ram* genes (*ramR*) can also partially restore aerial hyphae production to a complete 8× *chp* mutant on minimal media (Capstick *et al.*, 2007).

1.5.2.1 The Chaplins and the Fungal Hydrophobins

Filamentous fungi (ascomycetes and the basidiomycetes) produce proteins known as hydrophobins, which are functionally analogous to the *Streptomyces* chaplin and rodlin proteins but share no sequence homology. Like the chaplins (and SapB), the hydrophobins are surface-active proteins that are required for lowering the surface tension at air-aqueous interfaces, thus allowing fungi to extend aerial structures into the air. Hydrophobins are divided into two classes based on their biophysical properties (Wessels, 1994). Class I hydrophobins (e.g. SC3 from *Schizophyllum commune*) produce highly insoluble fibers that can only be disassociated by treatment with harsh solvents, such as trifluoroacetic acid (TFA). The insoluble aggregates formed by class I hydrophobins, like those of the chaplins, share characteristics with amyloid fibers, and readily bind the amyloid-specific dyes ThT and Congo red (Butko *et al.*, 2001, Mackay *et al.*, 2001). Also like the chaplins, fibers of class I hydrophobins are organized into rodlets on the cell surface (Wösten, 2001, Elliot & Talbot, 2004). Class II hydrophobins (e.g. HFBII from *Trichoderma reesei*) in contrast, do not form rodlets and are soluble in some organic solvents. There is little sequence similarity shared by different hydrophobins, but all have eight conserved Cys residues that form four disulfide bridges. The spacing of amino acids between Cys residues can vary in class I hydrophobins, but is well conserved among those from class II (Linder *et al.*, 2005). Structural studies carried out on members of class I and class II hydrophobins (EAS from *Neurospora crassa* and HFBII from *Trichoderma reesei*, respectively) revealed that hydrophobins adopt a structure consisting primarily of a central β -barrel comprising four β -strands. Two of the four disulfide bonds are found within the β -barrel and help to structurally constrain the protein in an amphiphilic conformation, thereby contributing to the surface activity of the hydrophobins (Hakanpaa *et al.*, 2004, Kwan *et al.*, 2006).

1.6 Amyloid Proteins

For over a century, amyloids were thought to be solely agents of disease (Kyle, 2001), and were presumed to be the byproducts of proteins that had become misfolded or dysfunctional (Kyle, 2001). Amyloids are associated with a number of devastating diseases, such as Alzheimer's, Huntington's, and type II diabetes, as well as prion-based diseases like bovine spongiform encephalopathy ('mad cow' disease) and Creutzfeldt-Jakob disease (Chiti & Dobson, 2006). Amyloids are defined as proteins that self-assemble into 4 - 12 nm wide unbranched fibers, having a characteristic cross- β sheet

secondary structure, where each β -strand is orientated perpendicular to the fiber axis. Amyloid fibers are highly insoluble, heat-stable structures that are also protease-resistant. In their monomeric state, amyloid fiber-forming proteins are largely unstructured, or may have a secondary structure composed of both α -helices and β -sheets. However, when these proteins polymerize to form amyloid fibers, they adopt the characteristic cross- β sheet structure. This polymerization process typically occurs via nucleation-dependent kinetics, having a lag, log and stationary phase. The lag phase is thought to represent the time required for the necessary amyloid ‘nuclei’ to form, which catalyze the formation of full-length amyloid fibers (Chiti & Dobson, 2006). During amyloidogenesis, proteins take on an intermediate structural configuration (‘protofibrils’) on their path towards forming mature amyloid fibers, and there is increasing evidence suggesting that these soluble intermediate species are the true source of the cellular toxicity associated with amyloids, and not the mature amyloid fibers (Lashuel & Lansbury, 2006, Chiti & Dobson, 2006). There is data indicating that the protofibrils can form channel-like structures, permeabilizing cell membranes. This results in ion leakage that in turn can cause the disruption of the membrane potential and homeostasis of the cell, potentially leading to cell death (Quist *et al.*, 2005, Lashuel & Lansbury, 2006). Once formed, mature amyloid fibers are thought to be relatively inert (Bucciantini *et al.*, 2002); however, the precise contribution that mature amyloid fibers make to the disease process remains controversial.

1.6.1 Functional Amyloids

Although many amyloids are cytotoxic, there have been a number of amyloids discovered over the last two decades that are greatly beneficial; instead of causing disease, they have important roles in cellular biology. Examples of these ‘functional amyloids’ are found in a wide range of organisms, including mammals, yeasts, and bacteria, and they have an equally diverse array of functions (Fowler *et al.*, 2007, Chiti & Dobson, 2006). In mammals, for example, Pmel17 is an amyloid protein that is involved in melanin biosynthesis (skin pigment) (Berson *et al.*, 2003). Another example is Sup35 from *Saccharomyces cerevisiae*, a regulatory protein that controls translation termination; when Sup35 forms amyloid fibers, it is no longer active and read-through of mRNA occurs (Wickner, 1994). Among bacteria, functional amyloids can act as toxins and virulence factors, such as microcin E492 (*Klebsiella pneumonia*) and HpaG (*Xanthomonas* sp.) (Bieler *et al.*, 2005, Oh *et al.*, 2007), as well as mediating cell adhesion and biofilm formation, in the case of MTP (*Mycobacterium tuberculosis*), TsaA (*Bacillus subtilis*), HfaA (*Caulobacter crescentus*), FapC (*Pseudomonas* sp.), and curli/tafi (*Escherichia coli/Salmonella*) (Alteri *et al.*, 2007, Romero *et al.*, 2010, Hardy *et al.*, 2010, Dueholm *et al.*, 2010, Barnhart & Chapman, 2006).

The one common feature that unites all functional amyloids is the strict regulation of their activity. Although functionally beneficial, it is possible that these proteins harbour the same potential for causing cell damage as their disease-associated counterparts. Cells must therefore have regulatory mechanisms in place that allow for the production of amyloids, while avoiding amyloid-related cytotoxicity. One strategy is to spatially

confine amyloid proteins to specific subcellular locations, keeping them in a state that does not promote aggregation. Pmel17, found in mammalian melanosomes, is initially membrane-bound, and must be cleaved (producing M α) before becoming amyloidogenic (Berson *et al.*, 2003). Following cleavage, M α remains attached to the membrane-bound M β protein (also derived from Pmel17), which prevents premature M α aggregation. Under the appropriate conditions, M β is degraded, allowing M α to aggregate into amyloid fibers (Berson *et al.*, 2001). In *E. coli*, curli amyloid fibers are produced by the gene products of the divergently transcribed *csgBA* and *csgDEFG* operons (Hammar *et al.*, 1995). Polymerization of the major curli subunit CsgA requires a nucleator protein (CsgB) to catalyze its polymerization on the cell surface (Bian & Normark, 1997). In the absence of CsgB, soluble monomers of CsgA are secreted from the cell surface and are lost to the extracellular environment (Hammar *et al.*, 1996, Chapman *et al.*, 2002). In contrast to the activity of CsgB, CsgE acts as an inhibitor, preventing the premature conversion of CsgA into amyloid fibers (Nenninger *et al.*, 2011). The transport of monomeric CsgA and CsgB to the cell surface is mediated through a curli-dedicated outer membrane lipoprotein encoded by *csgG* (Loferer *et al.*, 1997, Chapman *et al.*, 2002), ensuring the correct localization of curli fibers on the cell surface. Both Pmel17 and the curli proteins serve as prime examples of how multi-tier regulation of protein amyloidogenesis is necessitated in order to precisely control the spatial and temporal production of amyloid proteins.

1.7 Aims of this Thesis

Although it has been firmly established that the chaplins are essential for *S. coelicolor* morphological development, there is still much that remains unknown regarding their activity. In particular, how each of the chaplins contribute to the promotion of aerial development, and the importance that chaplin amyloidogenesis has in this process. The work outlined in Chapter 3 represents a comprehensive examination of chaplin amyloidogenesis (specifically that of ChpH) *in vitro*, identifying the sequence determinants that are crucial for ChpH amyloid fiber formation and relating these findings to the role ChpH has in promoting aerial morphogenesis *in vivo*. Chapter 4 includes a functional characterization of the unique short chaplin ChpE, in addition to an examination of the role the long chaplins play in ChpE cell surface attachment.

1.8 Figures

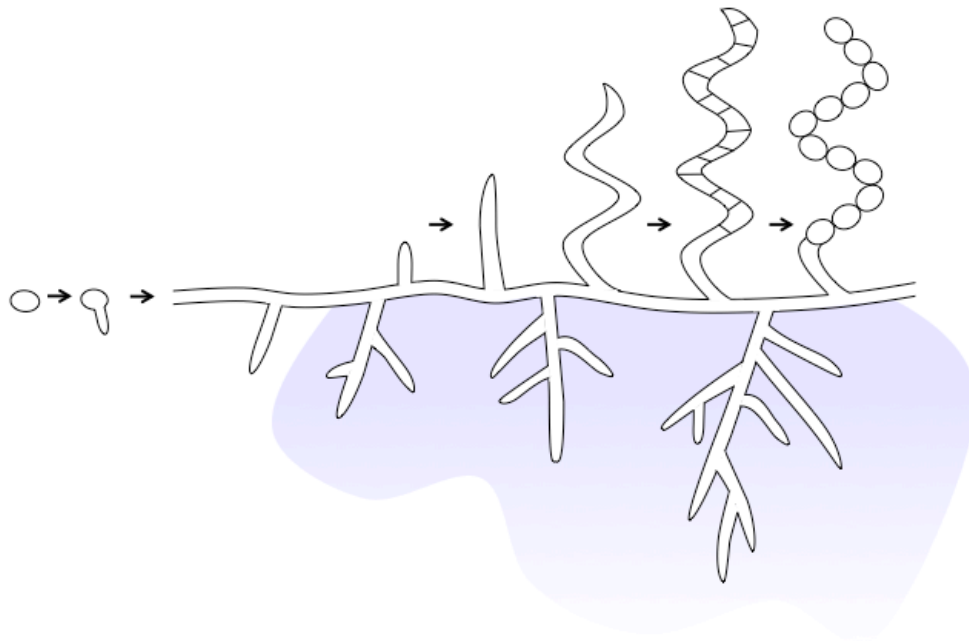


Figure 1.1: The life cycle of *S. coelicolor*. Growth initiates with spore germination and the emergence of one or more germ tubes, followed by a vegetative growth phase during which hyphae elongate and branch, ultimately forming the substrate mycelium. The vegetative growth is followed by the emergence of aerial hyphae that extend upwards from the colony surface. Aerial development occurs in conjunction with secondary metabolite production (purple). Aerial hyphae undergo a synchronous round of cell division, and these single genome compartments then mature, forming chains of reproductive spores. Image courtesy of J.P. Świercz.

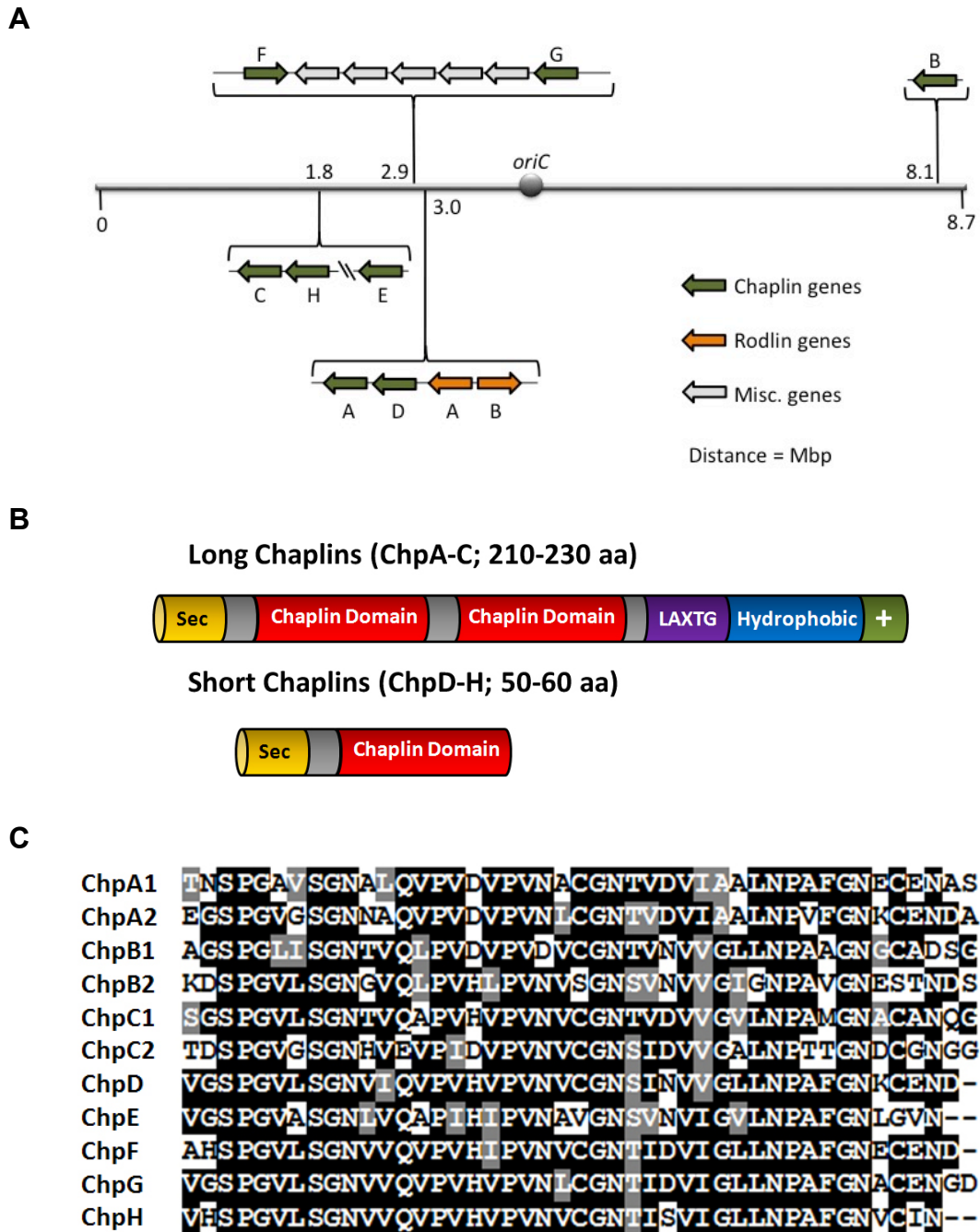


Figure 1.2: Overview of the chaplins. (A) Location of the chaplin genes on the chromosome. Rodlin genes are also indicated. (B) Chaplin proteins include a N-terminal Sec signal peptide (Sec) and one or more homologous regions (chaplin domain). The long chaplin C-terminal sortase-recognition motif (LAXTG) precedes a hydrophobic region and positively charged tail (+). (C) Alignment of chaplin domains.

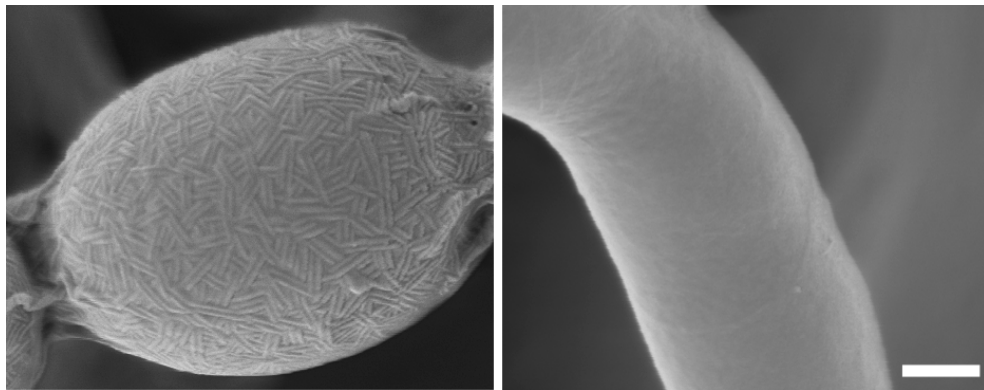


Figure 1.3: Paired-rod (‘rodlet’) ultrastructure on the surface of wild type *S. coelicolor* spores (left). Surface rodlets are absent in an 8× *chp* mutant (right). Scale bar, 200 nm. Images courtesy of K. Findlay.

CHAPTER 2

Materials and Methods

2.1 Bacterial culturing and microbiological techniques

2.1.1 Bacterial growth media

Growth media was sterilized by autoclaving at 121°C and 100 kPa for 20 min. Antibiotic solutions to be added to growth media [except those made with 100% ethanol or dimethyl sulfoxide (DMSO)] were sterilized by filtration through an Acrodisc[®] 25 mm syringe filter with a 0.2 µm Supor[®] membrane (Pall) and stored at -20°C. Unless otherwise indicated, antibiotics added to *Streptomyces* culture media were used at the following final concentrations (µg/ml): apramycin, 50; hygromycin B, 50; kanamycin sulfate, 50; naladixic acid, 25; thiostrepton, 50; vancomycin, 10; viomycin sulfate, 50. For *Escherichia coli*, antibiotics were added to media to the following final concentrations (µg/ml): ampicillin, 100; apramycin, 50; chloramphenicol, 25; hygromycin B, 50; kanamycin sulfate, 50; viomycin sulfate, 50. *S. coelicolor* was routinely cultured at 30°C on mannitol soy flour agar (MS) (Hobbs *et al.*, 1989), which consisted of (g/L): D-mannitol, 20; soy flour ('Bob's Red Mill' organic stone ground soy flour), 20; agar, 20 (prepared in tap water, not dH₂O). When harvesting mycelium, MS agar was covered with a sterile cellophane disc to facilitate biomass extraction, as *S. coelicolor* grows into the agar medium (it produces agarase). For rapid, non-differentiated growth, *S. coelicolor* was grown on Difco nutrient agar (DNA) (2.3 g DNA powder/100 ml dH₂O). When transforming with DNA, *S. coelicolor* protoplasts were plated on R2YE agar (Hopwood & Wright, 1978, Okanishi *et al.*, 1974) (g/800 ml): sucrose, 103; K₂SO₄, 0.25; MgCl₂•6H₂O, 10.12; glucose, 10; Difco casaminoacids, 0.1; agar, 22; after autoclaving, supplemented with (ml/80 ml): KH₂PO₄ (0.5%), 1; CaCl₂•2H₂O (3.68%), 8; L-proline (20%), 1.5; TES buffer (5.73%, pH 7.2), 10; NaOH (1 M), 0.5; trace elements [per L: ZnCl₂, 40 mg; FeCl₃•6H₂O, 200 mg; CuCl₂•2H₂O, 10 mg; MnCl₂•4H₂O, 10 mg; Na₂B₄O₇•10H₂O, 10 mg; (NH₄)₆Mo₇O₂₄•4H₂O, 10 mg], 0.2; yeast extract (10%), 5. When growing *Streptomyces* in liquid culture, a 1:1 mixture of YEME (yeast extract-malt extract) [(g/L): Difco yeast extract, 3; Difco Bacto-peptone, 5; malt extract, 3; glucose, 10; sucrose, 340; after autoclaving, amended with (ml/L): MgCl₂•6H₂O (2.5 M), 2; glycine (20%), 25] and TSB [(g/L): Oxoid tryptone soya broth, 30] was used. A metal spring was added to *Streptomyces* liquid cultures, and baffled flasks were used to reduce clumping of mycelium. Liquid cultures were grown at 30°C with shaking at 200 rpm in an Innova[®] 44 incubator shaker (New Brunswick Scientific). For *E. coli*, strains were cultured at 37°C in Luria Bertani (LB) media (Miller, 1972) and consisted of (g/L): tryptone, 10; yeast extract, 5; NaCl, 10; agar, 15 (for solid media). Liquid *E. coli* cultures were shaken at 200 rpm in an Innova[®] 44 shaking incubator (New Brunswick Scientific). When growing *E. coli* in the presence of salt-sensitive antibiotics (e.g. hygromycin), lower-salt liquid [2× YT broth (g/L): tryptone, 16; yeast extract, 10; NaCl, 5] or solid

(DNA) media was used. To enable blue-white screening when cloning, LB media was supplemented with EZ-GAL™ (4 µl/ml LB; Bioshop), which contains (exact quantities are not disclosed by the manufacturer) 5-bromo-4-chloro-3-indolyl-β-D-galactopyranoside (X-gal) and isopropyl β-D-1-thiogalactopyranoside (IPTG). When necessary, individual stocks of X-gal or IPTG (Bioshop) were made by dissolving the powder in 100% DMSO or dH₂O, respectively.

2.1.2 Bacterial strains and plasmids

All bacterial strains and plasmids used in this work are outlined in Table 2.1. For long-term storage of *S. coelicolor*, strains were grown on MS agar and incubated at 30°C until sporulation was evident (grey surface pigment). Mycelia were then scraped off the surface of the plate with a flame-sterilized metal spatula and transferred to ~10 ml of sterile dH₂O in a glass universal vial. The spore suspension was water bath sonicated until homogenous, after which the suspension was passed through a cotton syringe filter. The spore-containing filtrate was pelleted by centrifugation and the supernatant discarded before being resuspended in 40% glycerol and stored at -20°C. For non-sporulating *Streptomyces* strains, mycelia were collected and suspended in dH₂O and homogenized using a 15 ml Pyrex® homogenizer (Corning). The homogenized mixture was pelleted by centrifugation, resuspended in 40% glycerol, and stored at -20°C. For long-term storage of *E. coli* strains, overnight LB liquid cultures were mixed 1:1 with 40% glycerol and stored at -80°C.

2.2 Bacterial genetic and molecular biology techniques

2.2.1 *Streptomyces* conjugation

Conjugations were done as described previously (Kieser *et al.*, 2000). The *E. coli* ET12567 (methylation deficient) donor strain containing the pUZ8002 mobilizing plasmid and the target plasmid/cosmid (Table 2.1) was grown overnight in 5 ml LB broth and subcultured (1/100) in 25 ml fresh LB in a 250 ml flask. The *E. coli* subculture was grown to an OD₆₀₀ ~0.4, after which the cells were collected by centrifugation, washed twice with LB and finally suspended in 2 ml of LB. To prepare the recipient *S. coelicolor* strain, 5 µl of a concentrated spore stock (~10⁸ spores) was added to 500 µl of 2× YT broth and heat shocked at 50°C for 10 min. The spore suspension was allowed to cool to room temperature before 500 µl was removed and combined with 500 µl of washed *E. coli* donor cells. The mixture was vortexed briefly and centrifuged to collect the cells, which were then resuspended in the remaining liquid after discarding the supernatant, and plated on MS agar supplemented with 10 mM MgCl₂. After a 14 - 16 hour incubation at 30°C, the plates were overlaid with 1 ml sterile dH₂O supplemented with 25 µl apramycin (50 mg/ml)/viomycin (30 mg/ml) to select for the plasmid/cosmid and 20 µl naladixic acid (25 mg/ml) to kill the *E. coli* donor. Plates were then incubated at 30°C until colonies were visible (~4 days).

2.2.2 Protoplast transformation

Protoplast preparation and transformation were conducted using the method described by Kieser *et al.* (2000). Cosmid DNA to be transformed into *Streptomyces* was passaged through the methylation-deficient *E. coli* strain ET12567. For preparing protoplasts, a 10 ml YEME:TSB culture of *Streptomyces* was grown overnight before being transferred into a 250 ml baffled flask containing 30 ml fresh YEME:TSB (40 ml total). The subculture was incubated for 24 - 48 hrs until the culture exhibited a slight red/orange hue, indicating the start of pigmented antibiotic production. Mycelia were collected by centrifugation and washed with 10.3% sucrose before being re-suspended in 4 ml P buffer [(g/800 ml): sucrose, 103; K₂SO₄, 0.25; MgCl₂•6H₂O, 2.02; supplemented with 2 ml of R2YE trace elements solution; after autoclaving, amended with (ml/80 ml): KH₂PO₄ (0.5%), 1; CaCl₂•2H₂O (3.68%), 10; TES buffer (5.73%, pH 7.2), 10] containing 1 mg/ml lysozyme. The mixture was transferred to a glass universal vial and incubated in a 30°C water bath for 1 hour. To help separate the protoplasts from the cell wall, the mixture was gently drawn in and expelled three times from a 5 ml pipette, and then incubated at 30°C for 15 min. The mixture was diluted by adding 5 ml of P buffer (without lysozyme) and was then passed through a cotton syringe filter. The protoplast-containing filtrate was gently centrifuged at 1,000 g for 10 min. The supernatant was then discarded and the protoplast pellet was resuspended in ~1 ml of P buffer; of this 1 ml, 50 µl was then mixed with 5 µl of DNA. Immediately following mixing, 200 µl of P buffer containing 0.25% PEG1000 was added. The mixture was gently pipetted up and down, and was then plated on R2YE agar. Plates were incubated for ~14 - 20 hours at 30°C, before flooding the plates with kanamycin (200 µg/ml final) to select for the introduced cosmid (kanamycin-resistant). Plates were then incubated for an additional 3 - 4 days at 30°C until colonies were visible.

2.2.3 Preparing and transforming competent *E. coli* cells

Competent cell preparation using CaCl₂ and transformation methods are based on those described elsewhere (Sambrook & Russell, 2001). For the introduction of plasmid DNA into *E. coli*, cells were cultured overnight in 5 ml LB before being subcultured (1/100) in 50 ml fresh LB broth. Cultures were grown to an OD₆₀₀ of ~0.4 before cells were collected by centrifugation, and then suspended in 30 ml of an ice-cold MgCl₂/CaCl₂ solution (80 mM MgCl₂, 20 mM CaCl₂). Cells were recovered by centrifugation and were resuspended in 2 ml of ice-cold 0.1 M CaCl₂ containing 15% glycerol. Cells were used immediately for transformation or were stored in 200 µl aliquots at -80°C. To transform competent cells, 3 µl of plasmid DNA was mixed with 200 µl of competent cells, and the mixture was allowed to incubate on ice for 30 min before being heat shocked for 90 s at 42°C. After allowing the cells to rest on ice for ~2 min, 1 ml of LB broth was added and the cells were incubated with shaking (200 rpm) at 37°C for 20-60 min. Cells were then plated on LB agar containing the appropriate antibiotics and incubated at 37°C.

To prepare electrocompetent cells, an *E. coli* culture was grown and subcultured as above. Once the subculture reached an OD₆₀₀ of ~0.4, the cells were washed twice with ice-cold 10% glycerol. The cell pellet was resuspended in ~100 µl 10% glycerol and 50 µl of this was mixed with 1-2 µl of DNA (~100 ng). The mixture was transferred to an ice-cold 0.2 mm electroporation cuvette (BioRad) and electroporated using a BioRad MicroPulser™ (2.5 kV). Immediately afterwards, 1 ml of ice-cold LB was added to the cells, and the mixture was transferred to a 1.5 ml Eppendorf tube and allowed to incubate with shaking (200 rpm) at 37°C for 20 - 60 min. Cells were then plated on LB agar containing the appropriate antibiotics and incubated at 37°C overnight.

2.2.4 Bacterial two-hybrid assay

To assess protein-protein interactions, the bacterial two-hybrid assay was used (Karimova *et al.*, 1998). The *chpH*, *rldA*, and *rldB* genes were PCR-amplified using the primers listed in Table 2.2. All PCR primer pairs were designed to include *Pst*I and *Bam*HI sites, so that all resulting PCR products would include these restriction sites at their 5' and 3' ends, respectively, allowing them to be directionally cloned into plasmids pKT25/pKNT25 (*rldA* and *rldB*) or pUT18/pUT18C (*chpH*) cut with *Pst*I and *Bam*HI. Primers also included extra nucleotides to ensure that all inserts were fused in-frame with respect to the corresponding T18 or T25 adenylate cyclase subunit. As a positive control for the assay, pKNT25 and pUT18C carrying the leucine zipper of the yeast protein GCN4, which is known to dimerize, were used (Karimova *et al.*, 1998). Pairs of plasmids were transformed into *E. coli* DHM1 cells (Cya⁻), and plated on LB agar supplemented with kanamycin and ampicillin, to select for pKT25/pKNT25 and pUT18/pUT18C, respectively, plus 40 µg/ml X-gal and 0.5 mM IPTG, to facilitate blue-white screening.

2.2.5 DNA isolation

2.2.5.1 Isolation of genomic DNA from *Streptomyces*

A 10 ml YEME:TSB culture was grown overnight in a glass universal vial, before being transferred to a 250 ml baffled flask containing 40 ml fresh YEME:TSB (50 ml total) and grown for an additional ~24 hrs. Mycelia were collected by centrifugation and the pellet was washed with 10% glycerol. The washed pellet was resuspended in 6 ml fresh P buffer amended with 3 mg/ml lysozyme and incubated at 37°C for 1 hour before adding 1.32 ml EDTA (0.5 M, pH 8) and incubating for a further 10 min at 37°C. To the mixture was added 396 µl sodium dodecyl sulfate (SDS, 20%), followed by a 10 min incubation at 60°C. The mixture was diluted with 4 ml P buffer (no lysozyme) to a final volume of ~10 ml and at least two phenol:chloroform (1:1) extractions were done, each of which were followed by a 15 min centrifugation at 11,950 × g at 4°C (Sorvall RC6, SS34 rotor). The aqueous phase was mixed with one volume of chloroform and centrifuged as before. In a fresh tube, the aqueous phase was mixed with three volumes of 95% ethanol and incubated for 1 hour or overnight at -20°C. The precipitated nucleic acid was spooled around a sterile glass Pasteur pipette and transferred to a fresh 1.5 ml Eppendorf tube.

The pellet was air dried before adding 500 μ l T₁₀E₁ (10 mM Tris, 1 mM EDTA, pH 8) and leaving it overnight at 4°C to allow it to completely go into solution. RNase A was added to a final concentration of 30 μ g/ml, and the mixture was incubated at 37°C for 1 hour. To assess the quality of the genomic DNA, 5 μ l was run out on an ethidium bromide-stained 0.8% agarose gel. Preparations of genomic DNA were stored at 4°C (short-term) or -20°C (long-term).

2.2.5.2 Plasmid and cosmid DNA isolation from *E. coli*

Plasmid/cosmid isolation was performed as described previously (Sambrook & Russell, 2001). Cells from an overnight 5 ml *E. coli* culture were collected by centrifugation and suspended in 100 μ l TEG (50 mM Tris, 20 mM EDTA, 1% glucose, pH 8). Cells were lysed by adding 200 μ l (fresh) lysis buffer (0.2 M NaOH, 1% SDS) and incubating at room temperature for ~5 min before adding 150 μ l NaOAc (3 M, pH 4.8). The insoluble debris was collected by centrifugation and the supernatant transferred to a fresh tube, followed by a phenol:chloroform (1:1) extraction. The aqueous phase was transferred to a new tube and mixed with two volumes 95% ethanol and incubated at -20°C for 10 min. The nucleic acid was collected by centrifugation at 15,000 \times g for 10 min, and the pellet was then dried at room temperature before being resuspended in 40 μ l sterile dH₂O. RNase A was added to a final concentration of 10 μ g/ml, and the mixture was incubated at 37°C for 30 min.

For obtaining high-quality DNA suitable for sequencing, plasmids were prepared using the PureLink™ Quick Plasmid Miniprep kit (Invitrogen). For all isolated plasmids/cosmids, quality and concentration was determined by running 2 μ l on a 1% ethidium bromide-stained agarose gel and by measuring at 260 nm with an Ultrospec™ 3100 Pro spectrometer (Biochrom Ltd.).

2.2.6 Agarose gel electrophoresis

Standard agarose gels were prepared with 1 \times TBE buffer with an agarose concentration of 0.8 - 2.0%. For visualization of DNA fragments, 5 μ l of a 10 mg/ml ethidium bromide solution (BioShop) was added to 50 ml of molten agarose before pouring the gel. For estimation of DNA fragment size, 100 bp and/or 1 kb DNA ladders (New England BioLabs) were used. When excising DNA fragments from agarose gels, the MinElute® Gel Extraction kit (Qiagen) was used.

2.2.7 Restriction digestion of DNA

Restriction enzymes were purchased from New England BioLabs (NEB) and were used as recommended by NEB. Routine digests were carried out in a final volume of 20 μ l, containing 0.5-1 U of enzyme.

2.2.8 Phosphorylation and dephosphorylation of DNA

To prevent re-attachment of ‘sticky-end’ digestion products to be used for cloning purposes, DNA was dephosphorylated using calf intestine alkaline phosphatase (Roche) following the instructions from the manufacturer, before being phenol/chloroform (1:1) extracted and ethanol-precipitated to recover the linearized plasmid DNA. To phosphorylate DNA, T4 kinase (Invitrogen) was used as outlined by the manufacturer, and the DNA was recovered as before.

2.2.9 DNA ligations

Ligations were done using the Rapid Ligation Kit (Roche) as per the manufacturer’s instructions. Typically, insert DNA was combined with vector DNA in a 5:1 ratio, to a final reaction volume of 20 μ l, and allowed to incubate at room temperature for 20 min. Ligations were transformed into *E. coli* by gently mixing 3 μ l of the ligation mixture with 50 μ l Subcloning Efficiency™ (SE) DH5 α competent cells (Invitrogen), followed by an incubation on ice for 30 min, before heat shocking the cells at 37°C for 20 s. The cells were incubated on ice for 1 min before 1 ml of LB broth was added and the cells were transferred to 37°C for 1 hr. Cells were then collected by centrifugation, plated on LB agar containing the appropriate antibiotic, and incubated at 37°C overnight.

2.2.10 DNA amplification by PCR

For routine polymerase chain reaction (PCR) checks, *Taq* DNA polymerase (Norgen Biotek Corp.) was used, and PCR reactions were carried out in a Mastercycler® Thermal Cycler (Eppendorf). For PCR reactions requiring high-fidelity amplification, iProof™ High-Fidelity DNA polymerase (BioRad) was used.

For *E. coli* colony PCR, a small portion of the colony was transferred with a pipette tip to the PCR tube, and the PCR reaction was done without any further alteration. For *S. coelicolor* colony PCR, an initial lysis step was needed to facilitate effective extraction of DNA. A portion of a *S. coelicolor* colony was transferred with a pipette tip into 20 μ l of microLYSIS® solution (Gel Company), placed in the thermal cycler and incubated as follows (done twice): 65°C, 5 min; 96°C, 2 min; 65°C, 4 min; 96°C, 1 min; 65°C, 1 min; 96°C, 30 s. For subsequent PCR reactions, 3 μ l of the microLYSIS reaction was used as DNA template.

2.2.11 Creating gene knockouts in *S. coelicolor*

Gene knockouts were performed using the PCR-targeted method of Gust *et al.* (Gust *et al.*, 2003). Genes were replaced with *oriT*-containing cassettes conferring apramycin (*aac(3)IV*; from pIJ773) or viomycin (*vph*; from pIJ780) resistance (Gust *et al.*, 2003). A cosmid, from the ordered *S. coelicolor* genomic library [SuperCos-1 backbone conferring kanamycin-resistance (Redenbach *et al.*, 1996)] carrying the gene of interest, was electroporated into *E. coli* BW25113 (Datsenko & Wanner, 2000).

Following this, the target gene carried on the cosmid was disrupted through electroporation of the knockout cassette, which included gene-specific 39 bp 5' and 3' extensions, generated via PCR (Table 2.2). Knockout cosmids were confirmed by PCR and digestion to ensure correct cassette localization and loss of the target gene (Table 2.2). The knockout cosmid was then electroporated into ET12567/pUZ8002 cells, which were used to conjugate the knockout cosmid into *S. coelicolor*. Transconjugants were screened for a double-crossover event between the *S. coelicolor* chromosome and the mutant cosmid by replica-plating on DNA agar containing kanamycin or apramycin/viomycin. Colonies that were apramycin/viomycin-resistant (gain of the cassette) and kanamycin-sensitive (loss of the cosmid) and were screened using PCR to confirm the presence and correct chromosomal location of the knockout cassette (Table 2.2).

When necessary, unmarked mutants (i.e. lacking a selectable marker) were created by first removing the cassette from the knockout cosmid via a FLP recombinase-mediated event. The knockout cosmid was introduced by electroporation into *E. coli* BT340 (Datsenko & Wanner, 2000), which carries a temperature-sensitive plasmid (replicates at 30°C) that expresses the FLP recombinase at 42°C, conditions that cause the concurrent loss of the FLP plasmid (Cherepanov & Wackernagel, 1995). Knockout cassettes are flanked by two FLP recognition target (FRT) sites that target the removal of the central portion of the cassette, leaving behind an 81 bp sequence, which is in-frame and lacks any stop codons (Gust *et al.*, 2003). After an overnight incubation at 42°C, colonies were screened for kanamycin-resistance and apramycin/viomycin-sensitivity, due to the loss of the selectable marker from the cosmid, which was confirmed by PCR (Table 2.2). Protoplasts of the cassette-containing mutant were prepared and transformed with the cassette-less cosmid. Transformants were initially selected for using kanamycin, after which they were screened for kanamycin- and apramycin/viomycin-sensitivity, and putative unmarked mutants were confirmed by PCR (Table 2.2).

2.2.12 Generating substitution mutations via PCR

The *chpH* gene was excised from pIJ6935 (Elliot *et al.*, 2003) using *EcoRI* and ligated into *EcoRI*-digested pIJ2925 (Janssen & Bibb, 1993). The *chpH*-pIJ2925 plasmid was used as template for all *chpH* PCR-based mutagenesis. The entire *chpH*-pIJ2925 plasmid was PCR-amplified using Pfu enzyme (Stratagene) with the primers listed in Table 2.2. The PCR program included an initial denaturing at 95°C for 5 min, followed by 5 cycles at 95°C for 1 min, 65°C for 1 min, and 72°C for 10 min, and then 19 cycles at 95°C for 1 min, 62°C for 1 min, and 72°C for 10 min, followed by a final elongation at 72°C for 15 min. The original template DNA was removed by digestion with *DpnI* (which selectively cleaves methylated DNA) for 2 hrs at 37°C. Next, 3 µl of the reaction mixture was introduced in *E. coli* XL-1 Blue cells via electroporation, and cells were plated on LB media supplemented with ampicillin. To replace the entire 'VIGLL' sequence with five alanine residues, *chpH* was PCR-amplified as two halves using iProof DNA polymerase (BioRad) with M13 forward/VIGLL-AAAAA1 and M13 reverse/VIGLL-AAAAA2 primers (Table 2.2). The two halves were combined together

and used as template DNA for a second PCR reaction with M13 universal primers to amplify the entire construct (Table 2.2). All mutations were confirmed by sequencing. Mutant (*chpH**) genes were excised using *EcoRI* and cloned into *EcoRI*-digested pIJ2925 containing *chpC*. Following confirmation of the orientation by PCR, the *chpH**-*chpC* fragments were then excised with *BglII*, cloned into the *BamHI* site of pSET152 (Bierman *et al.*, 1992), and conjugated into *S. coelicolor* strain J3149A.

2.2.13 Creating gene deletions via PCR

PCR mutagenesis to delete portions of *chpH* was performed using iProof DNA polymerase and *chpH*-pIJ2925 plasmid DNA as template. *chpH* deletions were created by PCR-amplifying *chpH* as two halves. The 5' sequence common to all three N-terminal deletions was amplified using the universal M13 reverse primer together with ChpHdelRev (Table 2.2), while the 3' sequence was amplified using the universal M13 forward primer and a *chpH*-specific primer that annealed immediately down from the sequence to be deleted, and included a 5' extension homologous to the 3' end of the first PCR product. The two products were combined together and used as template for a second PCR reaction using the M13 universal primers. A similar strategy was used to remove the C-terminal 'VIGLL' sequence, only using different primer combinations: ChpHVIGLL1/M13 reverse and ChpHVIGLL2/M13 forward primers (Table 2.2). All mutant plasmids were sequenced to ensure that only the desired mutation was introduced. Each mutant *chpH* gene was cloned upstream of *chpC* and introduced into *S. coelicolor* J3149A by conjugation.

2.2.14 Construction of *chpH/chpH** expression vectors

*chpH/chpH** was PCR-amplified from pUC19 carrying *chpH/chpH** (Di Berardo *et al.*, 2008) using ChpH Up New and M13 Fwd primers (Table 2.2). The PCR product was blunt-end ligated into *SmaI*-digested pIJ2925, and the orientation of *chpH/chpH** was confirmed by restriction digestion. The *chpH/chpH**-pIJ2925 construct was then digested with *BamHI/EcoRI* and directionally cloned into pIJ2925 cut with the same enzymes. The P_{vanJ} promoter was PCR amplified from pIJ2925 + P_{vanJ} (Di Berardo *et al.*, 2008) using M13 universal primers (Table 2.2) and the PCR product was digested with *HindIII/SalI* in order to directionally clone it upstream of *chpH/chpH**. The entire P_{vanJ} -*chpH/chpH** fragment was excised from pIJ2925 using *BglII* and cloned into the *BamHI* site of pIJ82.

2.3 Protein biochemical techniques

2.3.1 Purification and mass spectrometry analysis of chaplin proteins

S. coelicolor strains were grown on cellophane discs on the surface of MS agar, and the mycelium was harvested by scraping it off with a sterile metal spatula and suspending it in 10 ml Tris buffer (0.1 M, pH 8). The mixture was sonicated on ice for 3 × 15 s and then centrifuged for 10 min at 7,800 × g. The supernatant was discarded and the

pellet was suspended in 3 ml 2% SDS, followed by heating the pellet at 100°C for 10 min. After allowing it to cool, the mixture was pelleted by centrifugation at $7,800 \times g$ for 10 min, before repeating the SDS/heat-treatment. The insoluble material was washed 10× with dH₂O to remove any trace of SDS, before being flash-frozen in an ethanol-dry ice bath, and dried by rotary evaporation (Eppendorf Vacufuge™ connected to a Büchi® V-500 vacuum pump). Trifluoroacetic acid (TFA) was added to the dried pellet, and the mixture was water bath sonicated for 10 min before being centrifuging at $15,000 \times g$ for 10 min. The TFA-soluble fraction was transferred to a new tube and rapidly dried down under a stream of air. Matrix-assisted laser desorption/ionization time-of-flight (MALDI-ToF) mass spectrometry analysis of chaplin samples was done at the McMaster Regional Centre for Mass Spectrometry and as described previously (Elliot *et al.*, 2003). Briefly, the protein sample was suspended in ~2-4% TFA and then mixed 1:1 with sinapinic acid (10 mg/ml) in 50% acetonitrile containing 1% TFA. The mixture was spotted onto a thin layer of sinapinic acid that was applied to the sample template. After drying, a second thin layer of sinapinic acid was applied and allowed to dry. The resulting crystals were washed twice in 0.1% TFA before being analyzed.

2.3.2 Synthetic peptide and amyloid ‘seed’ preparation

Synthetic peptides (Proteintech Group Inc.) were suspended in TFA and water bath sonicated for 30 min. Aliquots of the peptide/TFA solution were transferred to pre-weighed tubes before the TFA was quickly evaporated under a stream of air. The tubes were then weighed to calculate the amount of dried peptide per tube, and were stored at -80°C. To prepare amyloid seeds, 1 week-old amyloid fibers were sonicated on ice 3×15 s before immediately being added to peptide samples.

2.3.3 Measuring amyloidogenesis with thioflavin T

Lyophilized peptides were dissolved to a concentration of 0.5 mg/ml in ice-cold 50 mM KPi buffer (pH 7.2) immediately before the start of the experiment. At each time point, 98 μ l of peptide was mixed with 2 μ l 1 mM thioflavin T (ThT) in duplicate and deposited in the wells of a black, flat-bottom 96-well plate (Microfluor, Thermo Scientific). Plates were covered with ABSolute™ QPCR seal (Thermo Scientific) to prevent sample evaporation. ThT fluorescence was measured with a BioTek Synergy 4 microplate reader (Fisher Scientific) at 450 nm excitation and 490 nm emission.

2.3.4 Circular dichroism secondary structure analysis

Circular dichroism (CD) spectra were collected at the same time as the ThT assays were being performed, using the same peptide mixture. Peptides were diluted from 0.5 mg/ml to 0.25 mg/ml with ice-cold 50 mM KPi buffer (pH 7.2) (5 mg/ml samples were also tested for the C-terminal mutant peptides and these too were diluted to 0.25 mg/ml) and transferred to a 1-mm quartz cuvette. CD spectra of the buffer (no protein) were

subtracted from peptide-containing solution values. Spectra were recorded from 190 to 260 nm using an Aviv 410 spectrometer.

2.3.5 Protease-resistance assay

Proteinase K (Roche) was added to two week-old fibers or freshly purified SCO3571 (Crp) (both 0.5 mg/ml) in 50 mM KPi buffer to a final concentration of 10 µg/ml. Samples were incubated at 37°C and reactions were stopped by freezing at -80°C. Samples were thawed immediately before analysis by CD spectroscopy.

2.4 Microscopy techniques

2.4.1 Scanning electron microscopy (SEM)

For obtaining high-resolution SEM surface images, colonies were excised from MS agar and mounted on the surface of an aluminum stub with optimal cutting temperature compound (Miles Scientific). The stub was plunged into a liquid nitrogen slush at approximately -210°C and transferred to the cryostage of an Alto 2500 cryotransfer system (Gatan, Oxford, England) attached to a Zeiss Supra 55 VP field emission gun SEM (Zeiss SMT, Germany). The surface frost was sublimated at -95°C for 3 min before sputter coating the sample with platinum for 2 min at 10 mA and below -110°C. The sample was moved to the cryostage of the microscope, held at approximately -130°C, and viewed at 1.2 to 5.0 kV.

To assess relative spore abundance, colonies were excised from MS agar and fixed overnight in 2% glutaraldehyde, before being rinsed 2× with dH₂O and post-fixed in 1% osmium tetroxide for 1 hour. Samples were dehydrated using an ethanol gradient (50, 70, 95, and 100% ethanol) and transferred to a critical point dryer. Dried samples were mounted onto an aluminum stub and gold sputter-coated, before being viewed with a JEOL JSM 840 SEM. Relative numbers of spore chains were determined by counting chains captured in at least five independent micrographs. All SEM images were saved as TIF graphic files and manipulated in Adobe Photoshop 8.0.

2.4.2 Transmission electron microscopy (TEM)

Peptide samples for TEM were prepared on freshly made continuous carbon grids with a previous glow-discharge treatment of 10 s. Grids were floated on a 5 µl drop of peptide solution (0.5 or 5 mg/ml) for 2 min. Excess sample was blotted and the grids were stained with 2% phosphotungstic acid (PTA) solution (Canemco and Marivac Inc.) for 1 min. The 2% PTA solution was prepared in dH₂O and the final pH of the solution was adjusted with 5 M NaOH to pH 7.0. The stain solution was filtered with an Acrodisc[®] 25 mm syringe filter with a 0.2 µm Supor[®] membrane (Pall) before use. Specimens were imaged at a nominal magnification of 75,000× or 120,000× in a JEOL 1200-EX electron microscope operated at 80 kV. All images were acquired on AMT XR-41 Side-Mount

Cooled 4 megapixel format CCD camera. All TEM images were saved as TIF graphic files and manipulated in Adobe Photoshop 8.0.

Table 2.1: Strains and plasmids used in this work

Name	Description	Reference
<i>Streptomyces coelicolor</i>		
M600	SCP1 ⁻ SCP2 ⁻	(Chakraborty & Bibb, 1997)
J3149A	M600 Δ <i>chpAD</i> Δ <i>chpCH::aadA</i> Δ <i>chpB</i> Δ <i>chpF</i> Δ <i>chpG</i> (7 \times <i>chp</i>)	(Capstick <i>et al.</i> , 2007)
‘Minimal chaplin’ strain	J3149A + <i>chpHC</i> -pSET152	(Di Berardo <i>et al.</i> , 2008)
J3144	M600 Δ <i>chpB::aac(3)IV</i>	(Elliot <i>et al.</i> , 2003)
E206	M600 Δ <i>chpA::aac(3)IV</i> Δ <i>chpB</i> Δ <i>chpC::vph</i>	This work
<i>Escherichia coli</i>		
DH5 α	<i>fhuA2</i> Δ (<i>argF-lacZ</i>)U169 <i>phoA</i> <i>glnV44</i> Φ 80 Δ (<i>lacZ</i>)M15 <i>gyrA96</i> <i>recA1</i> <i>relA1</i> <i>endA1</i> <i>thi-1</i> <i>hsdR17</i>	(Hanahan, 1983)
SE DH5 α	Highly-competent (Subcloning Efficiency TM) DH5 α cells	Invitrogen
ET12567	<i>dam</i> , <i>dcm</i> , <i>hsdS</i> , <i>cat</i> , <i>tet</i> ; carries plasmid pUZ8002	(MacNeil <i>et al.</i> , 1992)
BW25113	Δ <i>araBAD</i> , Δ <i>rhaBAD</i>	(Datsenko & Wanner, 2000)
BT340	DH5 α carrying pCP20	(Cherepanov & Wackernagel, 1995)
XL-1 Blue	<i>ecA1</i> , <i>endA1</i> , <i>gyrA96</i> , <i>thi-1</i> , <i>hsdR17</i> , <i>supE44</i> , <i>relA1</i> , <i>lac</i>	Stratagene
DHM1	F ⁻ , <i>cya-854</i> , <i>recA1</i> , <i>gyrA96</i> (Nal ^r), <i>thi1</i> , <i>hsdR17</i> , <i>spoT1</i> , <i>rfbD1</i> , <i>glnV44(AS)</i>	(Karimova <i>et al.</i> , 2005)
Plasmids		
pUZ8002	<i>tra</i> , <i>neo</i> , RP4	(Paget <i>et al.</i> , 1999)
pCP20	FLP-recombination plasmid: <i>flp</i> , <i>bla</i> , <i>cat</i> , <i>rep101</i> ^{ts}	(Cherepanov & Wackernagel, 1995)
pIJ2925	<i>E. coli</i> cloning vector; pUC18 derivative, <i>bla</i>	(Janssen & Bibb, 1993)
pSET152	Integrative cloning vector; <i>ori</i> pUC18, <i>apr</i> , <i>oriT</i> , RK2, <i>int</i> Φ C31, <i>attP</i> Φ C31	(Bierman <i>et al.</i> , 1992)
pIJ82	Derivative of pSET152 that has a <i>hyg</i> gene instead of <i>aac(3)IV</i>	Gift from H. Kieser
pKT25	Bacterial two-hybrid plasmid; derivative of pSU40; creates	(Karimova <i>et al.</i> , 1998)

	fusions to C-terminus of CyaA T25 fragment; <i>neo</i>	
pKNT25	Bacterial two-hybrid plasmid; derivative of pSU40; creates fusions to N-terminus of CyaA T25 fragment; <i>neo</i>	(Karimova <i>et al.</i> , 1998)
pUT18	Bacterial two-hybrid plasmid; derivative of pUC19; creates fusions to N-terminus of CyaA T18 fragment; <i>bla</i>	(Karimova <i>et al.</i> , 1998)
pUT18C	Bacterial two-hybrid plasmid; derivative of pUC19; creates fusions to N-terminus of CyaA T18 fragment; <i>bla</i>	(Karimova <i>et al.</i> , 1998)
SuperCos-1	<i>bla, neo, cos</i>	Stratagene
pIJ773	<i>aac(3)IV, oriT</i>	(Gust <i>et al.</i> , 2003)
pIJ780	<i>vph, oriT</i>	(Gust <i>et al.</i> , 2003)
pIJ6935	pSET152 + <i>chpHC</i>	(Elliot <i>et al.</i> , 2003)
pIJ6917	pIJ82 + P <i>vanJ</i> + <i>chpE</i>	(Di Berardo <i>et al.</i> , 2008)
pMC146	pIJ82 + P <i>vanJ</i> + <i>chpH</i>	This work
pMC147	pIJ82 + P <i>vanJ</i> + <i>chpH*</i>	This work
pMC102	pIJ2925 + <i>chpH</i>	This work
pMC103	pSET152 + Δ <i>chpH-chpC</i>	This work
pMC104	pSET152 + <i>chpH(I60A)-chpC</i>	This work
pMC105	pSET152 + <i>chpH(S61A)-chpC</i>	This work
pMC106	pSET152 + <i>chpH(S61D)-chpC</i>	This work
pMC107	pSET152 + <i>chpH(V62A)-chpC</i>	This work
pMC108	pSET152 + <i>chpH(I63A)-chpC</i>	This work
pMC109	pSET152 + <i>chpH(G64A)-chpC</i>	This work
pMC110	pSET152 + <i>chpH(L65A)-chpC</i>	This work
pMC111	pSET152 + <i>chpH(L66A)-chpC</i>	This work
pMC112	pSET152 + <i>chpH(V73A)-chpC</i>	This work
pMC113	pSET152 + <i>chpH(VIGLL- AAAAA)-chpC</i>	This work
pMC114	pSET152 + <i>chpH(ΔVIGLL)- chpC</i>	This work
pMC115	pSET152 + <i>chpH(Δ30-35)- chpC</i>	This work
pMC116	pSET152 + <i>chpH(Δ30-41)- chpC</i>	This work
pMC117	pSET152 + <i>chpH(Δ30-51)- chpC</i>	This work
pMC148	pUT18 + <i>chpH</i>	This work
pMC149	pUT18C + <i>chpH</i>	This work

pMC150	pKT25 + <i>rdlA</i>	This work
pMC151	pKNT25 + <i>rdlA</i>	This work
pMC152	pKT25 + <i>rdlB</i>	This work
pMC153	pKNT25 + <i>rdlB</i>	This work

Table 2.2: Oligonucleotides used in this work

Name	Sequence (5' to 3')*	Comments
I52.17c up	CGGAGTGGACGAGCGGGTGC	Cloning of Δ <i>chpH-chpC</i>
I6c end	CGAGTACGGACACTGGGAG	Cloning of Δ <i>chpH-chpC</i>
I60A1	GTCTGCGGCAACACGGCCTCCGTG ATCGGTCT	I60A mutagenesis
I60A2	AGACCGATCACGGAGGCCGTGTTG CCGCAGAC	I60A mutagenesis
S61A1	GCGGCAACACGATCGCCGTGATCG GTCTG	S61A mutagenesis
S61A2	CAGACCGATCACGGCGATCGTGTT GCCGC	S61A mutagenesis
S61D1	CTGCGGCAACACGATCGACGTGAT CGGTCTGCTG	S61D mutagenesis
S61D2	CAGCAGACCGATCACGTCGATCGT GTTGCCGAG	S61D mutagenesis
V62AFwd	AACACGATCTCCGCGATCGGTCTG CTGA	V62A mutagenesis
V62ARvs	TCAGCAGACCGATCGCGGAGATCG TGTT	V62A mutagenesis
I63AFwd	CACGATCTCCGTGGCCGGTCTGCT GAACCC	I63A mutagenesis
I63ARvs	GGGTTTCAGCAGACCGGCCACGGA GATCGTG	I63A mutagenesis
G64AFwd	GATCTCCGTGATCGCTCTGCTGAA CCCCG	G64A mutagenesis
G64ARvs	CGGGGTTTCAGCAGAGCGATCACGG ACATC	G64A mutagenesis
L65A1	GATCTCCGTGATCGGTGCGCTGAA CCCCGCC	L65A mutagenesis
L65A2	GGCGGGGTTTCAGCGCACCGATCAC GGAGATC	L65A mutagenesis
L66A1	CCGTGATCGGTCTGGCGAACCCCG CCTTCG	L66A mutagenesis
L66A2	CGAAGGCGGGGTTTCGCCAGACCG ATCACGG	L66A mutagenesis
V73A1	CCGCCTTCGGCAACGCCTGCATCA ACAAGTG	V73A mutagenesis
V73A2	CACTTGTTGATGCAGGCGTTGCCG AAGGCGG	V73A mutagenesis
VIGLL- AAAAA-1	GGCAACACGATCTCCGCGGCCGC TGCGGCGAACCCCGCCTTCGGCA AC	VIGLL/AAAAA mutagenesis

VIGLL- AAAAA-2	GTTGCCGAAGGCGGGGTT CGCCG CAGCGGCCGCGGAGATCGTGTTG CC	VIGLL/AAAAA mutagenesis
ChpHVIGLL1	GGAGATCGTGTTGCCGCAGA	VIGLL deletion
ChpHVIGLL2	TGCGGCAACACGATCTCCAACCCC GCCTTCGGCAACGT	VIGLL deletion
ChpHdelRev	GGCACCGGAGTCGGCGACGG	ChpH N-terminal deletions
ChpHdelFwd1	GTCGCCGACTCCGGTGCCCTCGCCC GGCGTCCTTTCCGG	aa 30-35 deletion
ChpHdelFwd2	GTCGCCGACTCCGGTGCCGGCAAC GTCGTTCAAGTTCC	aa 30-41 deletion
ChpHdelFwd3	GTCGCCGACTCCGGTGCCCCGGTG AACGTCTGCGGCAA	aa 30-51 deletion
ChpH Up New SCC46 forward	GGATCGCGTTTGCCAACTAGG CGTCATTCAGGCATGACCGCAGAG AAGGGAAAGTTCATGATTCCGGGG ATCCGTCGACC	Cloning <i>chpH</i> <i>chpA</i> knockout
SCC46 reverse	GGACCGGCCGGGGGCGTCGGGGTG GCGGGGGTGGGGTCATGTAGGCTG GAGCTGCTTC	<i>chpA</i> knockout
5H1.35c forward	ACTGCCCGCGACCATGTCTGGAAG GCAGGGAGCCTCATGATTCCGGGG ATCCGTCGACC	<i>chpB</i> knockout
5H1.35c reverse	CCGCCCTGACGGCGCGGGTGCCCC CGGTCGACGCGGTCATGTAGGCTG GAGCTGCTTC	<i>chpB</i> knockout
ChpC Fwd	TACCACGGGACCAGGACAAGGCA GGGATTCAGCAAATGATTCCGGG GATCCGTCGACC	<i>chpC</i> knockout
I52.16c reverse	GGTGCGGAGCCCCTGCGTGTACC GGTGCGCCCCTCATGTAGGCTG GAGCTGCTTC	<i>chpC</i> knockout
SCC46.02c up	GCTGTCCGGCGAACGGCGAGG	Confirming <i>chpA</i> knockout
SCC46.01c down	GGTCAGGGCGGCGATCACG	Confirming <i>chpA</i> knockout
5H1 up	CCGAGGGCCGAGTCTCCAGC	Confirming <i>chpB</i> knockout
5H1 down	GGGAGCTGCACGGTGTTGC	Confirming <i>chpB</i> knockout
SCI52.17c up	CGGAGTGGACGAGCGGGTGC	Confirming <i>chpC</i> knockout
SCI52.16c down	CCGTGTTGCCCGACAGCACGC	Confirming <i>chpC</i>

		knockout
M13 Fwd	CGCCAGGGTTTTCCAGTCACG	Cloning and sequencing
M13 Rev	GCGGATAACAATTTACACAGG	Cloning and sequencing
ChpH2HybF1	<i>GGCGCGCTGCAGGGACTCCGGTGC</i> CCAGGGTGCC	Cloning <i>chpH</i> into pUT18/pUT18C
ChpH2HybRev	<i>GGCGCGGGATCCTCCTTGTTGATG</i> CAGACGTTGCC	Cloning <i>chpH</i> into pUT18/pUT18C
RdlA2HybKTF	<i>GGCGCGCTGCAGGGATCGGGGACG</i> ACAACGGGCCG	Forward primer for cloning <i>rdlA</i> into pKT25
RdlA2HybKNTF	<i>GGCGCGCTGCAGGATCGGGGACGA</i> CAACGGGCCG	Forward primer for cloning <i>rdlA</i> into pKNT25
RdlA2HybRev	<i>GGCGCGGGATCCTCGCGGCCCTCG</i> CCGTTCGCCGA	Reverse primer for cloning <i>rdlA</i> into pKT25/pKNT25
RdlB2HybKTF	<i>GGCGCGCTGCAGGGGCCGCGGCC</i> CGCAGGCGATG	Forward primer for cloning <i>rdlB</i> into pKT25
RdlB2HybKNTF	<i>GGCGCGCTGCAGGGGCCGCGGCC</i> GCAGGCGATG	Forward primer for cloning <i>rdlB</i> into pKNT25
RdlB2HybRev	<i>GGCGCGGGATCCTCGCCCTTGCCG</i> CCCTCGCCGT	Reverse primer for cloning <i>rdlB</i> into pKT25/pKNT25

* Sequences corresponding to aa substitutions are indicated in bold; engineered restriction enzyme sites are underlined; extra nucleotides added to allow for efficient enzyme digestion or to ensure PCR products are in the proper reading frame when cloned into the corresponding target vector are italicized.

CHAPTER 3

Chaplin Amyloidogenesis and Its Role in Aerial Development

Preface

The work detailed in this chapter (excluding Sections 3.2.7 and 3.2.8, and portions of Section 3.2.1) has been published in the *Proceedings of the National Academy of Sciences USA* (Capstick *et al.*, 2011). Most figures used in this chapter are reproduced from the original manuscript, as *PNAS* allows authors to retain copyright of their published work. All TEM images were obtained and formatted with the assistance of Ahmad Jomaa (Ph.D. candidate, Ortega Lab) and Dr. Joaquin Ortega (Department of Biochemistry and Biomedical Sciences, McMaster University). Chan Gao (Ph.D. candidate, Elliot Lab) provided purified Crp (SCO3571) protein for use in the protease-resistance assays. The ChpH(V62A), ChpH(I63A), and ChpH(G64A) mutants were constructed by Christopher Hanke (undergraduate thesis student, Elliot Lab). Kim Findlay (John Innes Centre, Norwich, England) prepared samples for and performed cryo-SEM, and Marcia Reid (Electron Microscopy Facility, McMaster University) prepared samples for low-resolution SEM.

3.1 Introduction

The chaplin family of proteins (ChpA-H) plays a multifunctional role during the developmental program of *S. coelicolor*. At the start of aerial development, the surface-active chaplin proteins help to lower the surface tension at the colony-air interface, allowing aerial hyphae to extend from the colony surface into the air. The chaplins also polymerize on the surfaces of aerial structures, forming a hydrophobic layer that protects these structures from desiccation (Elliot *et al.*, 2003, Claessen *et al.*, 2003). Chaplin fibers are organized into a tight, ‘basket weave’-like matrix, producing a characteristic paired-rod (‘rodlet’) ultrastructure. The organization of chaplin fibers is believed to be mediated through the activity of another class of proteins, the rodlins (RdIA and RdIB) (Claessen *et al.*, 2004, Claessen *et al.*, 2002). Although not required for aerial development, deletion of one or both of the rodlin-encoding genes results in a loss of the rodlet ultrastructure (Claessen *et al.*, 2004). Interestingly, chaplin fibers have characteristics that are shared with amyloid fibers (Claessen *et al.*, 2003, de Jong *et al.*, 2009b), protein aggregates that were once thought to only be associated with human diseases (Chiti & Dobson, 2006). The functional importance of chaplin amyloidogenesis has remained elusive, and biochemical factors that are responsible for this extensive structural transition have not yet been identified.

For many amyloid proteins, there can exist one or more ‘amyloid domains’ within the protein: short stretches of sequence that by themselves are highly amyloidogenic *in vitro*, and together, are believed to be the driving force behind amyloidogenesis *in vivo*

(Esteras-Chopo *et al.*, 2005, Pastor *et al.*, 2007). It is therefore highly probable that, like many amyloids, the chaplins also contain one or more amyloid domains that orchestrate the structural changes required to form amyloid fibers. The presence of such amyloidogenic regions within proteins, however, cannot simply be predicted through examination of the primary protein sequence, as there is no universal ‘amyloid motif’ that is shared by all amyloid proteins. For example, the A β protein and the islet amyloid polypeptide, associated with Alzheimer’s disease and type II diabetes, respectively, have a hydrophobic core that promotes the aggregation of these proteins during amyloidogenesis (Li *et al.*, 1999, Lopes *et al.*, 2007). Other amyloids, such as the Huntington’s protein, contain higher than average glutamine and asparagine residues, often occurring in long repeated sequences; the length of these repeats can enhance the amyloidogenicity of the protein, and also the severity of the associated disease (Li & Li, 1998). Consequently, although amyloid proteins produce fibers that are morphologically similar, the primary sequence determinants that direct their formation can differ significantly from one protein to another. A number of bioinformatic programs have been developed that attempt to predict aggregation-prone/amyloidogenic sequences within proteins (Fernandez-Escamilla *et al.*, 2004, Conchillo-Sole *et al.*, 2007, Garbuzynskiy *et al.*, 2010, Maurer-Stroh *et al.*, 2010, Trovato *et al.*, 2007), but such programs have their limitations, and a comprehensive *in vitro/vivo* examination is always necessary.

In this work, I identify the primary sequence determinants underlying chaplin amyloidogenesis, and provide a direct link between chaplin amyloid fiber formation and chaplin-dependent aerial development. I focused my studies on the short chaplin ChpH, as ChpH, along with ChpE and ChpC, are the only chaplins that are conserved among the streptomycetes. Moreover, a strain that only produces these three chaplins is capable of raising a robust level of aerial hyphae; in this ‘minimal chaplin strain’, ChpH appears to be the primary contributor to aerial hypha formation (Di Berardo *et al.*, 2008). In this work I show that ChpH contains at least two domains, located at the N and C termini, which are highly amyloidogenic *in vitro*. Furthermore, I show that both amyloid domains are important for amyloid fiber formation and stimulating aerial development, however, the C-terminal domain has a greater role in forming and organizing the chaplin surface fibers *in vivo*.

3.2 Results

3.2.1 *In vitro* characterization of ChpH amyloidogenesis

To study ChpH amyloidogenesis *in vitro*, a 49 amino acid (aa) peptide was synthesized that represented the mature ChpH protein (lacking the Sec signal peptide and the first 3 aa) (Figure 3.1). The standard method for following amyloid fiber formation *in vitro* is by using the amyloid-specific fluorescent dye thioflavin T (ThT) (LeVine, 1999), which fluoresces at 490 nm when bound to mature amyloid fibers, after excitation at 450 nm. The ChpH peptide (0.5 mg/ml) was mixed with ThT and fluorescence production was followed over 72 hrs (Figure 3.2A). Generally, when amyloids form fibers *in vitro*, there is an initial delay before mature amyloid fibers are detectable (a ‘lag phase’), which

is believed to correspond to the time required for an initial amyloid ‘nucleus’ to form, and can last for minutes, hours, or even days. Once formed, the amyloid nuclei cause a rapid increase in aggregation, as neighbouring monomers become quickly incorporated into the growing fiber. When fluorescence of the ChpH/ThT mixture was followed during the initial 10 hrs of the experiment, taking readings every 10 min (Figure 3.2A), there was no evidence of an obvious lag phase, as fluorescence increased immediately after shifting the peptide to room temperature. No lag phase was ever observed, even when ChpH concentrations were varied (Figure 3.2A). After 24 hrs, the level of ThT fluorescence plateaued, and remained constant for a further 48 hrs (72 hrs total) (Figure 3.2A). Circular dichroism (CD) spectroscopy showed that the dramatic increase in ThT fluorescence during the first 24 hrs could be correlated with a change in the secondary structure of ChpH, as it transitioned from a relatively unstructured state, to a β -sheet-rich structure after 24 hrs (Figure 3.2B). When viewed with transmission electron microscopy (TEM), amyloid fibers formed by ChpH were very long and had a strong tendency to form large aggregates, with individual fibers twisting and tangling around one another, forming tightly packed fiber clusters (Figure 3.2C-D). The morphology of ChpH amyloid fibers did not appear to change appreciably after the first day, as fiber clusters imaged at 24 hrs appeared similar to those viewed at 120 hrs (Figure 3.3).

One of the hallmarks of the chaplin domain is the presence of two highly conserved cysteine (Cys) residues. *In vivo*, these disulfide bond-forming Cys residues are essential for the ability of ChpH to promote aerial development and form surface rodlet fibers (Di Berardo *et al.*, 2008, Elliot *et al.*, 2003). It is not known, however, whether disulfide bond formation is an essential component of ChpH amyloidogenesis. To this end, we followed ChpH amyloid fiber formation *in vitro* using the ThT fluorescence-based assay as before, but compared the polymerization kinetics of ChpH in the presence and absence of a reducing agent [10 mM dithiothreitol (DTT)]. Under reducing conditions, ChpH polymerization was not impaired, as there was no significant difference between the polymerization kinetics of ChpH in the presence or absence of DTT (Figure 3.2E). This indicates that disulfide bond formation is not necessary for ChpH amyloidogenesis *in vitro*.

In general, amyloid fibers are extremely heat-stable, insoluble protein aggregates, which are only dissociated after treatment with strong solvents, such as trifluoroacetic acid (TFA), hexafluoro-2-isopropanol (HFIP), or DMSO (Hirota-Nakaoka *et al.*, 2003, Jao *et al.*, 1997, Chen & Wetzel, 2001). Another feature of amyloid fibers is their resistance to proteolysis. To test whether ChpH amyloid fibers were affected by protease exposure, two week-old mature ChpH amyloid fibers (0.5 mg/ml) were incubated with Proteinase K (10 μ g/ml) for 30 min. Protease resistance was assessed by analyzing the secondary structure of ChpH using CD spectroscopy, with the assumption that protease degradation of ChpH fibers would cause a loss in detectable secondary structure. After 30 min, ChpH still exhibited a predominantly β -rich structure, although the CD spectra was altered slightly, indicating some loss of structure likely occurred (Figure 3.4). In contrast, the non-amyloid protein SCO3571 (Crp) was unstructured after only 5 min of incubation with Proteinase K (Figure 3.4). Taken together with the above results, it can be concluded that ChpH can form β -sheet-rich, protease-resistant amyloid fibers *in vitro*.

3.2.2 Nucleation-dependence of ChpH polymerization

As the rapid polymerization of ChpH suggested that it may assemble into amyloid fibers through a nucleation-independent pathway, we wanted to further examine whether this was in fact the case. When pre-formed amyloid fibers are added to a solution of a nucleation-dependent amyloid protein (a process known as ‘seeding’), the pre-formed amyloid ‘seeds’ act as nuclei to catalyze amyloid polymerization, which reduces the lag phase, or even eliminates it entirely (Wood *et al.*, 1996, Evans *et al.*, 1995). When two week-old ChpH amyloid seeds were added to fresh ChpH peptide (10% w/w), they could accelerate the aggregation of ChpH, as measured by ThT fluorescence (Figure 3.2F). The results of these seeding experiment provided evidence in favour of ChpH polymerization occurring in a nucleation-dependent manner. The immediate and rapid increase in fluorescence generated when ChpH was mixed with ThT could be explained by the presence of pre-formed aggregates in the preparations of ChpH, present prior to the start of the experiments. Using TEM, we screened multiple samples of ChpH peptide preparations and found that there were routinely small oligomeric aggregates present in the samples of ChpH at the start of the experiments (Figure 3.3). These small aggregates could influence the polymerization of ChpH, acting as amyloid fiber nuclei, and thus negating the requirement for a lag phase. There are two explanations for the presence of these small pre-formed aggregates. First, it is possible that the method for preparing the peptide (solubilizing with 100% TFA) was not completely effective at eliminating pre-formed aggregates (discussed further below). Alternatively, it could be due to the ability of ChpH to aggregate relatively quickly, even when stored (< 5 min) at low temperature (on ice), as was done prior to the start of all kinetic experiments.

3.2.3 The C-terminus of ChpH is amyloidogenic

As ChpH was found to be highly amyloidogenic, it was of interest to explore the sequence determinants that define this process. To begin, the primary aa sequence of ChpH was analyzed using three different bioinformatic software programs that predict aggregation-prone/amyloidogenic sequences within proteins: Tango, FoldAmyloid, and AGGRESCAN (Fernandez-Escamilla *et al.*, 2004, Garbuzynskiy *et al.*, 2010, Conchillo-Sole *et al.*, 2007). Although each program predicted slightly different sequences, all three identified the same 5 aa sequence (SVIGL) within the C-terminus of ChpH as being aggregation-prone/amyloidogenic (Figure 3.1). This region was also predicted to have β -strand secondary structure using the PSIPRED protein prediction server (Bryson *et al.*, 2005). In an effort to determine whether this region of ChpH may represent a potential ‘amyloid domain’, a 9 aa peptide (TISVIGLLN) was synthesized and tested for its ability to form amyloid fibers. When mixed with ThT, the peptide was unable to induce reproducible fluorescence, and no changes in secondary structure were detected using CD spectroscopy, even after 12 days (not shown). It was possible that the neighbouring sequence was important, as the SVIGL sequence is found in a region of ChpH that is structurally constrained by a disulfide bridge (Elliot *et al.*, 2003). For this reason, a

second, larger (16 aa) C-terminal peptide was synthesized (GNTISSVIGLLNPAFGN) that included all sequences flanked by the two Cys residues in ChpH (Figure 3.1). In contrast to the shorter peptide, this larger C-terminal peptide reproducibly bound ThT (Figure 3.5A). Unlike the full-length ChpH peptide, which caused an immediate and rapid increase in ThT fluorescence (Figure 3.2A), the C-terminal peptide exhibited a pronounced lag phase during the initial 24 hrs of incubation (Figure 3.5A). This was followed by a sharp increase in fluorescence, and then an equally sharp drop in fluorescence at approximately 96 hrs. The C-terminal peptide required significantly more time (~96 hrs) to transition from an unstructured state to one rich in β -sheet structure (Figure 3.5B), compared to the full-length ChpH peptide, which only required 24 hrs (Figure 3.2B). Like the full-length ChpH peptide, 2 week-old amyloid seeds of the C-terminal peptide could promote the polymerization of ChpH, although not to the same degree as when ChpH was amended with full-length ChpH seeds (Figure 3.2F). In addition, two week-old amyloid fibers produced by the C-terminal peptide were protease-resistant, maintaining their secondary structure after a 30 min treatment with Proteinase K (Figure 3.4). When viewed with TEM at 72 hrs, the C-terminal fibers were very long and twisted, forming tangles of fibers (although not to the same extent as full-length ChpH) (Figure 3.5C-D). Interestingly, at 96 hrs, the fiber tangles were much less dense than those observed at 72 hrs, and by 120 hrs, the C-terminal fibers were significantly shorter and thicker (Figure 3.3). The dramatic change in fiber association and morphology after 96 hrs may account for the large drop in ThT fluorescence observed during this time (Figure 3.5A). These results show that the C-terminus of ChpH represents an amyloid domain capable of forming amyloid fibers *in vitro*.

3.2.4 *In vitro* characterization of C-terminal ChpH mutants

Since the 16 aa C-terminal region of ChpH was capable of forming amyloid fibers, we wanted to explore whether the SVIGL region contributed to this process, or whether other sequences (not predicted by the bioinformatics software) were important in promoting amyloidogenesis. Two mutant C-terminal peptides were synthesized containing alanine (Ala) substitutions: V62A (GNTISAIGLLNPAFGN) and AAAAA (GNTISAAAAANPAFGN). V62 was selected arbitrarily for mutagenesis, while the 5 \times Ala substitution was made to examine the collective importance of the hydrophobic VIGLL sequence. When mixed with ThT, both mutant peptides failed to produce significant levels of fluorescence after incubating for 5 days (Figure 3.6A), and both remained unstructured, even after 16 days of incubation (Figure 3.6B). At 10 \times the concentration, the V62A mutant did show increased ThT fluorescence after 5 days (~2,000 compared to ~600 units), while the AAAAA mutant exhibited little ThT fluorescence (Figure 3.6A). The ThT fluorescence produced by the V62A mutant peptide at 10 \times the concentration was still very low in comparison to the wild type C-terminal peptide, which produced ~7,000 units of fluorescence after 72 hrs (Figure 3.5A). When imaged with TEM (Figure 3.6C-D), fibers produced by both mutant peptides were less abundant than the wild type C-terminal peptide, and fibers for the AAAAA mutant were only detectable at 10 \times the concentration of the wild type. Moreover, both mutants

produced fibers that were morphologically distinct from those of the wild type C-terminal peptide: the V62A mutant produced very short, needle-like fibers, which did not clump or aggregate, while the AAAAA mutant produced very thin, curved fibers (Figure 3.6C-D). Although fibers were observed for both mutant peptides, the inability to detect significant ThT-fluorescence or secondary structure indicative of amyloids suggests that the fibers may not be true amyloids. Alternatively, the fibers produced by the mutants may be amyloids, but they are present at such a low concentration that they are not detectable by ThT fluorescence or CD spectroscopy. Either scenario provides evidence to conclude that the ability of both mutant peptides to form amyloid fibers is significantly impaired, and that the SVIGL-containing region of ChpH is important for ChpH amyloidogenesis.

3.2.5 ChpH amyloidogenesis is required for promoting aerial development

Morphological development of the minimal chaplin strain is primarily dependent on the activity of ChpH to promote the production of aerial hyphae (Di Berardo *et al.*, 2008). It was therefore of interest to determine, not only the importance of the SVIGL-containing region of ChpH to amyloid fiber formation, but the functional significance of this region to ChpH-mediated aerial development. To this end, single residues within this region were replaced with Ala by site-directed mutagenesis. To ensure that any alterations to ChpH functioning were not due solely to the substitution of residues with Ala, two residues outside of the C-terminal amyloid domain were also mutagenized (I60A and V73A) (Figure 3.1). To assess the *in vivo* effect of each mutation, wild type *chpH* was substituted with each mutant gene (*chpH**), upstream of *chpC* on an integrating plasmid (*chpH* is directly upstream of *chpC* on the *S. coelicolor* chromosome). The mutant plasmids were then introduced into a *S. coelicolor* mutant that produces only ChpE, thereby reconstituting the ‘minimal chaplin strain’ (*chpEH*C*). Since ChpH is essential for aerial hyphae formation by the minimal chaplin strain (Di Berardo *et al.*, 2008), mutants expressing functionally-compromised *chpH** can be readily identified by their reduced ability to raise aerial hyphae. After screening the mutants for developmental defects, the I60A and V73A mutations appeared to have little or no impact on aerial development after 5 days, and these mutants looked very similar to a strain expressing wild type *chpH* (Figure 3.7). This suggests that altering the overall hydrophobicity of ChpH is not sufficient to disrupt its functioning. In contrast, the S61A, V62A, I63A, G64A, L65A, and L66A mutants produced less white colouration on their surface, indicating reduced relative aerial hypha abundance (Figure 3.7). Each of these mutations occurs within, or immediately adjacent to, the SVIGL-containing amyloid domain, thus emphasizing the functional importance of this region of ChpH.

As single Ala substitutions within the putative amyloid domain had a significant impact on aerial development, the collective importance of this region was explored by completely deleting the hydrophobic VIGLL sequence (Figure 3.1), and observing what impact this deletion had on aerial development. The ChpH(Δ VIGLL) mutation caused, by far, the most severe developmental defect, resulting in a phenotype very similar to that of a strain completely lacking *chpH* (Δ *chpH*) after 5 days (Figure 3.7). It is possible that the deletion of five residues from between the two Cys residues that form a disulfide bridge

may have significantly altered the structure of ChpH. To address this possibility, the VIGLL sequence was instead replaced with five Ala residues, which ensured that the overall aa spacing in this region was maintained. The ChpH(VIGLL-AAAAA) mutant had a less severe developmental phenotype than the ChpH(Δ VIGLL) mutant after 5 days, and more closely resembled the single Ala mutants (Figure 3.7). However, when imaged with scanning electron microscopy (SEM) after 12 days, the ChpH(VIGLL-AAAAA) mutant produced very few spore chains, similar to what was observed for the Δ *chpH* mutant, while a single Ala mutant (V62A) produced abundant spore chains to almost the same level as the wild type (Figure 3.8). Comparison of the ChpH(Δ VIGLL) and ChpH(VIGLL-AAAAA) mutants revealed that the spacing of residues bridged by the disulfide bond is critical for ChpH activity; however, the specific biochemical characteristics of the residues within the VIGLL region are also of functional importance.

As it was possible that the developmental defects of the *chpH** mutants may have been due to reduced stability or improper ChpH* surface localization, chaplin extracts were obtained from those ChpH* mutants that exhibited a significant impairment in aerial development (V62A, VIGLL-AAAAA, Δ VIGLL) and these extracts were analyzed by MALDI-ToF mass spectrometry (Figure 3.9). For all strains tested, the mutant ChpH* proteins were effectively surface-localized and were found in relatively normal abundance, as compared to ChpE levels in each sample. This indicated that the observed phenotypes were due to ChpH* dysfunction, and not the result of impaired ChpH* secretion or stability.

In addition to mediating aerial development, ChpH also has an important role in assembling the rodlet ultrastructure on the surface of aerial hyphae and spores (Di Berardo *et al.*, 2008). Two of the ChpH* mutants, which exhibited impaired development, despite being cell surface-localized (V62A and VIGLL-AAAAA), were visualized with high-resolution SEM to determine whether either mutation altered surface fiber production/organization (Figure 3.10). As expected, the strain expressing wild type *chpH* produced abundant surface fibers, while the strain lacking *chpH* produced very few. Most notable was the effect that the VIGLL-AAAAA mutation had, as the surface fibers produced by this strain were sparse and disorganized. In contrast, the single V62A mutant had a surface ultrastructure similar to that of the wild type ChpH-expressing strain, revealing that single residues within the VIGLL region were not essential for surface rodlet production, but collectively, the VIGLL sequence was required for this activity of ChpH.

3.2.6 The ChpH N-terminus is amyloidogenic and important for aerial development

As the C-terminus of ChpH was determined to be important for both amyloidogenesis and aerial development, it was of interest to explore the functional importance of the N-terminal region. The *in silico* predictions unanimously identified the C-terminus as being important for aggregation/amyloidogenesis, however, one bioinformatic program [AGGRESCAN (Conchillo-Sole *et al.*, 2007)] also identified a second 10 aa-stretch (GVLSGNVQV) within the N-terminus of ChpH as having aggregative potential (Figure 3.1). Notably, this region was also predicted (by PSIPRED)

to adopt a β -strand secondary structure (Bryson *et al.*, 2005). To investigate the amyloidogenic potential of this region, a 17 aa peptide was synthesized, which included the predicted aggregative sequence (**GVLSGNVVQVPVHVPVN**). This specific peptide sequence was chosen due to its similar size relative to the 16 aa C-terminal peptide, in addition to having glycine and asparagine residues at its N- and C-termini, respectively, as is found in the C-terminal peptide. The N-terminal peptide reproducibly bound ThT, but the fluorescence profile was distinct from the other peptides, exhibiting a pronounced plateau from 24 to 48 hrs, before increasing again during the following 48 hrs (Figure 3.11A). Impressively, by 96 hrs the N-terminal peptide exhibited ThT fluorescence at levels that were similar to that of the full-length ChpH protein (~14,000 and ~17,000 units, respectively), and were twice that of the C-terminal peptide (~7,000 units). Moreover, 2 week-old amyloid seeds of the N-terminal peptide were very potent at stimulating ChpH aggregation, causing levels of ThT fluorescence that were even higher than the levels of ThT fluorescence generated by ChpH seeded with fibers of the full-length ChpH peptide (Figure 3.2F). Like the C-terminal peptide, the N-terminal peptide transitioned slower than the full-length ChpH peptide into a conformation rich in β -sheet structure, requiring ~120 hrs (Figure 3.11B) compared to 24 hrs for ChpH (Figure 3.2B). When viewed with TEM, N-terminal fibers were morphologically distinct from those produced by both the full-length and C-terminal peptides, appearing very long and straight, and forming fiber bundles primarily through lateral fiber-fiber associations (Figures 3.3 and 3.11C). Like the full-length ChpH and C-terminal peptides, the fibers produced by the N-terminal peptide were resistant to protease treatment (Figure 3.4). Thus, in addition to the C-terminus, the N-terminus of ChpH contains a second amyloidogenic region.

To probe the functional importance of the ChpH N-terminus *in vivo*, three deletions of varying sizes were generated (Figure 3.1), and their effect on ChpH activity was assessed by introducing them into the minimal chaplin strain in place of wild type *chpH*. The smallest 6 aa N-terminal deletion (Δ ChpH₃₀₋₃₅) removed sequence predicted to adopt β structure, but left the predicted aggregation-prone sequence (GVLSGNVVQV) intact. The 12 aa deletion (Δ ChpH₃₀₋₄₁) included the first predicted β strand and also removed the first four aa of the GVLSGNVVQV sequence. Finally, the largest 22 aa deletion (Δ ChpH₃₀₋₅₁) removed both N-terminal sequences predicted to have β structure, and included the entire predicted aggregation-prone region. The smallest, 6 aa deletion had little or no impact on aerial development (Figure 3.7). In contrast, the larger 12 and 22 aa deletions caused a noticeable reduction in aerial hypha abundance (Figure 3.7). The 12 aa ChpH deletion caused a developmental phenotype similar to that of the single C-terminal Ala mutants. Most notable was the developmental phenotype of the largest 22 aa deletion, which had a phenotype comparable to that of the ChpH(Δ VIGLL) and Δ *chpH* mutants, producing relatively sparse amounts of aerial hypha (Figure 3.7) and failed to form abundant spore chains (5-10-fold less than the wild type minimal chaplin strain) (Figure 3.8). When analyzed by MALDI-ToF mass spectrometry, the Δ ChpH₃₀₋₅₁ protein localized to the cell surface (Figure 3.9), indicating that secretion and stability of the mutant protein was not impaired. When the surface of the Δ ChpH₃₀₋₅₁-expressing strain was analyzed by high-resolution SEM, surface fiber formation and organization was

largely unaffected, and most closely resembled that of the V62A- and wild type ChpH-expressing strains (Figure 3.10). This was in contrast to the C-terminal VIGLL-AAAAA mutant, which, although it exhibited a developmental phenotype similar to that of the N-terminal Δ ChpH₃₀₋₅₁ mutant, was significantly impaired in its ability to form organized surface rodlet fibers (Figure 3.10). Collectively, these results show that the amyloidogenic N-terminus of ChpH is important for promoting aerial development, but is dispensable for the production and organization of rodlet fibers on the surfaces of aerial hyphae and spores.

3.2.7 ChpH mutations do not cause a dominant-negative phenotype

A selection of *chpH**-*chpC* mutant plasmids (L65A, V73A, Δ VIGLL, Δ ChpH₃₀₋₅₁) were introduced into wild type *S. coelicolor* (M600) encoding all eight chaplins (ChpA-H), to determine whether any of the ChpH mutants were capable of inhibiting aerial morphogenesis. The developmental phenotype of each ChpH*-containing strain was assessed by monitoring plate-grown cultures and by visualizing aerial hyphae and spore morphology using light microscopy. None of the mutants altered the developmental phenotype of the wild type (not shown), indicating that the ChpH mutants do not exhibit a dominant-negative effect on aerial morphogenesis.

3.2.8 Interactions between ChpH and the rodlin proteins

When the short chaplins polymerize on the surface of aerial structures, they produce an intricate matrix of paired rod-shaped fibers, known as ‘rodlets’ (Claessen *et al.*, 2004). In the minimal chaplin strain, ChpH is the primary polymerizing unit of surface rodlet fibers (Di Berardo *et al.*, 2008). The formation of the rodlet ultrastructure depends on two other proteins, known as the rodlins (RdlA and RdlB) (Claessen *et al.*, 2002). RdlA and RdlB are not redundant in their function, and deletion of either rodlin-encoding gene causes the rodlet ultrastructure to be absent from the surface of aerial structures (Claessen *et al.*, 2002). It has been proposed that the function of the rodlin proteins is to organize the individual chaplin fibers into rodlets (Claessen *et al.*, 2004). Since the ChpH(VIGLL-AAAAA) mutant failed to produce a robust surface rodlet ultrastructure (Figure 3.10), it may be that the C-terminus of ChpH is important for rodlin-mediated chaplin fiber organization. Although it is possible that either of the rodlins may directly interact with chaplin fibers to influence their organization, such an interaction has never been shown experimentally. Thus, before we could investigate whether the C-terminus of ChpH is important for its interaction with the rodlins, we first had to establish whether the rodlins directly interact with ChpH.

To determine whether ChpH directly interacts with RdlA and RdlB, a bacterial two-hybrid approach was taken (Karimova *et al.*, 1998), cloning each rodlin gene (*rdlA* and *rdlB*) into T25 plasmids and wild type *chpH* into T18 plasmids, to generate N-/C-terminal fusions to each domain of adenylate cyclase. If RdlA/B and ChpH interact, the T25 and T18 subunits will be brought in close enough proximity to enable cAMP synthesis, which is required to activate *lacZ* expression. When cells are plated on X-Gal-

containing media, a direct interaction between the two fusion proteins results in a blue colony phenotype. When *E. coli* DHM1 cells (*cya*⁻) were transformed with combinations of *rdlA/B*- and *chpH*-containing plasmids, none produced a result indicative of a direct ChpH-RldA/RdlB interaction, as all colonies appeared white. In contrast, DHM1 colonies containing the positive control plasmids, which express T25/T18 fusions to the dimer-forming leucine zipper region of the yeast GCN4 protein (Karimova *et al.*, 1998), appeared blue. These results suggest that ChpH and RdlA/B do not directly interact; however, there are several reasons that could explain why a direct interaction was not detected using this assay, which are discussed below.

3.3 Discussion

The chaplins are functional amyloid proteins that are essential for the aerial development of *S. coelicolor* (Elliot *et al.*, 2003, Claessen *et al.*, 2003, Capstick *et al.*, 2007). How the chaplins form amyloid fibers and whether chaplin amyloidogenesis is important for promoting aerial development has never been investigated. The work presented here provides the first functional link between chaplin amyloidogenesis and aerial development, and shows that ChpH amyloid fiber formation depends on two amyloid domains that are disparate in their functional contributions to ChpH activity.

The multi-amyloid domain architecture of ChpH is not unique among functional amyloids. The *E. coli* CsgA curli protein, for example, contains five imperfect repeat units, three of which are amyloidogenic *in vitro* (Wang *et al.*, 2007b), and two of which are essential for CsgA amyloid fiber formation *in vivo* (Wang *et al.*, 2008). Curli are important for biofilm formation and *E. coli* pathogenesis, as curli promote *E. coli*-host cell attachment during the infection process (Barnhart & Chapman, 2006). It is not clear, however, what functional contribution each domain of CsgA makes towards these cellular activities. In ChpH, both amyloid domains are necessary for promoting aerial development, but the C-terminal domain has a greater functional role in promoting surface rodlet formation. The functional disparity between the two domains is also evident in the distinct morphologies of fibers produced by each domain, in addition to the higher-order interactions between fibers. Both amyloid domains of ChpH produce amyloid fibers that are morphologically distinct from those of the full-length ChpH peptide, indicating that both domains contribute to the wild type morphology.

When followed *in vitro*, the full-length ChpH peptide polymerized relatively quickly, without exhibiting a detectable lag phase. Amyloid assembly is typically characterized by a delay ('lag') in mature amyloid fiber detection. This lag phase is thought to represent the period of time required for monomeric protein species to begin aggregating, eventually forming an amyloid 'nucleus'. Once a nucleus has formed, it then catalyzes the rapid polymerization of other neighbouring monomeric/oligomeric species, leading to the formation of a mature amyloid fiber. Despite polymerizing with seemingly nucleation-independent kinetics, ChpH did respond to the addition of pre-formed ChpH fibers (full-length, N-terminal or C-terminal peptides), which enhanced ChpH polymerization. When samples of ChpH were observed with TEM at the start of polymerization experiments (Time = 0 min), small oligomeric species were routinely

observed. It is possible that these small aggregates influence the rate of ChpH polymerization by nucleating ChpH polymerization, negating the requirement for a lag phase, and causing rapid ChpH polymerization. In the literature, there are numerous techniques cited for eliminating pre-formed aggregates from amyloid peptide preparations (Stine *et al.*, 2003, Hirota-Nakaoka *et al.*, 2003, Jao *et al.*, 1997), including: filtering and/or ultra-centrifugation to remove pre-formed aggregates, sonication to break-up aggregates, and/or the use of dilute solvents to slow peptide aggregation (e.g. dimethyl sulfoxide, hexafluoro-2-propanol, trifluoroacetic acid). In practice, I found that none of these methods were able to completely remove pre-formed ChpH aggregates from peptide preparations.

In contrast to full-length ChpH, peptides representing the N- and C-termini of ChpH polymerized with very different kinetics. Aggregation of the N-terminal peptide progressed through two distinct stages, plateauing after 24 hrs, before increasing again after 48 hrs. Unlike the full-length ChpH peptide, which produced very dense clusters of twisted fibers, the N-terminus produced fibers that were much straighter and formed bundles through lateral fiber associations. The C-terminal peptide behaved differently still. After a more gradual increase in ThT fluorescence, in comparison to full-length ChpH, which included a lag phase during the first 24 hrs, this peptide exhibited a large drop in ThT fluorescence after 96 hrs of incubation. When imaged with TEM after 72 hrs, C-terminal amyloid fibers produced were very long and twisted, and formed large tangles of fibers, although not to the extent of full-length ChpH. However, at 96 hrs, these fibers were significantly shorter and thicker and no longer formed the large fiber clusters observed 24 hrs earlier. This dramatic change, both in fiber morphology and organization, likely accounted for the drop in ThT fluorescence measured for the C-terminal peptide at this time, as there would be a significant reduction in amyloid fibers that would be exposed and available for interaction with the ThT dye. Both N- and C-terminal peptides polymerized much slower than the full-length ChpH peptide, which suggests that, *in vivo*, the two domains may act synergistically to catalyze the rapid amyloidogenesis of ChpH. This would be of particular importance in the context of amyloid toxicity. There is evidence to suggest that soluble oligomeric species produced during the intermediate stages of amyloidogenesis have the potential to be highly cytotoxic (Lashuel & Lansbury, 2006, Chiti & Dobson, 2006). By accelerating ChpH amyloidogenesis, this could minimize the generation or accumulation of potentially toxic intermediate species, and these oligomers would instead be incorporated into growing ChpH fibers.

Rodlet fibers, which decorate the surfaces of aerial hyphae and spores, are believed to comprise polymers of short chaplins (Claessen *et al.*, 2004). Although all five short chaplins are amyloidogenic *in vitro* (Sawyer *et al.*, 2011), it is not known how each contribute to these structures *in vivo*, and whether rodlet fibers comprise homo- or heteropolymers of short chaplins. When the TANGO-predicted aggregation propensities of the mature short chaplins (lacking N-terminal signal peptides) are compared (Fernandez-Escamilla *et al.*, 2004), ChpH, ChpE, and ChpD have the highest prediction scores (289, 224, and 147, respectively), while ChpF and ChpG have comparably very low scores (both 29), which may suggest that the short chaplins differ in their polymerization kinetics. Thus, the short chaplins may not contribute equally to the

formation of chaplin surface fibers. In addition, the short chaplins also distinguish themselves by their calculated isoelectric points. At pH 7, ChpD, ChpF, and ChpG are negatively charged (-3, -4.5, and -6, respectively), while ChpH and ChpE are positively charged (+0.5 and +1.0, respectively), which would promote electrostatic interactions between the two groups (Sawyer *et al.*, 2011). This, combined with the fact the *chp* genes are differentially expressed (*chpE* and *chpH* are expressed throughout development, while *chpD*, *chpF*, and *chpG* are expressed during aerial hyphae formation and sporulation) (Elliot *et al.*, 2003), suggests that the short chaplins may have distinct roles during *Streptomyces* development.

ChpH, like the other chaplins, is very hydrophobic, and it is this characteristic that likely helps promote its aggregation during amyloidogenesis. In particular, the C-terminus of ChpH is exceptionally hydrophobic (Figure 3.12), with the region flanked by the conserved Cys residues ranking significantly higher on a hydropathy scale (a measure of hydrophobicity) than the N-terminus of ChpH. Hydrophobicity alone, however, is not the only factor controlling ChpH amyloid fiber formation. Single Ala substitutions in this region of ChpH, which did not substantially alter the overall hydrophobicity of ChpH (Table 3.1), caused dramatic perturbations to ChpH amyloid fiber assembly and its capacity to stimulate aerial hyphae production. Impressively, single Ala substitutions in the C-terminal 'SVIGLL' region of ChpH caused a developmental phenotype that was as severe (or worse) than deleting 5 or 12 aa from the N-terminus of ChpH, highlighting the functional importance of the C-terminus. Most of the residues of functional importance were very hydrophobic (V62, I63, L65, L66), with the exception of S61 and G64. Interestingly, ChpH is the only chaplin to have serine at position 61; all other chaplins have an asparagine (ChpD, ChpE) or aspartic acid (ChpF, ChpG) residue at this position (see Figure 1.2B). This serine residue is also highly conserved among ChpH orthologs from other streptomycetes (Broad Institute actinomycete genomic database). A ChpH S61D mutant was generated and was found to have a developmental phenotype similar to that of the S61A mutant (Figure 3.13), showing that the conservation of serine at this position is important for ChpH activity. Aside from S61, the remaining residues (VIGLL) are highly conserved among the other short chaplins, with the exception of conservative isoleucine/leucine to valine substitutions in ChpD (VVGLL) and ChpE (VIGVL). Within the N-terminal portion of the chaplin domain there is also significant homology shared by the chaplins, although ChpE has three non-conservative substitutions, with alanine replacing leucine or valine at these positions.

The absence of abundant and well-organized rodlet fibers on the surface of the C-terminal VIGLL-AAAAA mutant suggested the C-terminus of ChpH may be important for coordinating ChpH surface fiber assembly. In addition to the chaplins, the formation of the rodlet ultrastructure also depends on the rodlin proteins (Claessen *et al.*, 2004, Claessen *et al.*, 2002). It has been suggested that the rodlins (RldA and RldB) are involved in organizing individual chaplin fibers into rodlets (Claessen *et al.*, 2004). However, this model has never been proven experimentally, and a direct interaction between RldA/RldB and the chaplins has never been demonstrated. Thus, as a first step to investigate the importance of the C-terminus of ChpH to rodlet assembly, it was necessary to establish whether wild type ChpH and either RldA or RldB directly interact.

Using a bacterial two-hybrid system (Karimova *et al.*, 1998), a positive, direct interaction could not be detected between wild type ChpH and RdlA/RdlB. It is possible that ChpH does not directly interact with the rodmins, and interaction with an additional protein(s) may be required for rodlet assembly. Alternatively, the lack of a positive interaction between ChpH and the rodmins may be due to limitations of the bacterial two-hybrid system. First, the production of ChpH in the reduced cytoplasmic environment of *E. coli* would mean that ChpH would not be oxidized to form disulfide bonds, a post-translational modification that may be important for its association with the rodmins. Secondly, the reporter tags fused to ChpH and the rodmin proteins may negatively affect the function of ChpH and/or RdlA/B, possibly by preventing proper protein folding. Finally, owing to its hydrophobicity, ChpH may aggregate into insoluble inclusion bodies once expressed in the *E. coli* cytoplasm, resulting in ChpH being inaccessible to RdlA/B. For these reasons, it is therefore not possible to conclude unequivocally that ChpH and RdlA/B do not interact directly *in vivo*. Further experimental evidence is needed in order to understand the details of the functional relationship between the chaplins and rodmins.

3.4 Figures and tables

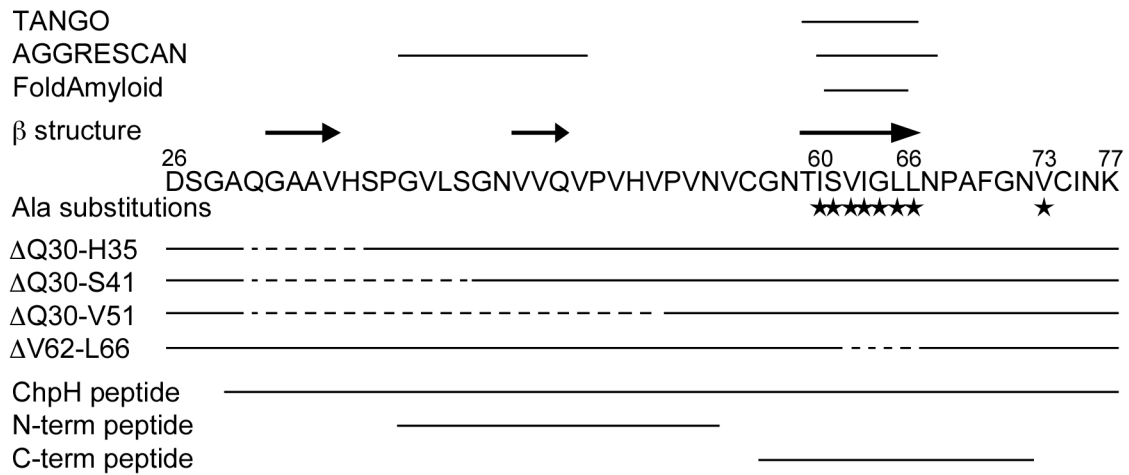


Figure 3.1: Sequence of the mature ChpH protein. (Top to bottom) Amyloidogenic- or aggregation-prone regions (marked by solid lines) predicted by the indicated software programs. Sequences predicted to adopt β secondary structure (arrows). Mutagenesis of ChpH: Ala substitutions (stars) and deletions (dashed lines). Synthetic peptides used to analyze the N- and C-terminal amyloid domains (solid lines).

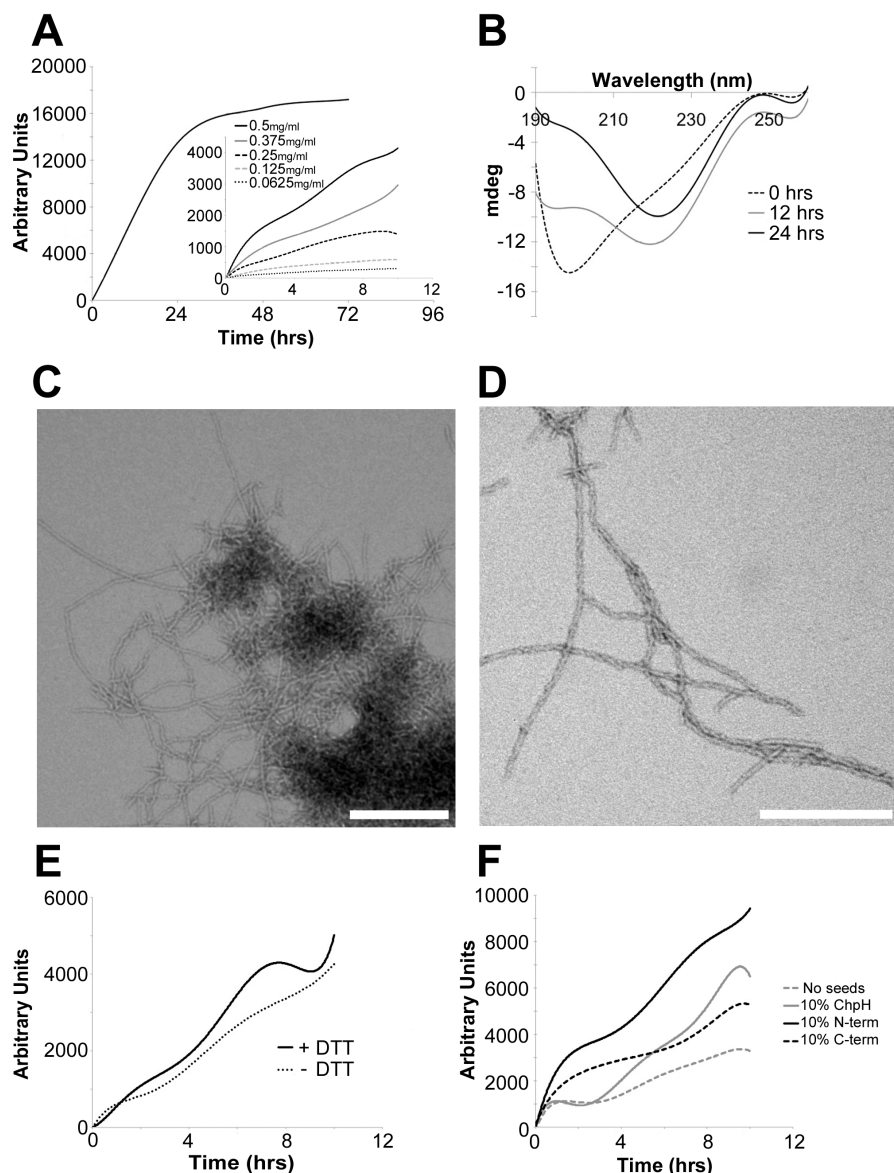
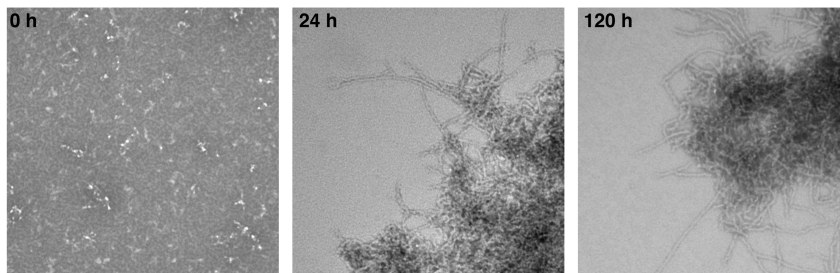
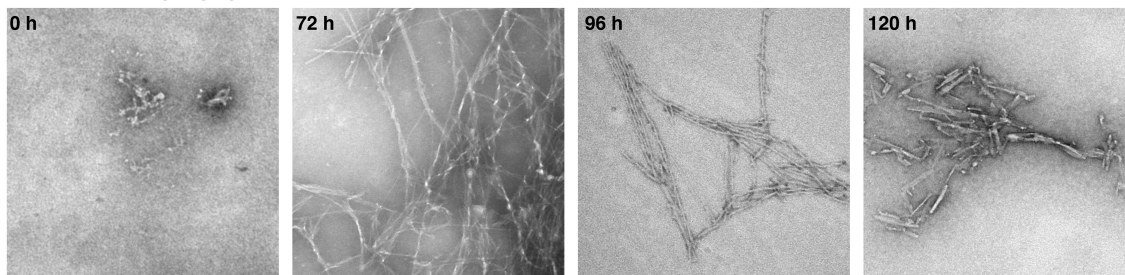


Figure 3.2: *In vitro* polymerization of the full-length ChpH peptide. (A) ThT fluorescence induced by ChpH (0.5 mg/ml) over 72 hrs (readings taken at 24 hr intervals). Fluorescence levels varied between replicates, but the overall trend was reproducible. Inset: ThT fluorescence of ChpH at different concentrations (readings taken every 10 min for 10 hr). (B) CD analysis of ChpH (diluted from 0.5 to 0.25 mg/ml) before incubation and after incubating for 12 and 24 hrs. (C-D) Negatively stained electron micrographs of a ChpH peptide solution (0.5 mg/ml) incubated at room temperature for 120 hrs. (Scale bar, 250 nm). (E) ThT fluorescence induced by ChpH (0.5 mg/ml) over 10 hrs in the presence and absence of 10 mM DTT (readings taken every 1 hr). (F) ThT fluorescence of ChpH (0.5 mg/ml) alone, or in the presence of 10% (w/w) sonicated ChpH, C-terminal or N-terminal fibers, over 10 hrs (readings taken every 10 min).

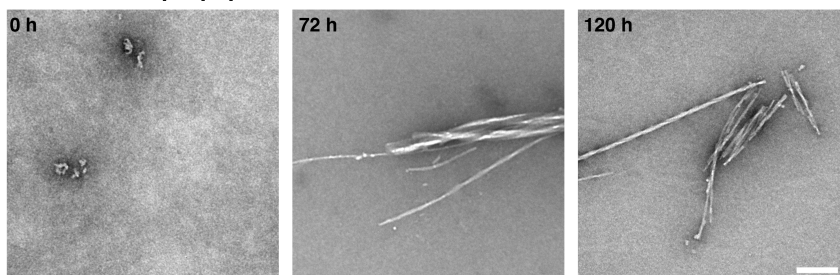
Full-length ChpH peptide



C-terminal ChpH peptide



N-terminal ChpH peptide



100 nm

Figure 3.3: Time course of negatively stained electron micrographs of the full-length ChpH peptide (top row), C-terminal ChpH peptide (center row) and N-terminal peptide (bottom row). Images of peptides (0.5 mg/ml) were captured following incubation at room temperature for the times indicated.

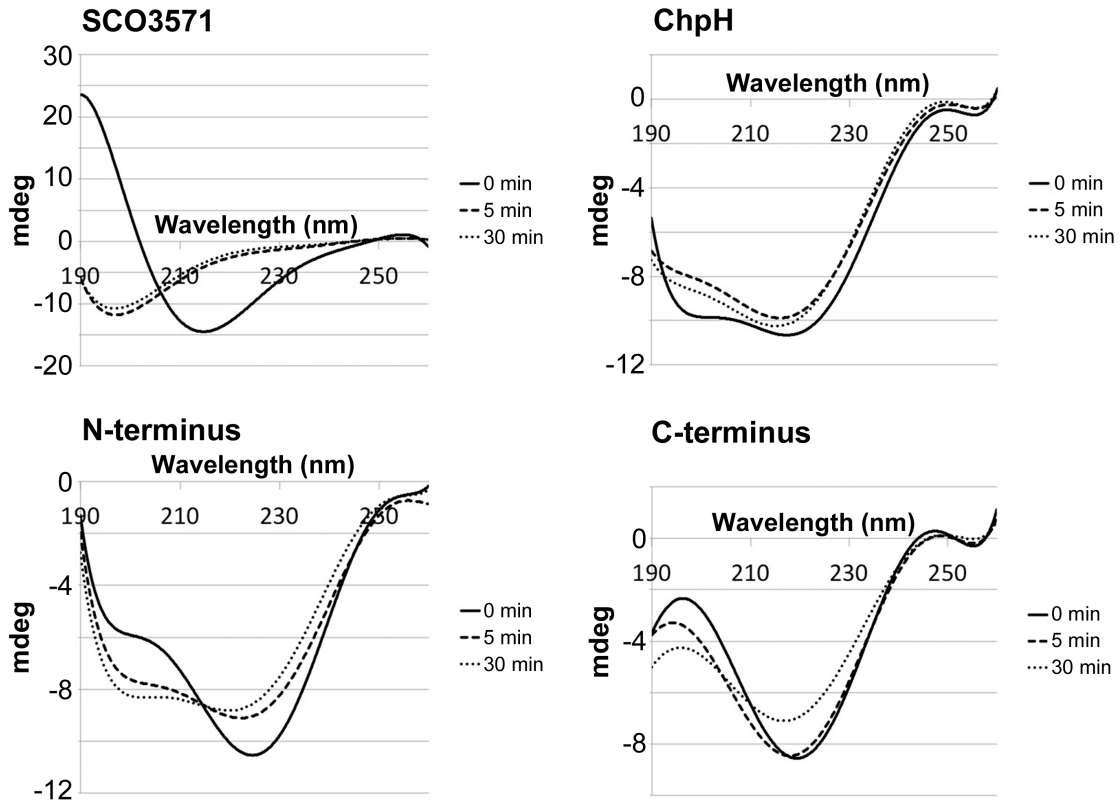


Figure 3.4: Proteinase K (10 $\mu\text{g/ml}$) was added to 0.5 mg/ml preparations of: SCO3571 (a non-amyloid transcription factor from *Streptomyces coelicolor*) (top left) or two week old fibers of ChpH (top right), N-terminal ChpH (bottom left) and C-terminal ChpH (bottom right). Within 5 min of protease treatment, SCO3571 was completely unstructured (as indicated by the pronounced minimum at 200 nm), while the ChpH-derived fibers all retained structure (specifically, β -rich structure), even after 30 min of protease exposure.

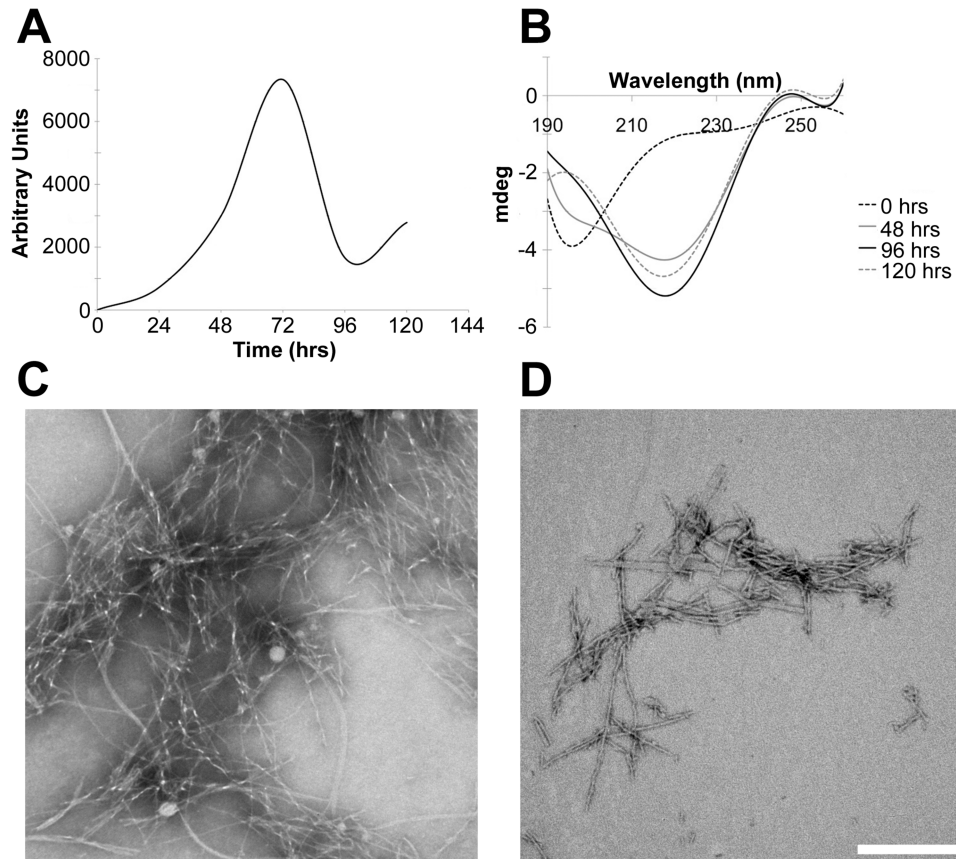


Figure 3.5: *In vitro* polymerization of the C-terminal ChpH peptide (GNTISVIGLLNPAFGN). (A) ThT fluorescence of the peptide (0.5 mg/ml) over 120 hrs (24 hr intervals). Fluorescence levels varied between replicates, but the overall trend was reproducible. (B) CD analysis of the peptide (diluted from 0.5 to 0.25 mg/ml) from 0 to 120 hrs. (C–D) Negatively stained electron micrographs of the peptide (0.5 mg/ml) incubated at room temperature for (C) 72 hrs or (D) 96 hrs. (Scale bar, 250 nm).

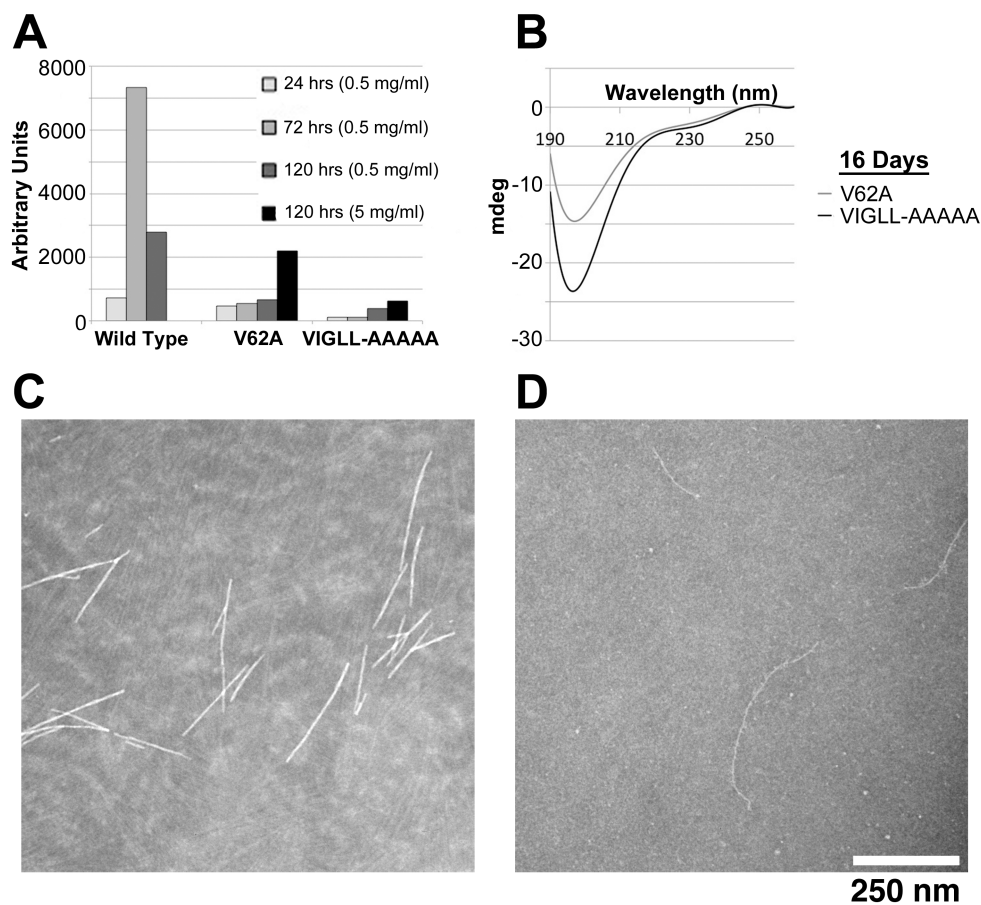


Figure 3.6: Analysis of the C-terminal ChpH V62A (GNTISAIGLLNPAFGN) and VIGLL-AAAAA (GNTISAAAAANPAFGN) mutant peptides *in vitro*. (A) ThT fluorescence of the two mutant peptides (incubated at 0.5 mg/ml or 5 mg/ml) compared to the wild type C-terminal peptide (0.5 mg/ml) after 24, 72 and 120 hrs. Mutant peptides incubated at 5 mg/ml were diluted to 0.5 mg/ml with buffer before measurements were taken. (B) Secondary structure analysis of the mutant peptides (0.5 mg/ml) using CD spectroscopy after 16 days. Peptides were diluted to 0.25 mg/ml for CD measurements. (C) and (D) Negative stained electron micrographs of (C) V62A and (D) VIGLL-AAAAA mutant C-terminal ChpH peptides (5 mg/ml) collected after 5 days of incubation at room temperature. (Scale bar, 250 nm).

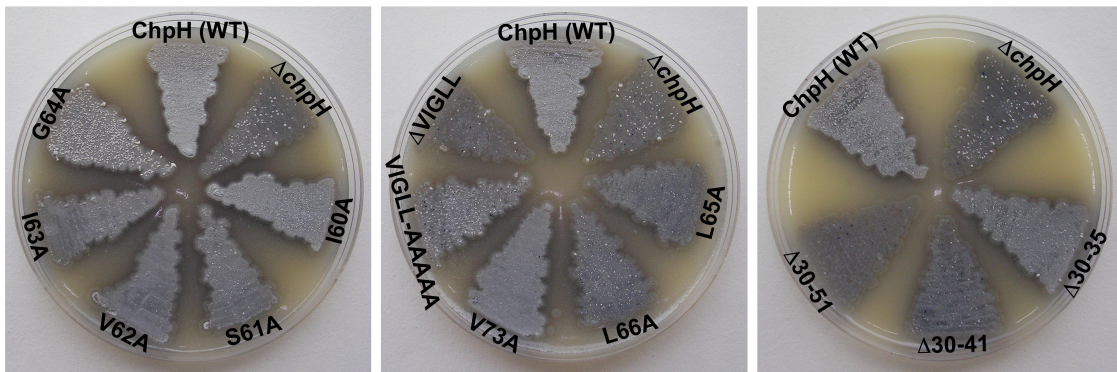


Figure 3.7: 120 hr cultures grown on MS medium, expressing wild type (WT) ChpH, lacking ChpH ($\Delta chpH$), and expressing mutant ChpH proteins bearing amino acid substitutions or deletions.

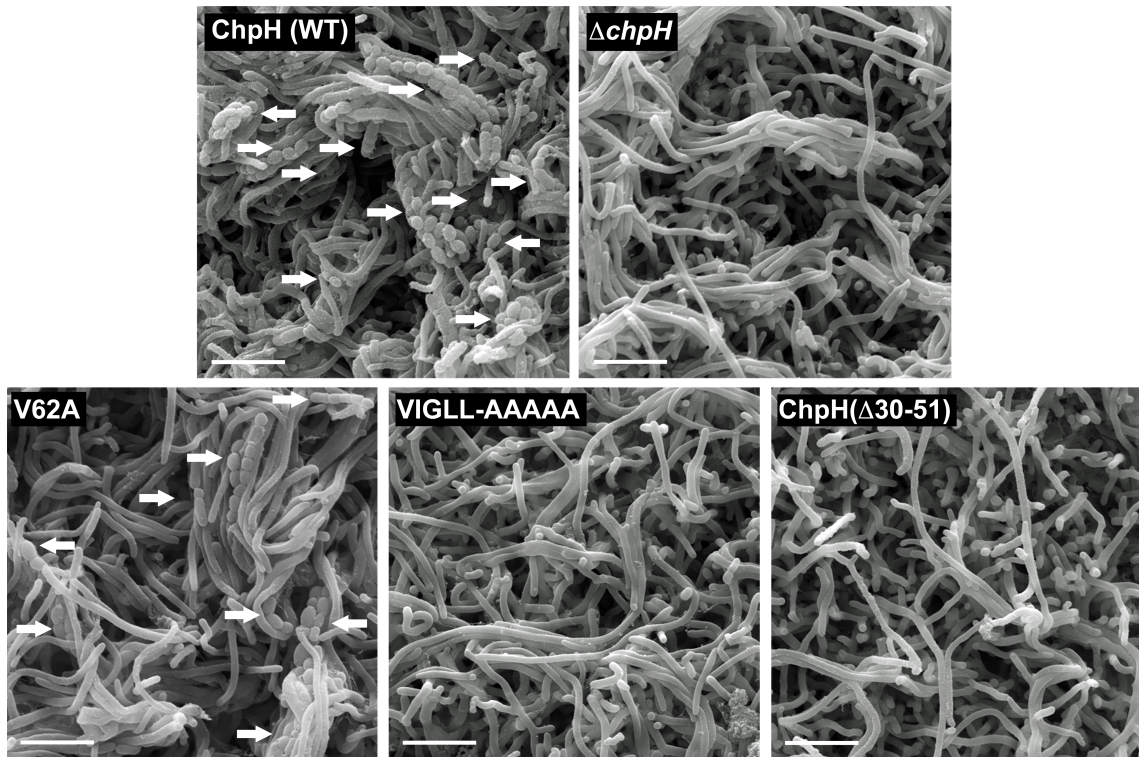


Figure 3.8: The phenotypic effect of ChpH mutations on aerial development, compared to a strain producing wild type ChpH (WT) and a strain completely lacking ChpH ($\Delta chpH$) after growth for 12 days on MS medium. Spore chains are indicated with arrows. (Scale bars, 5 μ m).

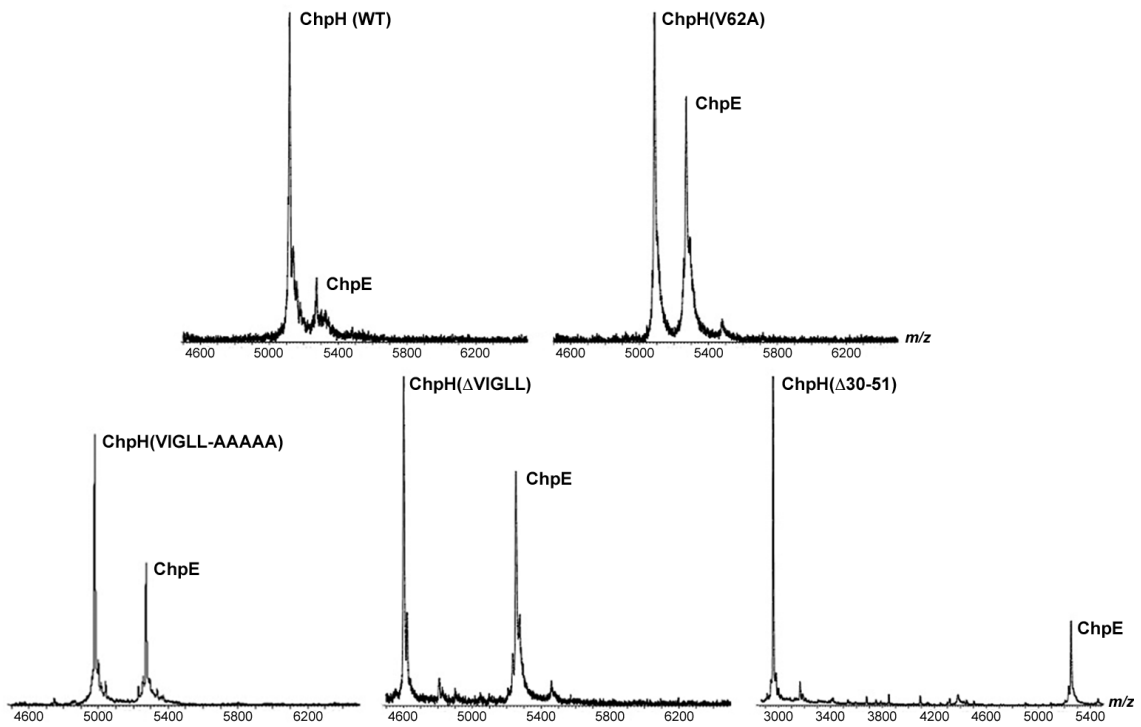


Figure 3.9: MALDI-ToF mass spectrometry of cell wall extracts from a selection of ChpH mutants and a strain producing wild type ChpH (WT) grown for 7 days on MS medium. Peaks corresponding to ChpH and ChpE are labeled. The x-axis represents the mass (m)/charge (z) ratio, where $z = 1$. Note that relative ChpH and ChpE levels vary between different preparations; the one consistent observation is that ChpH levels are always greater than ChpE levels in wild type strains when detected using MALDI-ToF mass spectrometry.

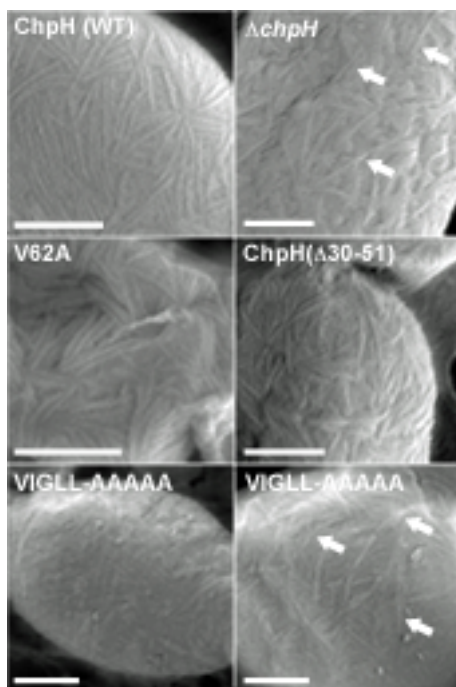


Figure 3.10: SEM micrographs focused on the surface ultrastructure of a strain producing wild type (WT) ChpH, lacking ChpH ($\Delta chpH$), and three strains expressing different mutant ChpH proteins. (Scale bars, 200 nm). For strains showing little ultrastructure, arrows point to occasional fibers on the aerial surfaces.

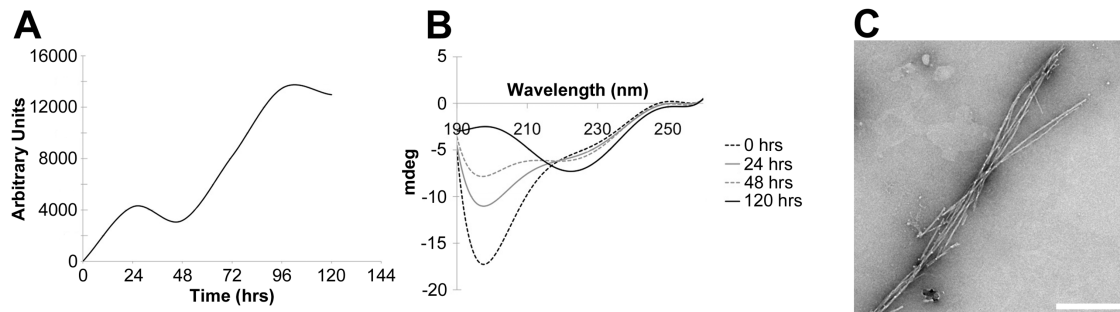


Figure 3.11: *In vitro* polymerization of the N-terminal ChpH peptide (GVLSGNVVQVPVHVPVN). (A) ThT fluorescence of the peptide (0.5 mg/ml) over 120 hrs (24 hr intervals). Fluorescence levels varied between replicates, but the overall trend was reproducible. (B) CD analysis of the peptide (diluted from 0.5 mg/ml to 0.25 mg/ml) from 0 to 120 hrs. (C) Negatively stained electron micrographs of the peptide (0.5 mg/ml) incubated for 120 hrs at room temperature. (Scale bar, 250 nm).

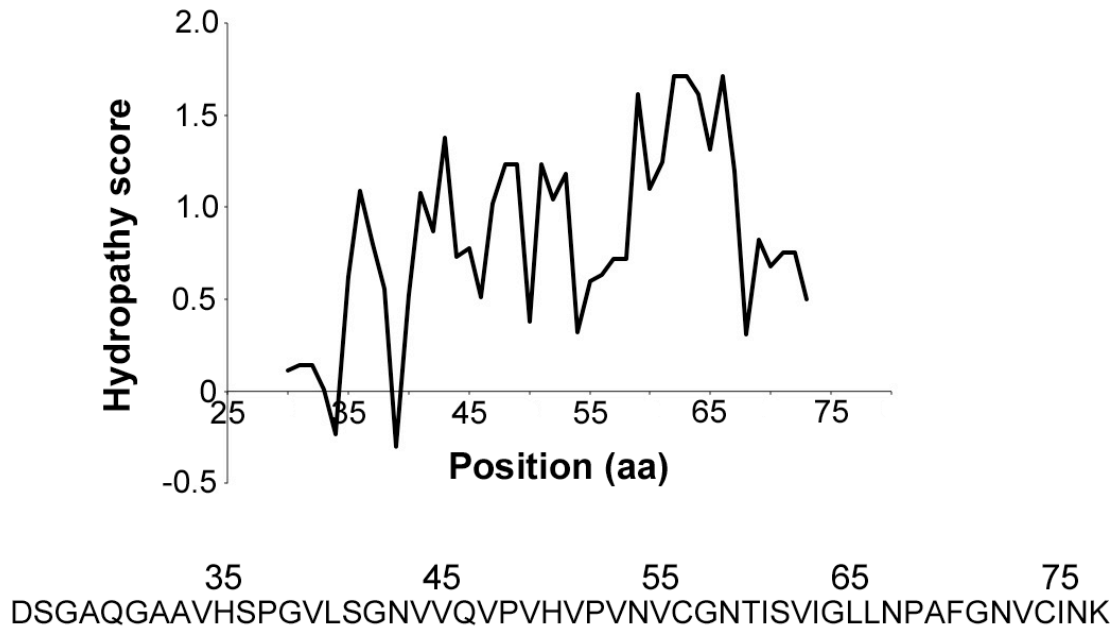


Figure 3.12: Hydropathy profile of ChpH as determined by ProtScale (Kyte & Doolittle, 1982, Wilkins *et al.*, 1999), with the mature sequence of ChpH (not including the signal peptide) shown below. Note the region flanked by Cys56 and Cys74 ranks higher on the hydropathy scale than the rest of ChpH (the higher the number, the greater the hydrophobicity).

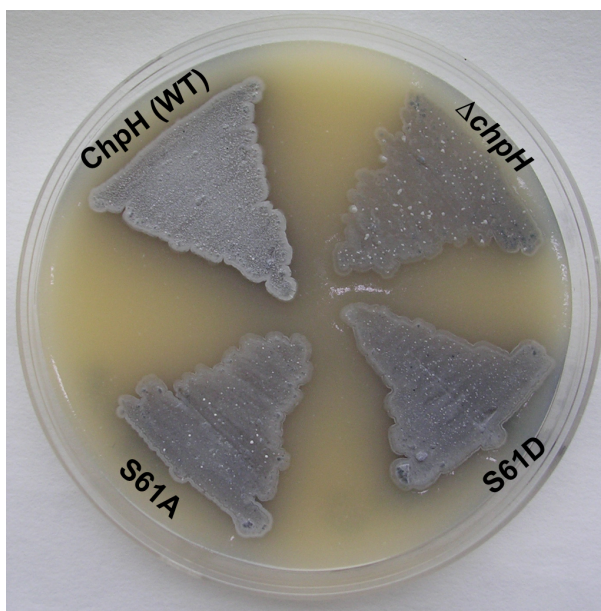


Figure 3.13: Four day cultures grown on MS medium, expressing wild type ChpH (WT), lacking ChpH ($\Delta chpH$), and expressing ChpH with either an Ala or Asp residue substituted for Ser61.

Table 3.1: Hydrophobicity scores of ChpH mutants

Chaplin	Hydrophobicity Score*
ChpH (Wild type)	0.6
I60A	0.548
S61A	0.65
V62A	0.554
I63A	0.548
G64A	0.642
L65A	0.562
L66A	0.562
V72A	0.554
VIGLL-AAAAA	0.467
Δ VIGLL	0.326
Δ Nterm ₃₀₋₃₅	0.663
Δ Nterm ₃₀₋₄₁	0.653
Δ Nterm ₃₀₋₅₁	0.577

*Calculated using GRAVY: Grand average of hydropathicity index. The larger the number, the more hydrophobic the protein (Kyte & Doolittle, 1982, Wilkins *et al.*, 1999).

CHAPTER 4

Characterization of the Unique Short Chaplin ChpE

Preface

Work outlined in section 4.2.1 has been published in the *Journal of Bacteriology* (Di Berardo *et al.*, 2008). Removal of the *chpB::aac(3)IV* cassette from cosmid 5H1, *chpH* site-directed mutagenesis (Cys₅₆-Val; Cys₇₄-Gly), construction of the inducible *chpE* plasmid (pIJ6917), and generating the *chpE* knockout cosmid [15(*chpE::aac(3)IV*)] was done by Dr. Marie Elliot. Kim Findlay (John Innes Centre, Norwich, England) prepared samples for and performed cryo-SEM.

4.1 Introduction

Although the chaplins share a high degree of sequence homology (see Figure 1.2), the short chaplin ChpE is unusual in that it lacks the two highly conserved Cys residues that are present in the chaplin domains of the other chaplins (with the exception of the second chaplin domain of the long chaplin ChpB). In place of the Cys residues, ChpE has a valine (Val) and glycine (Gly). In the other short chaplins, these Cys residues form intramolecular disulfide bonds (Elliot *et al.*, 2003) and are essential for chaplin functioning (Di Berardo *et al.*, 2008). The lack of Cys residues in ChpE implies that it adopts a different and possibly more ‘flexible’ structure than the other short chaplins. This structural disparity between ChpE and the other short chaplins suggests that ChpE may be functionally distinct among the chaplins. What specific role ChpE plays in streptomycete development, however, has yet to be uncovered.

In this chapter, I show that, unlike the other chaplins, ChpE is essential for cell viability, and the essential nature of ChpE depends primarily on its lack of Cys residues. I further demonstrate that ChpE cell surface localization does not rely on the long chaplins (ChpABC), but does require (at least) ChpC to form surface fibers *in vivo*.

4.2 Results

4.2.1 Generating a *chpE* knockout mutant

Previously, *chpE* knockouts have been generated in 5-fold (Δ *chpABCDH*) and 7-fold (Δ *chpABCDEFGH*) *chp* mutants (Claessen *et al.*, 2003, Capstick *et al.*, 2007). To explore the functional importance of ChpE alone, it was necessary to make a *chpE* knockout in a wild type background. Using a targeted PCR mutagenesis approach (Gust *et al.*, 2003), a *chpE* knockout cosmid [15(*chpE::aac(3)IV*)] was introduced into wild type (M600) cells by conjugation, and colonies were screened for a double-crossover event, whereby the chromosomally encoded wild type copy of *chpE* would be replaced by

the *aac(3)IV* cassette, with the concurrent loss of the introduced cosmid. Surprisingly, no *chpE* knockouts were isolated using this method, despite numerous attempts. To exclude the possibility that the inability to obtain *chpE* knockouts was due to a technical problem, a second copy of *chpE*, under the control of the vancomycin-inducible promoter P_{vanJ} (Hong *et al.*, 2004), was introduced on an integrating plasmid into the *chpE* knockout cosmid-containing strain. When grown in the presence of vancomycin, *chpE* knockouts were readily obtained (108/736 colonies); in contrast, without vancomycin present, no *chpE* knockouts were isolated, despite extensive screening (0/522). This strongly suggested that, in a wild type background, ChpE is essential for cell viability, as it can only be knocked out in the presence of a second copy of *chpE*.

4.2.2 Examining the importance of the lack of Cys residues in ChpE

One of the unique features of ChpE is its lack of Cys residues, which are conserved in all the other chaplins. In the Cys-containing short chaplin ChpH, these disulfide bond-forming Cys residues are critical for function (Di Berardo *et al.*, 2008, Elliot *et al.*, 2003). This raises the intriguing question as to whether the absence of Cys residues in ChpE is functionally relevant. If the lack of Cys residues in ChpE is the primary factor differentiating it from the other chaplins, then it may be possible to replace ChpE with another Cys-lacking short chaplin. To this end, the two Cys residues in ChpH were changed to Val and Gly, as found in ChpE, generating ChpH* (Cys₅₆-Val; Cys₇₄-Gly). ChpH was selected because, like ChpE, it is highly expressed throughout development and is conserved across the streptomycetes (Elliot *et al.*, 2003, Di Berardo *et al.*, 2008). Both *chpH* and *chpH** were cloned downstream of the P_{vanJ} vancomycin-inducible promoter on an integrating plasmid, and then introduced into the wild type strain that also contained the *chpE* knockout cosmid. In the absence of the vancomycin inducer, the presence of plasmid-borne *chpH* failed to facilitate the isolation of any *chpE* knockouts (0/157). When expression of wild type *chpH* was induced, a single *chpE* knockout was isolated (1/376 colonies). In contrast, induction of *chpH** by vancomycin enabled *chpE* knockouts to be readily obtained (39/512 colonies). However, when *chpH** expression was not induced, no *chpE* knockouts were isolated (0/218). These results show that ChpH* can functionally replace ChpE, suggesting that a major determinant of ChpE activity is its lack of Cys residues. The isolation of a single *chpE* knockout following induction of *chpH* expression may suggest that higher than normal levels of ChpH may partially compensate for the loss of ChpE, or that the *chpE* knockout that was isolated contained a suppressor mutation elsewhere in the chromosome.

4.2.3 *In vivo* ChpE polymerization

The chaplins polymerize on the cell surface, creating a robust matrix of fibers that coat and protect aerial structures. Previously, it was shown that ChpE alone is insufficient to stimulate aerial hypha production or form surface fibers (Di Berardo *et al.*, 2008). This latter phenotype was observed for a mutant only expressing *chpE* (7x *chp*). It is possible, however, that ChpE may require other factors, which are absent in the 7x *chp* mutant, in

order to polymerize on the surface. In particular, the long chaplins (ChpABC) have been predicted to interact with short chaplin polymers on the surface, possibly acting as ‘molecular anchors’ for short chaplin fibers (Elliot *et al.*, 2003).

To examine whether the long chaplins are required for ChpE surface polymerization, a derivative of the ‘minimal chaplin strain’ was constructed. The minimal chaplin strain encodes only ChpH (short, Cys-containing), ChpC (long) (both carried on an integrating plasmid), and ChpE (short, Cys-lacking; native chromosomal copy). The minimal chaplin strain allows each ‘type’ of chaplin to be studied individually, in a more simplified genetic background (Di Berardo *et al.*, 2008). Therefore, to explore the importance of ChpC to the surface polymerization of ChpE, *chpH* was deleted from plasmid pIJ6935 (*chpHC*-pSET152), and the resulting plasmid was introduced into the 7x *chp* mutant to generate a strain expressing only *chpE* and *chpC*. When viewed by SEM, the surface of the *chpEC* strain revealed the presence of definite surface fibers (Figure 4.1A); the fibers, though, were far less abundant and organized compared to the surface fibers produced by the wild type minimal chaplin strain. The *chpEC* strain, however, was still profoundly impaired at producing aerial hyphae, and looked similar a 7x *chp* mutant (Figure 4.1B).

4.2.4 Dependence of ChpE localization on the long chaplins

Prior evidence had suggested that the long chaplins were important for ChpE cell surface localization, as MALDI-ToF mass spectrometry profiles of *S. coelicolor* strains lacking two (Δ *chpACDH*) or all three long chaplins (Δ *chpABCDH*) exhibited relatively lower levels of ChpE in comparison to the wild type (Elliot *et al.*, 2003). In addition to the long chaplins, however, these strains also lacked *chpD* and *chpH*, making it difficult to establish a direct connection between the presence of the long chaplins and ChpE surface localization. Therefore, in order to directly examine whether the long chaplins are important for ChpE cell surface localization, a mutant only lacking the three long chaplins (Δ *chpABC*) was constructed. Beginning with a strain harboring an *aac(3)IV* cassette in *chpB* (Elliot *et al.*, 2003), the *chpB* cassette was removed and *chpA* and *chpC* were replaced with *aac(3)IV* and *vph* cassettes, respectively, using PCR-targeted mutagenesis (Gust *et al.*, 2003). Deletion of all three long chaplin genes had very little impact on aerial development, as the Δ *chpABC* mutant could still produce a robust aerial mycelium that was comparable to the wild type (Figure 4.2A), with only a slight delay in the timing sporulation was observed (~24 hrs slower than the wild type). To compare ChpE surface localization in the long chaplin mutant and the wild type strain, chaplin extracts were isolated from each and analyzed by MALDI-ToF mass spectrometry. The mass spectrometry analysis revealed that relative ChpE levels (and those of the other short chaplins) were unchanged between the Δ *chpABC* mutant and the wild type (Figure 4.2B). In addition, when the surface of the long chaplin was examined using SEM, it had a very robust rodlet ultrastructure (Figure 4.2C). On closer inspection, however, the individual fibers that comprise the rodlets from the Δ *chpABC* mutant appeared to be longer [\sim 293 nm (\pm 82), n = 12] than those observed for the wild type [\sim 144 nm (\pm 40), n = 12]. Taken together with the findings from Section 4.2.3, the long chaplins appear to be dispensable

for ChpE surface localization, but may be important for ChpE polymerization, as surface fibers are absent in a strain only expressing *chpE* (Di Berardo *et al.*, 2008).

4.3 Discussion

The chaplins are surface-active proteins that are believed to lower the surface tension at the colony surface and form a protective hydrophobic coat around aerial structures (Elliot *et al.*, 2003, Claessen *et al.*, 2003). As ChpE is predicted to adopt a unique structure in comparison to the other chaplins, due to its lack of Cys residues, it is likely that ChpE has an equally unique function among the chaplins during *S. coelicolor* development.

4.3.1 ChpE is essential for cell viability

It was surprising to find that *chpE* was recalcitrant to deletion, indicating that it is essential for maintaining cell viability. ChpE, like the other chaplins, was assumed to only be involved in promoting aerial morphogenesis, a developmental process that is not required for *S. coelicolor* viability (Merrick, 1976). However, *chpE* (and *chpH*) is highly expressed (Elliot *et al.*, 2003) during vegetative growth, suggesting that ChpE has a role that precedes the emergence of aerial hyphae.

The essential nature of *chpE* is conditional, as it can be deleted in the absence of five or more of the other *chp* genes (Claessen *et al.*, 2003, Claessen *et al.*, 2004, Capstick *et al.*, 2007). This dependence on the presence/absence of the other chaplins points to a possible role of ChpE in regulating the activity of the other chaplins. The chaplins are amyloid proteins, and as such, have the potential for causing cell damage (Lashuel & Lansbury, 2006). It is tempting to speculate that ChpE may have a role in controlling unwanted chaplin amyloid fiber formation: in the absence of ChpE, aberrant chaplin aggregation may occur, having potentially lethal consequences. This type of inhibitory activity has recently been documented in *E. coli* for the regulation of curli amyloid fiber assembly, where CsgE is able to prevent the aggregation of CsgA (the primary polymerizing unit of curli fibers) *in vitro* (Nenninger *et al.*, 2011). It is not known whether CsgE exhibits similar activity *in vivo*, but it may function as a safeguard against pre-mature CsgA polymerization, which could occur prior to its secretion to the cell surface. In *S. coelicolor* mutants that are lacking five or more of the other *chp* genes, the total concentration of chaplin proteins produced would be far less than in the wild type; it is possible that when the overall short chaplin concentration is below a certain threshold, ChpE is dispensable. Among the short chaplins, however, only *chpE* and *chpH* are expressed early in the *S. coelicolor* life cycle, while *chpD*, *chpF*, and *chpG* are transcribed at the highest level during the later stages of aerial development and sporulation (Elliot *et al.*, 2003). Since the essential function of ChpE is presumably required during the early stages of growth, the presence/absence of these particular three chaplins (ChpD, F, G) is likely irrelevant to ChpE-dependent cell viability. It is interesting to note that in the published reports of chaplin mutants lacking *chpE*, all were also missing *chpH*, and in all cases, *chpH* was deleted prior to the removal of *chpE*

(Capstick *et al.*, 2007, Claessen *et al.*, 2003, Claessen *et al.*, 2004). Furthermore, *chpE* and *chpH* are the only two short chaplins that are conserved across all streptomycete genomes sequenced to date, which may suggest that the presence ChpE is necessitated by the production of ChpH. It is possible that ChpE may function to specifically control ChpH activity. One fact to consider, however, is that *chpHC* can be introduced on an integrating plasmid into a complete 8× *chp* mutant (lacking *chpE*), and the resulting strain is viable (Di Berardo *et al.*, 2008). However, the ectopic transcription/translation of the plasmid-borne *chpH* gene may be reduced compared to *chpH* expressed from its native chromosomal location. In this scenario, ChpH levels may be low enough to make *chpE* dispensable. By comparing the expression of the native copy of *chpH* to the plasmid-encoded copy of *chpH*, by reverse transcription PCR (to monitor transcription) and western blot analysis (to monitor translation), it would provide evidence as to whether there is a disparity in expression between the two alleles.

Another possible explanation as to why the deletion of most/all of the chaplins allows for *chpE* to be deleted may have more to do with the expression of other genes in chaplin mutant backgrounds, and less to do directly with the absence of the chaplins. For example, *rdlAB* transcription is severely reduced in a mutant lacking six or more of the chaplins (Claessen *et al.*, 2004). This is particularly interesting since *chpE* can be readily deleted in a *rdlAB* mutant (Di Berardo *et al.*, 2008). The reduced expression of *rdlAB* in a multiple *chp* mutant may therefore permit the deletion of *chpE*. The dependence on *rdlAB* for maintaining ChpE-dependent cell viability, however, is perplexing, as the rodlinins are only expressed in growing aerial hyphae (after ~2 days), and the essential function of ChpE would be expected to be required long before the emergence of aerial hyphae. It is therefore not obvious what the connection is between the rodlinins and the maintenance of ChpE-dependent viability.

The deletion of all eight *chp* genes causes differential expression of not only *rdlAB*, but a host of other genes. In total, 100 genes are down-regulated in an 8× *chp* mutant (which includes the *chp* and *rdl* genes), and of these, 12 are predicted to encode secreted proteins (excluding *chp* and *rdl* genes) (de Jong *et al.*, 2009a). It is possible that one or more of these proteins is required for the maintenance of ChpE-dependent cell viability.

In addition to chaplin (5-fold or more) and rodlin mutants, *chpE* can also be deleted in mutants defective in twin arginine transport (Tat) (Di Berardo *et al.*, 2008), a translocation system encoded by *tatA*, *tatB* and *tatC* (Berks *et al.*, 2000). In bacteria, the Tat system is responsible for transporting pre-folded proteins across the cytoplasmic membrane. This is in contrast to the Sec system, which is involved in the secretion of unfolded proteins (Berks *et al.*, 2000). Neither the chaplins nor the rodlinins are Tat substrates, so it seems likely that ChpE-dependent cell viability requires the activity of another protein(s) that is a substrate of the Tat system (discussed below).

When the expression data of those genes that are down-regulated in an 8× *chp* mutant (de Jong *et al.*, 2009a) is compared to genes encoding predicted Tat substrates (Schaerlaekens *et al.*, 2004), there are two genes common to both data sets. The first, *SCO4142* (*pstS*), encodes a lipoprotein involved in phosphate transport. In *S. coelicolor*, phosphate availability impacts both morphological differentiation and secondary

metabolism; specifically, inactivation of *pstS* causes aerial differentiation to be accelerated, which is accompanied by an overproduction of the blue pigmented antibiotic actinorhodin (Diaz *et al.*, 2005). The other Tat substrate-encoding gene is *SCO3244*, which specifies a secreted protein of unknown function. It is possible that either of these proteins may have a role in maintaining ChpE-dependent cell viability; however, whether this is the case, will require further investigation.

4.3.2 The role of Cys in the activity of the chaplins

The essential function of ChpE is primarily dependent on its lack of Cys residues. By merely replacing the two Cys residues found in ChpH with Val and Gly, as is found in ChpE, the resulting ChpH* mutant could functionally substitute for ChpE. The Cys residues found in the other chaplins form intramolecular disulfide bonds (Elliot *et al.*, 2003); the absence of such linkages in ChpE would suggest that ChpE requires a more ‘flexible’ structure in order to function properly. Functionally analogous to the chaplins are the hydrophobins, which are produced by filamentous fungi and contain eight highly conserved Cys residues (Wösten, 2001). These Cys residues form disulfide bonds that provide structural rigidity, locking the hydrophobin protein in an amphipathic conformation (Hakanpaa *et al.*, 2004, Kwan *et al.*, 2006), a characteristic that is likely important for maintaining the protein in a surface-active form. It is possible that the disulfide bonds formed within the Cys-containing chaplins also have a similar role in maintaining chaplin surface activity. Despite the absence of a disulfide bond, however, ChpE exhibits a similar level of surface activity as the other short chaplins (Sawyer *et al.*, 2011). Likewise, when ChpE is deposited on the surface of a 6× *chp* mutant (Δ *chpABCDEH*), it is able to partially restore aerial hyphae formation; however, the amount of aerial hyphae produced after the application of ChpE is much less when compared to the extracellular application of ChpD, ChpG, or ChpF (Sawyer *et al.*, 2011). This suggests that ChpE is not as potent as the other short chaplins in stimulating aerial development. This is also supported by the severe developmental phenotype exhibited by strains only producing ChpE (Di Berardo *et al.*, 2008) or ChpE and ChpC, both of which closely resemble a complete 8× *chp* mutant (Capstick *et al.*, 2007, Claessen *et al.*, 2004). Like the other short chaplins, ChpE can form amyloid fibers *in vitro* (Sawyer *et al.*, 2011), and produces surface fibers *in vivo* (Capstick *et al.*, 2011), albeit very sparsely in comparison to the Cys-containing ChpH protein (Di Berardo *et al.*, 2008), and only in the presence of the long chaplin ChpC. Thus, although disulfide bond formation does not appear to be essential for chaplin polymerization (as ChpH can also form amyloid fibers under reducing conditions) or surface activity *in vitro*, it does appear to have an important functional role *in vivo*, in both the promotion of aerial development and the formation of surface rodlets by the chaplins.

Interestingly, the *S. coelicolor* Tat system (which is required for maintaining ChpE-dependent cell viability) is predicted to translocate ‘Dsb-like’ (disulfide bond) proteins (e.g. SCO4472), enzymes that are responsible for catalyzing disulfide bond formation in bacteria (Kadokura *et al.*, 2003). These Tat-dependent Dsb-like proteins catalyze chaplin disulfide bond formation. In general, the mechanism underlying disulfide

bond formation in streptomycetes and other Gram-positive bacteria is not well understood. In Gram-negative *E. coli* cells, disulfide bond formation occurs in the periplasm and is primarily mediated by DsbA, DsbB, DsbC, and DsbD (Messens & Collet, 2006). DsbA is directly responsible for the rapid oxidation of Cys residues found in proteins secreted into the periplasm, and is characterized by having a redox active Cys-X-X-Cys sequence (Martin *et al.*, 1993). Once the Cys-X-X-Cys active site of DsbA becomes reduced, the cytoplasmic membrane-spanning protein DsbB is responsible for restoring DsbA to its oxidized form via the electron transport chain, transferring two electrons from DsbA onto oxidized ubiquinone (Bader *et al.*, 2000). In proteins that have more than two Cys residues, there is the potential for DsbA to form disulfide bonds that cause the protein to fold improperly. When this occurs, the disulfide bond isomerase DsbC (and its paralog DsbG) is able to rescue proteins from such misfolded fates (Shevchik *et al.*, 1994, Bessette *et al.*, 1999). DsbC is maintained in a reduced form by the cytoplasmic membrane protein DsbD (Missiakas *et al.*, 1995).

In Gram-positive bacteria, it is not known how proteins become oxidized on the cell surface to form disulfide bonds. Moreover, although many bacterial genomes encode homologs of DsbA, not all encode homologs of DsbB (Dutton *et al.*, 2008), suggesting that more than one pathway exists among bacteria for the formation of disulfide bonds. Evidence for such an alternate pathway was recently uncovered in the actinomycete *M. tuberculosis*. Instead of DsbB, *M. tuberculosis* encodes a homolog of the eukaryotic vitamin K epoxide reductase (VKOR) (Rv2968c), which can functionally replace DsbB in *E. coli* (Dutton *et al.*, 2008, Dutton *et al.*, 2010). In eukaryotes, a protein disulfide isomerase (PDI) is responsible for disulfide bond formation (Wilkinson & Gilbert, 2004), and similar to the relationship between DsbA and DsbB in *E. coli*, VKOR functions to transfer electrons from PDI to a quinone, restoring PDI to its oxidized state (Wallin *et al.*, 2007). In humans, VKOR is important for maintaining vitamin K in a reduced state, which acts as a cofactor during the carboxylation of prothrombin, a protein involved in blood clotting (Sun *et al.*, 2005). VKOR homologs are found in other bacterial genomes that lack a DsbB homolog (Dutton *et al.*, 2008), including *S. coelicolor* (SCO1507). Despite these recent advances in our understanding of disulfide bond formation in Gram-positive bacteria, further research is required in order to completely understand the mechanisms underlying disulfide bond formation in bacteria such as *S. coelicolor*, and specifically, whether Dsb-like proteins like SCO4472 or the VKOR homolog SCO1507 are involved in generating disulfide bonds in the chaplin proteins.

4.3.3 The role of the long chaplins

In the original model that was put forth to explain the function of the chaplins (Elliot *et al.*, 2003), the cell wall-attached long chaplins (ChpA-C) were predicted to interact with polymers of short chaplins, anchoring them to the cell surface. However, the work presented here suggests this is not the case, as the long chaplins are not required for short chaplin cell surface attachment. Moreover, deletion of all three long chaplin-encoding genes only caused a slight impairment in development, as a Δ *chpABC* mutant could raise a very robust aerial mycelium, although sporulation was delayed by ~1 day.

However, in the minimal chaplin strain, the developmental contribution of the long chaplins is much more evident. Although a strain expressing only *chpE* and *chpH* is capable of raising aerial hyphae, the resulting aerial mycelium is much less robust than the wild type minimal chaplin strain expressing *chpE*, *chpH*, and *chpC* (Di Berardo *et al.*, 2008). While the Δ *chpABC* mutant produced wild type-levels of surface fibers, upon closer inspection, the fibers appeared measurably longer than those of the wild type. It is possible that the long chaplins control the length of chaplin surface fibers, acting as molecular markers to signify the ‘start’ and ‘end’ points during short chaplin polymerization. Whether this ‘long surface fiber’ phenotype contributes to the delay in aerial development exhibited by the long chaplin mutant is not clear. Likewise, in the minimal chaplin strain, removal of the long chaplin ChpC causes a similar disorganization in rodlet surface fibers. When only *chpE* and *chpH* are expressed, chaplin fibers can be readily observed on the surfaces of aerial structures; however, these fibers are much more sparse and do not occur in pairs (rodlets). When *chpC* is introduced into a *chpEC* strain, surface fiber abundance is greatly enhanced, and while individual fibers are observed, paired rodlets are also found. Interestingly, many of the fibers on the surface of a *chpEHC*-expressing strain appear to emanate from a common focus, producing a ‘starburst-like’ pattern (Di Berardo *et al.*, 2008). It is therefore apparent that the long chaplins are not essential for short chaplin attachment to the cell surface, but instead are critical for the organization of short chaplin fibers on the cell surface.

4.4 Figures

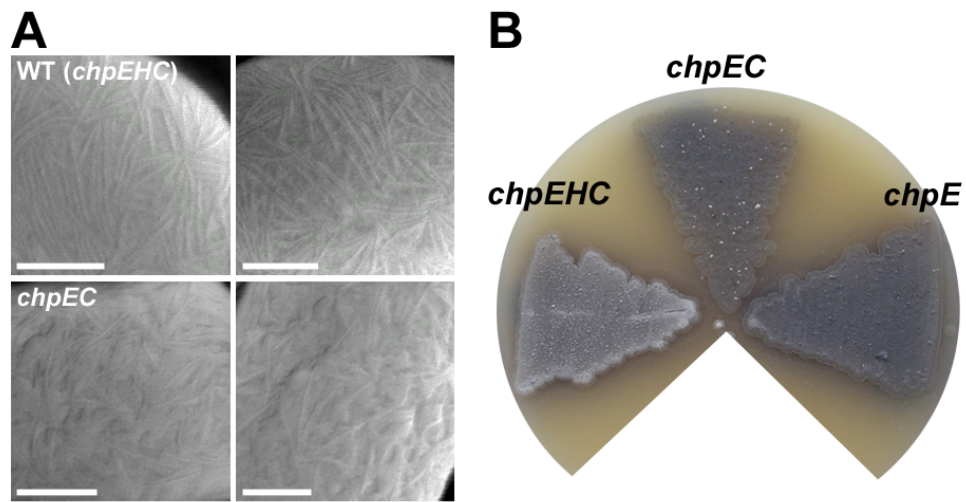


Figure 4.1: (A) SEM micrographs focused on the surface ultrastructure of the minimal chaplin strain (WT) (expressing *chpEHC*) (top) compared to a strain producing ChpE and ChpC only (bottom) (Scale bars, 200 nm). (B) Four day cultures grown on MS medium of the minimal chaplin strain and mutant derivatives that produce ChpE and ChpC, or ChpE only.

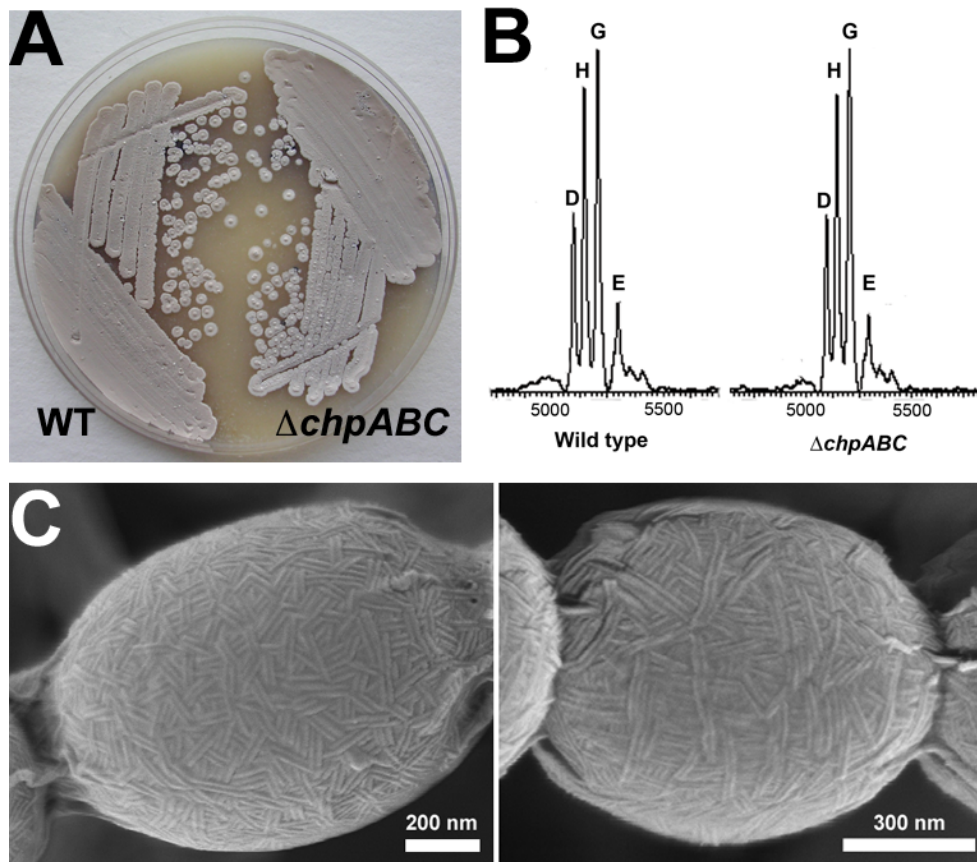


Figure 4.2: (A) Four day cultures grown on MS medium of the wild type (WT; expressing all eight chaplins) and the $\Delta chpABC$ mutant. (B) MALDI-ToF analysis of chaplin extracts isolated from both strains, showing that the loss of the long chaplins does not impact the cell surface localization of the short chaplins. (C) SEM micrographs comparing the surface ultrastructure of the wild type (left) vs. the $\Delta chpABC$ mutant (right). Scale bars are as indicated.

CHAPTER 5

Summary and Future Directions

5.1 Summary of research

The continual discovery of beneficial, functional amyloids from a diverse range of organisms has meant that amyloids can no longer be regarded simply as agents of disease, or the product of aberrant, uncontrolled protein aggregation. Instead, amyloids have important roles in numerous aspects of cellular biology. The discovery of the *S. coelicolor* chaplin proteins expanded the functional roles of amyloids to include the promotion of bacterial cellular differentiation. It is well established that the chaplins are essential for *S. coelicolor* aerial development (Elliot *et al.*, 2003, Capstick *et al.*, 2007, Claessen *et al.*, 2003); however, there was no evidence showing that chaplin amyloidogenesis was a critical component of chaplins functioning in promoting *S. coelicolor* morphological development.

The work outlined in Chapter 3 represents the first evidence of a direct structure-function relationship between chaplin amyloidogenesis and *S. coelicolor* aerial development. Mutations that severely compromised ChpH amyloid fiber formation also caused significant impairment to aerial development. Both the amyloidogenic activity of ChpH and its ability to promote aerial development were traced to separate N- and C-terminal domains. The C-terminal domain appears to have greater functional importance, as it is essential for surface rodlet assembly, whereas the N-terminus is not. Similar to ChpH, there are other amyloid proteins that contain more than one amyloid domain (Wang *et al.*, 2008, Wang *et al.*, 2007b, Ross *et al.*, 2005, Watt *et al.*, 2009); however, ChpH is the first example of a functional amyloid having multiple amyloid domains that are functionally disparate. Thus, amyloid domains can have the potential to not only influence protein amyloid fiber formation, but can have additional activities, which are important for the overall biological role of the amyloid protein.

The primary focus of Chapter 4 was to explore the functional role of the unique short chaplin ChpE. Surprisingly, ChpE is essential for cell viability, which suggests that it has activity that extends beyond the stimulation of aerial hyphae growth. What this essential role may be, however, remains unclear. From a genetic perspective, it is evident that the essential nature of ChpE depends on other factors, as it is possible to delete *chpE* in the presence of a variety of second site suppressor mutations. Possible directions for future research into understanding the role of ChpE are discussed below.

A secondary focus of the research presented in Chapter 4 was to examine the functional importance of the long chaplins (ChpA, ChpB, and ChpC) in relation to ChpE and the other short chaplins. The original chaplin model proposed that the long chaplins anchor polymers of short chaplins to the cell wall (Elliot *et al.*, 2003, Claessen *et al.*, 2003). Although deletion of all three long chaplin genes caused a slight delay in development, it did not impact short chaplin surface localization, or reduce relative surface rodlet abundance. The rodlet ultrastructure, however, was altered in the absence

of the long chaplins, with individual rodlet fibers being longer than those of the wild type. Thus, the long chaplins are not necessary for chaplin surface fiber attachment, per se, but are important for influencing rodlet surface fiber organization.

5.2 A revised model for chaplin assembly and function

When the chaplins were discovered in 2003, a model was put forth that attempted to explain how the chaplins might promote aerial development in *S. coelicolor* (Elliot *et al.*, 2003, Claessen *et al.*, 2003). During the early stages of aerial development, the highly surface-active chaplin proteins are required to lower the surface tension at the air-colony interface, an event that is presumed to be required in order to allow aerial hyphae to escape the aqueous colony environment. Aerial hyphae are coated in a hydrophobic layer of chaplin fibers as they grow by hyphal tip extension, which would cause a displacement of water molecules in contact with the hydrophobic aerial hyphae, resulting in a reduction in local surface tension. As aerial hyphae continue to grow, the hydrophobic layer would protect these structures from desiccation and confer structural stability.

One of the tenets of this model is that the short chaplins heteropolymerize with the long chaplins, presumably through hydrophobic interactions between the homologous chaplin domains. The heteropolymerization between short and long chaplins would serve to securely attach the hydrophobic chaplin layer to the peptidoglycan layer of the cell wall. However, it is now evident that the long chaplins are not the primary means by which the short chaplins are bound to the cell surface. Instead, there is likely another factor(s) present that mediates chaplin cell surface attachment. The functionally analogous class I hydrophobins that are produced by filamentous fungi, which also adopt a rodlet ultrastructure, are not believed to require accessory proteins for attachment; instead, the hydrophobins are predicted to form an amphiphilic film over aerial structures: the hydrophilic face would be in contact with the hydrophilic cell wall, while the hydrophobic side would be exposed to the air (Wösten *et al.*, 1993).

The functional relationship between the short and long chaplins may be analogous to that of TasA and TapA in *B. subtilis*. TasA is an amyloid protein from *B. subtilis*, which forms amyloid fibers that help bind cells together and provide structural integrity to biofilms (Romero *et al.*, 2010). Like the short chaplins, TasA interacts with a cell wall-bound accessory protein, TapA (TasA anchoring/assembly protein) (Romero *et al.*, 2011). In the absence of TapA, the amount of TasA fibers is significantly reduced; the few TasA fibers that are produced by a *tapA* mutant are disorganized and usually detached from the cell surface (Romero *et al.*, 2011). Thus, TapA has a dual role, first to anchor TasA to the cell surface, and to promote the formation of TasA amyloid fibers. Unlike the long chaplins, TapA does not appear to be a substrate of a sortase enzyme, and it is not clear whether it is covalently attached to the cell wall (Romero *et al.*, 2011). Similar to TapA, the long chaplins promote short chaplin fiber assembly, and, although the long chaplins are not essential for short chaplin cell surface localization, they may be important for the anchoring of fimbriae that are produced by the chaplins when *S. coelicolor* is grown in standing liquid culture. Under these growth conditions, a mutant of *S. coelicolor* lacking the long chaplins (Δ *chpABCDH*) is impaired in its ability to attach to

solid surfaces (~20% less biomass attached) and produces fewer fimbriae (de Jong *et al.*, 2009b). However, in order to directly assess the importance of the long chaplins for attachment and fimbriae assembly, these experiments would need to be repeated with a mutant only lacking the long chaplins ($\Delta chpABC$).

Another aspect of the proposed chaplin model is that the short chaplins (specifically ChpH and ChpE), along with SapB, are primarily responsible for the precipitous drop in surface tension that is a prerequisite for aerial hyphae emergence. This, however, may not necessarily be the functional fate of ChpE. By itself, ChpE exhibits surface activity *in vitro* that is comparable to the other short chaplins, but is unable to stimulate comparable levels of aerial development *in vivo* (Sawyer *et al.*, 2011). And although ChpE is able to form surface fibers *in vivo*, it does so much less effectively relative to ChpH. Most significantly, ChpE is essential for cell viability. Together, this implies that surface activity and/or surface fiber formation are likely not the primary utilities of ChpE. Further research is required to determine how ChpE precisely fits into the functional model describing chaplin activity.

5.3 Future directions

5.3.1 Regulation of chaplin activity

One of the most interesting areas of chaplin research that has yet to be explored in any great detail are the mechanisms that control chaplin activity. Given that the chaplins are amyloids, forming highly insoluble, protease-resistant aggregates, which may have the potential for causing amyloid-related cytotoxicity, it is anticipated that chaplin activity is highly regulated at multiple levels. At the transcriptional level, *chp* gene expression depends on the *bld* genes (Elliot *et al.*, 2003), a class of genes in *S. coelicolor* that are essential for the early stages of aerial development (Merrick, 1976). In fact, the chaplins were originally discovered through their dependence on *bldN* (Elliot *et al.*, 2003), which encodes an extracytoplasmic function (ECF) sigma factor (Bibb *et al.*, 2000). However, the upstream regions of both *chpE* and *chpH* do not contain an obvious σ^{BldN} consensus sequence, suggesting that σ^{BldN} -dependent regulation of the chaplins is indirect (Elliot *et al.*, 2003). A direct target of σ^{BldN} is *bldM*, which encodes a developmental response-regulator (Bibb *et al.*, 2000). It is conceivable that σ^{BldN} -dependent *chp* expression is mediated directly through the activity of BldM, as *chp* gene expression is also significantly reduced in a *bldM* mutant background (Elliot *et al.*, 2003). However, using electrophoretic mobility shift assays, a direct interaction between BldM and the *chpE* promoter (P_{chpE}) failed to be observed *in vitro* (Capstick and Elliot, unpublished), but this may be because the binding conditions were not ideal for promoting BldM binding, and does not conclusively rule out the possibility that BldM binds P_{chpE} . Using a more systematic approach to identify a transcriptional regulator of the chaplins, I have begun work using an affinity purification-based approach, in an effort to isolate proteins that bind the upstream region of *chpH*. By identifying a transcriptional regulator of *chpH*, it will provide important information regarding the placement of the chaplins in the developmental regulatory cascade.

5.3.2 Surface localization of the chaplins

There is still much that remains unclear about the contribution of each of the chaplins on the cell surface and the specific localization of each. The short chaplins polymerize on the cell surface, but it is not known whether the resulting fibers are homo- or heteropolymers of short chaplins. Surface fibers produced by the minimal chaplin strain, which expresses only *chpE*, *chpH*, and *chpC*, appear to comprise polymers primarily of ChpH (Di Berardo *et al.*, 2008). This is based on the fact that only mutant derivatives of the minimal chaplin strain that express *chpH* (e.g. *chpEH* or *chpHC*) have robust surface fibers; in the absence of ChpH (e.g. *chpE* or *chpEC*), surface fiber abundance is dramatically reduced or fibers are entirely absent [see Figure 4.1A and (Di Berardo *et al.*, 2008)]. However, there is no direct evidence to show that ChpH is the primary polymerizing unit of chaplin fibers in the case of the minimal chaplin strain. Similarly, it is not known where the cell wall-bound long chaplins (e.g. ChpC) reside with respect to chaplin surface fibers. If the long chaplins represent the ‘start’ and ‘stop’ points for the polymerization of chaplin fibers (as was hypothesized based on the results presented in Chapter 4), then it would be expected that the long chaplins would be present at the fiber poles. Moreover, by following the specific cell surface localization of ChpE, in particular, it could provide important insight into the function of ChpE. To this end, chaplin surface localization could be followed using immunogold electron microscopy. However, a challenge with doing this type of experiment stems from the homology that exists between chaplin proteins. For example, there is 66 - 78% identity between the chaplin domain of ChpH and that of ChpE and the dual chaplin domains of ChpC. Thus, it is likely not possible to obtain an antibody with specificity for a single chaplin protein. To circumvent this, chaplin localization could be monitored using tagged chaplin proteins [e.g. FLAG tag (Einhauer & Jungbauer, 2001)] in conjunction with tag-specific antibodies. Each FLAG construct could then be introduced into the minimal chaplin in place of the native copy of each gene in order to follow ChpH, ChpE, or ChpC surface localization via immunogold electron microscopy. It would also be of great value to not only examine the individual localization patterns of each chaplin, but to perform co-localization experiments, to see whether there are any trends with regard to the spatial distribution of each chaplin protein relative to one another. This could be achieved by using multiple tags (e.g. FLAG and Strep tags). Similar studies using immunogold electron microscopy have been used to great effect in the functional dissection of other bacterial amyloid proteins, including the *E. coli* curli proteins and the *B. subtilis* TsaA and TapA proteins (Bian & Normark, 1997, Hammar *et al.*, 1996, Romero *et al.*, 2010, Romero *et al.*, 2011). Knowing how the chaplins interact on the cell surface may provide important clues to their specific functional roles.

5.3.3 Towards understanding the essential function of ChpE

The precise function of ChpE that renders it essential for cell viability remains unclear. What is very evident is that the essential nature of ChpE depends on additional

factors, as suppressor mutations have been isolated that permit *chpE* deletion, namely $\Delta rdlAB$ and mutants of the Tat system (Di Berardo *et al.*, 2008). Interestingly, during the initial attempts to obtain *chpE* knockouts, an additional class of ChpE suppressor was isolated (Elliot, unpublished). The spontaneous *chpE* suppressor mutant exhibited a small colony phenotype, which is characteristic of *tat* mutants when grown on mannitol-containing media, but did not exhibit any of the other phenotypes associated with a *tat* mutant (e.g. lack of agarase and actinorhodin production, failure to develop aerial hyphae on rich media, inability to grow in high-sucrose liquid media). Furthermore, this mutant does not have mutations in any of the *tat* or *rdl* genes, and genetic complementation experiments have failed to narrow down possible candidate genes (Capstick and Elliot, unpublished). Due to its partial *tat* mutant phenotype (small colony size), it is possible that this unmarked mutation is present in a gene encoding a substrate of the Tat system. In an effort to isolate additional *chpE* suppressor mutants, a more direct approach has been taken in the past using a genome-wide, transposon-based strategy (Capstick, unpublished). But these attempts failed, owing largely to an insufficient yield of transposon mutants to use in screening for mutations that permit *chpE* deletion. Through the analysis of expression data from a complete chaplin mutant (de Jong *et al.*, 2009a), a list of potential candidates that may be responsible for maintaining ChpE-dependent viability was assembled. This is centered on the idea that deletion of *chpE* in a mutant lacking most of the other chaplins is less to do with the actual loss of the chaplins, and may have more to do with the down-regulation of other genes that are required for maintaining ChpE-dependent viability. In particular, there are 12 genes that are down-regulated in the absence of the chaplins that encode proteins predicted to be exported to the cell surface, and thus could represent potential interacting partners of ChpE. The functions of most of these gene products are not known, with the exception of *nepA*, which encodes a protein involved in the maintenance of spore dormancy (de Jong *et al.*, 2009a). Interestingly, two of these genes, *SCO4142* (*pstS*) and *SCO3244*, encode proteins that are also predicted to be targets of the Tat system. It is possible that *pstS*, *SCO3244*, or one of the other genes down-regulated in a complete chaplin mutant, may be required for ChpE-dependent viability. A direct mutational analysis of each of these genes would easily confirm whether this is the case. This would involve knocking out the genes individually, and then screening to see if *chpE* deletions could be created in each mutant background. Since PstS and SCO3244 are substrates of the Tat system, knocking them out may cause a *tat* mutant-like phenotype (small colonies on mannitol-containing media). Understanding what other factors are required for the essential activity of ChpE may offer some important insight into the role ChpE plays in *S. coelicolor* biology.

REFERENCES

- Adams, D. W. & J. Errington, (2009) Bacterial cell division: assembly, maintenance and disassembly of the Z ring. *Nature Reviews Microbiology* **7**: 642-653.
- Aínsa, J. A., H. D. Parry & K. F. Chater, (1999) A response regulator-like protein that functions at an intermediate stage of sporulation in *Streptomyces coelicolor* A3(2). *Molecular Microbiology* **34**: 607-619.
- Alam, M. S., S. K. Garg & P. Agrawal, (2007) Molecular function of WhiB4/Rv3681c of *Mycobacterium tuberculosis* H37Rv: a [4Fe-4S] cluster co-ordinating protein disulphide reductase. *Molecular Microbiology* **63**: 1414-1431.
- Alteri, C. J., J. Xicohtencatl-Cortes, S. Hess, G. Caballero-Olin, J. A. Giron & R. L. Friedman, (2007) *Mycobacterium tuberculosis* produces pili during human infection. *Proceedings of the National Academy of Sciences of the United States of America* **104**: 5145-5150.
- Bader, M. W., T. Xie, C. A. Yu & J. C. Bardwell, (2000) Disulfide bonds are generated by quinone reduction. *Journal of Biological Chemistry* **275**: 26082-26088.
- Barnhart, M. M. & M. R. Chapman, (2006) Curli biogenesis and function. *Annual Review of Microbiology* **60**: 131-147.
- Bennett, J. A., J. Yarnall, A. B. Cadwallader, R. Kuennen, P. Bidey, B. Stadelmaier & J. R. McCormick, (2009) Medium-dependent phenotypes of *Streptomyces coelicolor* with mutations in *ftsI* or *ftsW*. *Journal of Bacteriology* **191**: 661-664.
- Bentley, S. D., K. F. Chater, A. M. Cerdeno-Tarraga, G. L. Challis, N. R. Thomson, K. D. James, D. E. Harris, M. A. Quail, H. Kieser, D. Harper, A. Bateman, S. Brown, G. Chandra, C. W. Chen, M. Collins, A. Cronin, A. Fraser, A. Goble, J. Hidalgo, T. Hornsby, S. Howarth, C. H. Huang, T. Kieser, L. Larke, L. Murphy, K. Oliver, S. O'Neil, E. Rabinowitsch, M. A. Rajandream, K. Rutherford, S. Rutter, K. Seeger, D. Saunders, S. Sharp, R. Squares, S. Squares, K. Taylor, T. Warren, A. Wietzorrek, J. Woodward, B. G. Barrell, J. Parkhill & D. A. Hopwood, (2002) Complete genome sequence of the model actinomycete *Streptomyces coelicolor* A3(2). *Nature* **417**: 141-147.
- Berdy, J., (2005) Bioactive microbial metabolites. *Journal of Antibiotics* **58**: 1-26.
- Berks, B. C., F. Sargent & T. Palmer, (2000) The Tat protein export pathway. *Molecular Microbiology* **35**: 260-274.
- Berson, J. F., D. C. Harper, D. Tenza, G. Raposo & M. S. Marks, (2001) Pmel17 initiates premelanosome morphogenesis within multivesicular bodies. *Molecular Biology of the Cell* **12**: 3451-3464.
- Berson, J. F., A. C. Theos, D. C. Harper, D. Tenza, G. Raposo & M. S. Marks, (2003) Proprotein convertase cleavage liberates a fibrillogenic fragment of a resident glycoprotein to initiate melanosome biogenesis. *The Journal of Cell Biology* **161**: 521-533.
- Bessette, P. H., J. J. Cotto, H. F. Gilbert & G. Georgiou, (1999) *In vivo* and *in vitro* function of the *Escherichia coli* periplasmic cysteine oxidoreductase DsbG. *Journal of Biological Chemistry* **274**: 7784-7792.

- Bian, Z. & S. Normark, (1997) Nucleator function of CsgB for the assembly of adhesive surface organelles in *Escherichia coli*. *The EMBO Journal* **16**: 5827-5836.
- Bibb, M. J., R. F. Freeman & D. A. Hopwood, (1977) Physical and genetic characterization of a second sex factor, SCP2, for *Streptomyces coelicolor* A3(2). *Molecular & General Genetics* **154**: 155-166.
- Bibb, M. J., V. Molle & M. J. Buttner, (2000) σ^{BldN} , an extracytoplasmic function RNA polymerase sigma factor required for aerial mycelium formation in *Streptomyces coelicolor* A3(2). *Journal of Bacteriology* **182**: 4606-4616.
- Bibb, M. J., J. M. Ward, T. Kieser, S. N. Cohen & D. A. Hopwood, (1981) Excision of chromosomal DNA sequences from *Streptomyces coelicolor* forms a novel family of plasmids detectable in *Streptomyces lividans*. *Molecular & General Genetics* **184**: 230-240.
- Bieler, S., L. Estrada, R. Lagos, M. Baeza, J. Castilla & C. Soto, (2005) Amyloid formation modulates the biological activity of a bacterial protein. *Journal of Biological Chemistry* **280**: 26880-26885.
- Bierbaum, G. & H. G. Sahl, (2009) Lantibiotics: mode of action, biosynthesis and bioengineering. *Current Pharmaceutical Biotechnology* **10**: 2-18.
- Bierman, M., R. Logan, K. O'Brien, E. T. Seno, R. N. Rao & B. E. Schoner, (1992) Plasmid cloning vectors for the conjugal transfer of DNA from *Escherichia coli* to *Streptomyces* spp. *Gene* **116**: 43-49.
- Bryson, K., L. J. McGuffin, R. L. Marsden, J. J. Ward, J. S. Sodhi & D. T. Jones, (2005) Protein structure prediction servers at University College London. *Nucleic Acids Research* **33**: W36-38.
- Bucciantini, M., E. Giannoni, F. Chiti, F. Baroni, L. Formigli, J. Zurdo, N. Taddei, G. Ramponi, C. M. Dobson & M. Stefani, (2002) Inherent toxicity of aggregates implies a common mechanism for protein misfolding diseases. *Nature* **416**: 507-511.
- Butko, P., J. P. Buford, J. S. Goodwin, P. A. Stroud, C. L. McCormick & G. C. Cannon, (2001) Spectroscopic evidence for amyloid-like interfacial self-assembly of hydrophobin Sc3. *Biochemical and Biophysical Research Communications* **280**: 212-215.
- Capstick, D. S., A. Jomaa, C. Hanke, J. Ortega & M. A. Elliot, (2011) Dual amyloid domains promote differential functioning of the chaplin proteins during *Streptomyces* aerial morphogenesis. *Proceedings of the National Academy of Sciences of the United States of America* **108**: 9821-9826.
- Capstick, D. S., J. M. Willey, M. J. Buttner & M. A. Elliot, (2007) SapB and the chaplins: connections between morphogenetic proteins in *Streptomyces coelicolor*. *Molecular Microbiology* **64**: 602-613.
- Chakraborty, R. & M. Bibb, (1997) The ppGpp synthetase gene (*relA*) of *Streptomyces coelicolor* A3(2) plays a conditional role in antibiotic production and morphological differentiation. *Journal of Bacteriology* **179**: 5854-5861.
- Champness, W. C., (1988) New loci required for *Streptomyces coelicolor* morphological and physiological differentiation. *Journal of Bacteriology* **170**: 1168-1174.

- Champness, W. C. & K. Chater, (1994) Regulation and integration of antibiotic production and morphological differentiation in *Streptomyces* spp. In: Regulation of Bacterial Development. P. J. Piggot, C. P. Moran & P. Youngman (eds). Washington, D.C.: American Society for Microbiology, pp. 61-93.
- Chandra, G. & K. F. Chater, (2008) Evolutionary flux of potentially *bldA*-dependent *Streptomyces* genes containing the rare leucine codon TTA. *Antonie Van Leeuwenhoek* **94**: 111-126.
- Chapman, M. R., L. S. Robinson, J. S. Pinkner, R. Roth, J. Heuser, M. Hammar, S. Normark & S. J. Hultgren, (2002) Role of *Escherichia coli* curli operons in directing amyloid fiber formation. *Science* **295**: 851-855.
- Chater, K. F., (1972) A morphological and genetic mapping study of white colony mutants of *Streptomyces coelicolor*. *Journal of General Microbiology* **72**: 9-28.
- Chater, K. F., (1975) Construction and phenotypes of double sporulation deficient mutants in *Streptomyces coelicolor* A3(2). *Journal of General Microbiology* **87**: 312-325.
- Chater, K. F., (2001) Regulation of sporulation in *Streptomyces coelicolor* A3(2): a checkpoint multiplex? *Current Opinion in Microbiology* **4**: 667-673.
- Chater, K. F., C. J. Bruton, K. A. Plaskitt, M. J. Buttner, C. Mendez & J. D. Helmann, (1989) The developmental fate of *S. coelicolor* hyphae depends upon a gene product homologous with the motility sigma factor of *B. subtilis*. *Cell* **59**: 133-143.
- Chen, S. & R. Wetzel, (2001) Solubilization and disaggregation of polyglutamine peptides. *Protein Science* **10**: 887-891.
- Cherepanov, P. P. & W. Wackernagel, (1995) Gene disruption in *Escherichia coli*: TcR and KmR cassettes with the option of Flp-catalyzed excision of the antibiotic-resistance determinant. *Gene* **158**: 9-14.
- Chiti, F. & C. M. Dobson, (2006) Protein misfolding, functional amyloid, and human disease. *Annual Review of Biochemistry* **75**: 333-366.
- Claessen, D., R. Rink, W. de Jong, J. Siebring, P. de Vreugd, F. G. Boersma, L. Dijkhuizen & H. A. Wösten, (2003) A novel class of secreted hydrophobic proteins is involved in aerial hyphae formation in *Streptomyces coelicolor* by forming amyloid-like fibrils. *Genes & Development* **17**: 1714-1726.
- Claessen, D., I. Stokroos, H. J. Deelstra, N. A. Penninga, C. Bormann, J. A. Salas, L. Dijkhuizen & H. A. Wösten, (2004) The formation of the rodlet layer of streptomycetes is the result of the interplay between rodlines and chaplins. *Molecular Microbiology* **53**: 433-443.
- Claessen, D., H. A. Wösten, G. van Keulen, O. G. Faber, A. M. Alves, W. G. Meijer & L. Dijkhuizen, (2002) Two novel homologous proteins of *Streptomyces coelicolor* and *Streptomyces lividans* are involved in the formation of the rodlet layer and mediate attachment to a hydrophobic surface. *Molecular Microbiology* **44**: 1483-1492.
- Conchillo-Sole, O., N. S. de Groot, F. X. Aviles, J. Vendrell, X. Daura & S. Ventura, (2007) AGGRESCAN: a server for the prediction and evaluation of "hot spots" of aggregation in polypeptides. *BMC Bioinformatics* **8**.

- Crawford, D. L., (1978) Lignocellulose decomposition by selected *Streptomyces* strains. *Applied and Environmental Microbiology* **35**: 1041-1045.
- Datsenko, K. A. & B. L. Wanner, (2000) One-step inactivation of chromosomal genes in *Escherichia coli* K-12 using PCR products. *Proceedings of the National Academy of Sciences of the United States of America* **97**: 6640-6645.
- Datta, P., A. Dasgupta, S. Bhakta & J. Basu, (2002) Interaction between FtsZ and FtsW of *Mycobacterium tuberculosis*. *Journal of Biological Chemistry* **277**: 24983-24987.
- Datta, P., A. Dasgupta, A. K. Singh, P. Mukherjee, M. Kundu & J. Basu, (2006) Interaction between FtsW and penicillin-binding protein 3 (PBP3) directs PBP3 to mid-cell, controls cell septation and mediates the formation of a trimeric complex involving FtsZ, FtsW and PBP3 in mycobacteria. *Molecular Microbiology* **62**: 1655-1673.
- Davis, N. K. & K. F. Chater, (1990) Spore colour in *Streptomyces coelicolor* A3(2) involves the developmentally regulated synthesis of a compound biosynthetically related to polyketide antibiotics. *Molecular Microbiology* **4**: 1679-1691.
- de Jong, W., A. Manteca, J. Sanchez, G. Bucca, C. P. Smith, L. Dijkhuizen, D. Claessen & H. A. Wösten, (2009a) NepA is a structural cell wall protein involved in maintenance of spore dormancy in *Streptomyces coelicolor*. *Molecular Microbiology* **71**: 1591-1603.
- de Jong, W., H. A. Wösten, L. Dijkhuizen & D. Claessen, (2009b) Attachment of *Streptomyces coelicolor* is mediated by amyloid fimbriae that are anchored to the cell surface via cellulose. *Molecular Microbiology* **73**: 1128-1140.
- den Hengst, C. D., N. T. Tran, M. J. Bibb, G. Chandra, B. K. Leskiw & M. J. Buttner, (2010) Genes essential for morphological development and antibiotic production in *Streptomyces coelicolor* are targets of BldD during vegetative growth. *Molecular Microbiology* **78**: 361-379.
- Di Berardo, C., D. S. Capstick, M. J. Bibb, K. C. Findlay, M. J. Buttner & M. A. Elliot, (2008) Function and redundancy of the chaplin cell surface proteins in aerial hypha formation, rodlet assembly, and viability in *Streptomyces coelicolor*. *Journal of Bacteriology* **190**: 5879-5889.
- Diaz, M., A. Esteban, J. M. Fernandez-Abalos & R. I. Santamaria, (2005) The high-affinity phosphate-binding protein PstS is accumulated under high fructose concentrations and mutation of the corresponding gene affects differentiation in *Streptomyces lividans*. *Microbiology* **151**: 2583-2592.
- Dietz, A. & J. Mathews, (1971) Classification of *Streptomyces* spore surfaces into five groups. *Applied Microbiology* **21**: 527-533.
- Dueholm, M. S., S. V. Petersen, M. Sonderkaer, P. Larsen, G. Christiansen, K. L. Hein, J. J. Enghild, J. L. Nielsen, K. L. Nielsen, P. H. Nielsen & D. E. Otzen, (2010) Functional amyloid in *Pseudomonas*. *Molecular Microbiology*.
- Dutton, R. J., D. Boyd, M. Berkmen & J. Beckwith, (2008) Bacterial species exhibit diversity in their mechanisms and capacity for protein disulfide bond formation. *Proceedings of the National Academy of Sciences of the United States of America* **105**: 11933-11938.

- Dutton, R. J., A. Wayman, J. R. Wei, E. J. Rubin, J. Beckwith & D. Boyd, (2010) Inhibition of bacterial disulfide bond formation by the anticoagulant warfarin. *Proceedings of the National Academy of Sciences of the United States of America* **107**: 297-301.
- Einhauer, A. & A. Jungbauer, (2001) The FLAG peptide, a versatile fusion tag for the purification of recombinant proteins. *Journal of Biochemical and Biophysical Methods* **49**: 455-465.
- Elliot, M., F. Damji, R. Passantino, K. Chater & B. Leskiw, (1998) The *bldD* gene of *Streptomyces coelicolor* A3(2): a regulatory gene involved in morphogenesis and antibiotic production. *Journal of Bacteriology* **180**: 1549-1555.
- Elliot, M. A., M. J. Bibb, M. J. Buttner & B. K. Leskiw, (2001) BldD is a direct regulator of key developmental genes in *Streptomyces coelicolor* A3(2). *Molecular Microbiology* **40**: 257-269.
- Elliot, M. A., M. J. Buttner & J. R. Nodwell, (2007) Multicellular development in *Streptomyces*. In: Myxobacteria: Multicellularity and Differentiation. D. E. Whitworth (ed). Washington, DC.: American Society for Microbiology Press, pp. 419-438.
- Elliot, M. A., N. Karoonuthaisiri, J. Huang, M. J. Bibb, S. N. Cohen, C. M. Kao & M. J. Buttner, (2003) The chaplins: a family of hydrophobic cell-surface proteins involved in aerial mycelium formation in *Streptomyces coelicolor*. *Genes & Development* **17**: 1727-1740.
- Elliot, M. A. & B. K. Leskiw, (1999) The BldD protein from *Streptomyces coelicolor* is a DNA-binding protein. *Journal of Bacteriology* **181**: 6832-6835.
- Elliot, M. A. & N. J. Talbot, (2004) Building filaments in the air: aerial morphogenesis in bacteria and fungi. *Current Opinion in Microbiology* **7**: 594-601.
- Enoch, D. A., J. M. Bygott, M. L. Daly & J. A. Karas, (2007) Daptomycin. *The Journal of Infection* **55**: 205-213.
- Esteras-Chopo, A., L. Serrano & M. Lopez de la Paz, (2005) The amyloid stretch hypothesis: recruiting proteins toward the dark side. *Proceedings of the National Academy of Sciences of the United States of America* **102**: 16672-16677.
- Evans, K. C., E. P. Berger, C. G. Cho, K. H. Weisgraber & P. T. Lansbury, Jr., (1995) Apolipoprotein E is a kinetic but not a thermodynamic inhibitor of amyloid formation: implications for the pathogenesis and treatment of Alzheimer disease. *Proceedings of the National Academy of Sciences of the United States of America* **92**: 763-767.
- Fekkes, P. & A. J. Driessen, (1999) Protein targeting to the bacterial cytoplasmic membrane. *Microbiology and Molecular Biology Reviews* **63**: 161-173.
- Fernandez-Escamilla, A. M., F. Rousseau, J. Schymkowitz & L. Serrano, (2004) Prediction of sequence-dependent and mutational effects on the aggregation of peptides and proteins. *Nature Biotechnology* **22**: 1302-1306.
- Fernandez-Moreno, M. A., J. L. Caballero, D. A. Hopwood & F. Malpartida, (1991) The *act* cluster contains regulatory and antibiotic export genes, direct targets for translational control by the *bldA* tRNA gene of *Streptomyces*. *Cell* **66**: 769-780.

- Fowler, D. M., A. V. Koulov, W. E. Balch & J. W. Kelly, (2007) Functional amyloid-- from bacteria to humans. *Trends in Biochemical Sciences* **32**: 217-224.
- Garbuzynskiy, S. O., M. Y. Lobanov & O. V. Galzitskaya, (2010) FoldAmyloid: a method of prediction of amyloidogenic regions from protein sequence. *Bioinformatics* **26**: 326-332.
- Goodfellow, M. & S. T. Williams, (1983) Ecology of actinomycetes. *Annual Review of Microbiology* **37**: 189-216.
- Grantcharova, N., U. Lustig & K. Flärdh, (2005) Dynamics of FtsZ assembly during sporulation in *Streptomyces coelicolor* A3(2). *Journal of Bacteriology* **187**: 3227-3237.
- Guijarro, J., R. Santamaria, A. Schauer & R. Losick, (1988) Promoter determining the timing and spatial localization of transcription of a cloned *Streptomyces coelicolor* gene encoding a spore-associated polypeptide. *Journal of Bacteriology* **170**: 1895-1901.
- Gust, B., G. L. Challis, K. Fowler, T. Kieser & K. F. Chater, (2003) PCR-targeted *Streptomyces* gene replacement identifies a protein domain needed for biosynthesis of the sesquiterpene soil odor geosmin. *Proceedings of the National Academy of Sciences of the United States of America* **100**: 1541-1546.
- Haiser, H. J., M. R. Yousef & M. A. Elliot, (2009) Cell wall hydrolases affect germination, vegetative growth, and sporulation in *Streptomyces coelicolor*. *Journal of Bacteriology* **191**: 6501-6512.
- Hakanpää, J., A. Paananen, S. Askolin, T. Nakari-Setälä, T. Parkkinen, M. Penttilä, M. B. Linder & J. Rouvinen, (2004) Atomic resolution structure of the HFBII hydrophobin, a self-assembling amphiphile. *Journal of Biological Chemistry* **279**: 534-539.
- Hammar, M., A. Arnqvist, Z. Bian, A. Olsen & S. Normark, (1995) Expression of two *csg* operons is required for production of fibronectin- and congo red-binding curli polymers in *Escherichia coli* K-12. *Molecular Microbiology* **18**: 661-670.
- Hammar, M., Z. Bian & S. Normark, (1996) Nucleator-dependent intercellular assembly of adhesive curli organelles in *Escherichia coli*. *Proceedings of the National Academy of Sciences of the United States of America* **93**: 6562-6566.
- Hanahan, D., (1983) Studies on transformation of *Escherichia coli* with plasmids. *Journal of Molecular Biology* **166**: 557-580.
- Hardy, G. G., R. C. Allen, E. Toh, M. Long, P. J. Brown, J. L. Cole-Tobian & Y. V. Brun, (2010) A localized multimeric anchor attaches the *Caulobacter* holdfast to the cell pole. *Molecular Microbiology* **76**: 409-427.
- Harz, C. O., (1877) *Actinomyces bovis*: ein neuer Schimmel in den Geweben des Rindes. *Deutsche Zeitschrift für Tiermedizin* **1877-1878**: 125-140.
- Heichlinger, A., M. Ammelburg, E. M. Kleinschnitz, A. Latus, I. Maldener, K. Flärdh, W. Wohlleben & G. Muth, (2011) The MreB-like protein Mbl of *Streptomyces coelicolor* A3(2) depends on MreB for proper localization and contributes to spore wall synthesis. *Journal of Bacteriology* **193**: 1533-1542.

- Hirota-Nakaoka, N., K. Hasegawa, H. Naiki & Y. Goto, (2003) Dissolution of beta2-microglobulin amyloid fibrils by dimethylsulfoxide. *Journal of Biochemistry* **134**: 159-164.
- Ho, T. F., C. J. Ma, C. H. Lu, Y. T. Tsai, Y. H. Wei, J. S. Chang, J. K. Lai, P. J. Cheuh, C. T. Yeh, P. C. Tang, J. Tsai Chang, J. L. Ko, F. S. Liu, H. E. Yen & C. C. Chang, (2007) Undecylprodigiosin selectively induces apoptosis in human breast carcinoma cells independent of p53. *Toxicology and Applied Pharmacology* **225**: 318-328.
- Hobbs, G., C. M. Frazer, D. C. J. Gardner, J. A. Cullum & S. G. Oliver, (1989) Dispersed growth of *Streptomyces* in liquid culture. *Applied Microbiology and Biotechnology* **31**: 272-277.
- Hong, H. J., M. I. Hutchings, J. M. Neu, G. D. Wright, M. S. Paget & M. J. Buttner, (2004) Characterization of an inducible vancomycin resistance system in *Streptomyces coelicolor* reveals a novel gene (*vanK*) required for drug resistance. *Molecular Microbiology* **52**: 1107-1121.
- Hopwood, D. A., (1967) Genetic analysis and genome structure in *Streptomyces coelicolor*. *Bacteriological Reviews* **31**: 373-403.
- Hopwood, D. A., (1999) Forty years of genetics with *Streptomyces*: from *in vivo* through *in vitro* to *in silico*. *Microbiology* **145**: 2183-2202.
- Hopwood, D. A., (2007) *Streptomyces in nature and medicine : the antibiotic makers*, p. viii, 250 p., 258 p. of plates. Oxford University Press, Oxford ; New York.
- Hopwood, D. A. & H. M. Wright, (1978) Bacterial protoplast fusion: recombination in fused protoplasts of *Streptomyces coelicolor*. *Molecular & General Genetics* **162**: 307-317.
- Hudson, M. E. & J. R. Nodwell, (2004) Dimerization of the RamC morphogenetic protein of *Streptomyces coelicolor*. *Journal of Bacteriology* **186**: 1330-1336.
- Hudson, M. E., D. Zhang & J. R. Nodwell, (2002) Membrane association and kinase-like motifs of the RamC protein of *Streptomyces coelicolor*. *Journal of Bacteriology* **184**: 4920-4924.
- Hunt, A. C., L. Servin-Gonzalez, G. H. Kelemen & M. J. Buttner, (2005) The *bluC* developmental locus of *Streptomyces coelicolor* encodes a member of a family of small DNA-binding proteins related to the DNA-binding domains of the MerR family. *Journal of Bacteriology* **187**: 716-728.
- Jakimowicz, P., M. R. Cheesman, W. R. Bishai, K. F. Chater, A. J. Thomson & M. J. Buttner, (2005) Evidence that the *Streptomyces* developmental protein WhiD, a member of the WhiB family, binds a [4Fe-4S] cluster. *Journal of Biological Chemistry* **280**: 8309-8315.
- Janssen, G. R. & M. J. Bibb, (1993) Derivatives of pUC18 that have *Bgl*III sites flanking a modified multiple cloning site and that retain the ability to identify recombinant clones by visual screening of *Escherichia coli* colonies. *Gene* **124**: 133-134.
- Jao, S. C., K. Ma, J. Talafous, R. Orlando & M. G. Zagorski, (1997) Trifluoroacetic acid pretreatment reproducibly disaggregates the amyloid beta-peptide. *Amyloid-International Journal of Experimental and Clinical Investigation* **4**: 240-252.

- Jones, D., H. J. Metzger, A. Schatz & S. A. Waksman, (1944) Control of Gram-negative bacteria in experimental animals by streptomycin. *Science* **100**: 103-105.
- Kadokura, H., F. Katzen & J. Beckwith, (2003) Protein disulfide bond formation in prokaryotes. *Annual Review of Biochemistry* **72**: 111-135.
- Karimova, G., N. Dautin & D. Ladant, (2005) Interaction network among *Escherichia coli* membrane proteins involved in cell division as revealed by bacterial two-hybrid analysis. *Journal of Bacteriology* **187**: 2233-2243.
- Karimova, G., J. Pidoux, A. Ullmann & D. Ladant, (1998) A bacterial two-hybrid system based on a reconstituted signal transduction pathway. *Proceedings of the National Academy of Sciences of the United States of America* **95**: 5752-5756.
- Kelemen, G. H., P. Brian, K. Flardh, L. Chamberlin, K. F. Chater & M. J. Buttner, (1998) Developmental regulation of transcription of *whiE*, a locus specifying the polyketide spore pigment in *Streptomyces coelicolor* A3 (2). *Journal of Bacteriology* **180**: 2515-2521.
- Kelemen, G. H. & M. J. Buttner, (1998) Initiation of aerial mycelium formation in *Streptomyces*. *Current Opinion in Microbiology* **1**: 656-662.
- Kelemen, G. H., P. H. Viollier, J. Tenor, L. Marri, M. J. Buttner & C. J. Thompson, (2001) A connection between stress and development in the multicellular prokaryote *Streptomyces coelicolor* A3(2). *Molecular Microbiology* **40**: 804-814.
- Kieser, T., M. J. Bibb, M. J. Buttner, K. F. Chater & D. A. Hopwood, (2000) *Practical Streptomyces genetics*. The John Innes Foundation, Norwich, United Kingdom.
- Kim, H. J., M. J. Calcutt, F. J. Schmidt & K. F. Chater, (2000) Partitioning of the linear chromosome during sporulation of *Streptomyces coelicolor* A3(2) involves an *oriC*-linked *parAB* locus. *Journal of Bacteriology* **182**: 1313-1320.
- Kodani, S., M. E. Hudson, M. C. Durrant, M. J. Buttner, J. R. Nodwell & J. M. Willey, (2004) The SapB morphogen is a lantibiotic-like peptide derived from the product of the developmental gene *ramS* in *Streptomyces coelicolor*. *Proceedings of the National Academy of Sciences of the United States of America* **101**: 11448-11453.
- Kwan, A. H., R. D. Winefield, M. Sunde, J. M. Matthews, R. G. Haverkamp, M. D. Templeton & J. P. Mackay, (2006) Structural basis for rodlet assembly in fungal hydrophobins. *Proceedings of the National Academy of Sciences of the United States of America* **103**: 3621-3626.
- Kyle, R. A., (2001) Amyloidosis: a convoluted story. *British Journal of Haematology* **114**: 529-538.
- Kyte, J. & R. F. Doolittle, (1982) A simple method for displaying the hydropathic character of a protein. *Journal of Molecular Biology* **157**: 105-132.
- Lakey, J. H., E. J. Lea, B. A. Rudd, H. M. Wright & D. A. Hopwood, (1983) A new channel-forming antibiotic from *Streptomyces coelicolor* A3(2) which requires calcium for its activity. *Journal of General Microbiology* **129**: 3565-3573.
- Lashuel, H. A. & P. T. Lansbury, Jr., (2006) Are amyloid diseases caused by protein aggregates that mimic bacterial pore-forming toxins? *Quarterly Reviews of Biophysics* **39**: 167-201.

- Lawlor, E. J., H. A. Baylis & K. F. Chater, (1987) Pleiotropic morphological and antibiotic deficiencies result from mutations in a gene encoding a tRNA-like product in *Streptomyces coelicolor* A3(2). *Genes & Development* **1**: 1305-1310.
- Leskiw, B. K., E. J. Lawlor, J. M. Fernandez-Abalos & K. F. Chater, (1991) TTA codons in some genes prevent their expression in a class of developmental, antibiotic-negative, *Streptomyces* mutants. *Proceedings of the National Academy of Sciences of the United States of America* **88**: 2461-2465.
- LeVine, H., III, (1999) Quantification of beta-sheet amyloid fibril structures with thioflavin T. *Methods in Enzymology* **309**: 274-284.
- Li, L., T. A. Darden, L. Bartolotti, D. Kominos & L. G. Pedersen, (1999) An atomic model for the pleated beta-sheet structure of Abeta amyloid protofilaments. *Biophysical Journal* **76**: 2871-2878.
- Li, S. H. & X. J. Li, (1998) Aggregation of N-terminal huntingtin is dependent on the length of its glutamine repeats. *Human Molecular Genetics* **7**: 777-782.
- Linder, M. B., G. R. Szilvay, T. Nakari-Setälä & M. E. Penttilä, (2005) Hydrophobins: the protein-amphiphiles of filamentous fungi. *FEMS Microbiology Reviews* **29**: 877-896.
- Loferer, H., M. Hammar & S. Normark, (1997) Availability of the fibre subunit CsgA and the nucleator protein CsgB during assembly of fibronectin-binding curli is limited by the intracellular concentration of the novel lipoprotein CsgG. *Molecular Microbiology* **26**: 11-23.
- Lopes, D. H., A. Meister, A. Gohlke, A. Hauser, A. Blume & R. Winter, (2007) Mechanism of islet amyloid polypeptide fibrillation at lipid interfaces studied by infrared reflection absorption spectroscopy. *Biophysical Journal* **93**: 3132-3141.
- Ma, H. & K. Kendall, (1994) Cloning and analysis of a gene cluster from *Streptomyces coelicolor* that causes accelerated aerial mycelium formation in *Streptomyces lividans*. *Journal of Bacteriology* **176**: 3800-3811.
- Mackay, J. P., J. M. Matthews, R. D. Winefield, L. G. Mackay, R. G. Haverkamp & M. D. Templeton, (2001) The hydrophobin EAS is largely unstructured in solution and functions by forming amyloid-like structures. *Structure* **9**: 83-91.
- MacNeil, D. J., K. M. Gewain, C. L. Ruby, G. Dezeny, P. H. Gibbons & T. MacNeil, (1992) Analysis of *Streptomyces avermitilis* genes required for avermectin biosynthesis utilizing a novel integration vector. *Gene* **111**: 61-68.
- Marraffini, L. A., A. C. Dedent & O. Schneewind, (2006) Sortases and the art of anchoring proteins to the envelopes of gram-positive bacteria. *Microbiology and Molecular Biology Reviews* **70**: 192-221.
- Martin, J. L., J. C. Bardwell & J. Kuriyan, (1993) Crystal structure of the DsbA protein required for disulphide bond formation *in vivo*. *Nature* **365**: 464-468.
- Maurer-Stroh, S., M. Debulpaep, N. Kuemmerer, M. Lopez de la Paz, I. C. Martins, J. Reumers, K. L. Morris, A. Copland, L. Serpell, L. Serrano, J. W. Schymkowitz & F. Rousseau, (2010) Exploring the sequence determinants of amyloid structure using position-specific scoring matrices. *Nature Methods* **7**: 237-242.
- Mazza, P., E. E. Noens, K. Schirner, N. Grantcharova, A. M. Mommaas, H. K. Koerten, G. Muth, K. Flardh, G. P. van Wezel & W. Wohlleben, (2006) MreB of

- Streptomyces coelicolor* is not essential for vegetative growth but is required for the integrity of aerial hyphae and spores. *Molecular Microbiology* **60**: 838-852.
- McCarthy, A. J., (1987) Lignocellulose-degrading actinomycetes. *FEMS Microbiology Reviews* **46**: 145-163.
- McCarthy, A. J. & S. T. Williams, (1992) Actinomycetes as agents of biodegradation in the environment - a review. *Gene* **115**: 189-192.
- McCormick, J. R., E. P. Su, A. Driks & R. Losick, (1994) Growth and viability of *Streptomyces coelicolor* mutant for the cell division gene *ftsZ*. *Molecular Microbiology* **14**: 243-254.
- Mendez, C., A. F. Brana, M. B. Manzanal & C. Hardisson, (1985) Role of substrate mycelium in colony development in *Streptomyces*. *Canadian Journal of Microbiology* **31**: 446-450.
- Merrick, M. J., (1976) A morphological and genetic mapping study of bald colony mutants of *Streptomyces coelicolor*. *Journal of General Microbiology* **96**: 299-315.
- Messens, J. & J. F. Collet, (2006) Pathways of disulfide bond formation in *Escherichia coli*. *The International Journal of Biochemistry & Cell Biology* **38**: 1050-1062.
- Miller, J. H., (1972) *Experiments in molecular genetics*, p. xvi, 466 p. Cold Spring Harbor Laboratory, Cold Spring Harbor, N.Y.
- Missiakas, D., F. Schwager & S. Raina, (1995) Identification and characterization of a new disulfide isomerase-like protein (DsbD) in *Escherichia coli*. *The EMBO Journal* **14**: 3415-3424.
- Mistry, B. V., R. Del Sol, C. Wright, K. Findlay & P. Dyson, (2008) FtsW is a dispensable cell division protein required for Z-ring stabilization during sporulation septation in *Streptomyces coelicolor*. *Journal of Bacteriology* **190**: 5555-5566.
- Molle, V. & M. J. Buttner, (2000) Different alleles of the response regulator gene *blmM* arrest *Streptomyces coelicolor* development at distinct stages. *Molecular Microbiology* **36**: 1265-1278.
- Molle, V., W. J. Palframan, K. C. Findlay & M. J. Buttner, (2000) WhiD and WhiB, homologous proteins required for different stages of sporulation in *Streptomyces coelicolor* A3(2). *Journal of Bacteriology* **182**: 1286-1295.
- Nenninger, A. A., L. S. Robinson, N. D. Hammer, E. A. Epstein, M. P. Badtke, S. J. Hultgren & M. R. Chapman, (2011) CsgE is a curli secretion specificity factor that prevents amyloid fibre aggregation. *Molecular Microbiology* **81**: 486-499.
- Nguyen, K. T., J. M. Willey, L. D. Nguyen, L. T. Nguyen, P. H. Viollier & C. J. Thompson, (2002) A central regulator of morphological differentiation in the multicellular bacterium *Streptomyces coelicolor*. *Molecular Microbiology* **46**: 1223-1238.
- Nodwell, J. R. & R. Losick, (1998) Purification of an extracellular signaling molecule involved in production of aerial mycelium by *Streptomyces coelicolor*. *Journal of Bacteriology* **180**: 1334-1337.

- Nodwell, J. R., K. McGovern & R. Losick, (1996) An oligopeptide permease responsible for the import of an extracellular signal governing aerial mycelium formation in *Streptomyces coelicolor*. *Molecular Microbiology* **22**: 881-893.
- Nodwell, J. R., M. Yang, D. Kuo & R. Losick, (1999) Extracellular complementation and the identification of additional genes involved in aerial mycelium formation in *Streptomyces coelicolor*. *Genetics* **151**: 569-584.
- Noens, E. E., V. Mersinias, B. A. Traag, C. P. Smith, H. K. Koerten & G. P. van Wezel, (2005) SsgA-like proteins determine the fate of peptidoglycan during sporulation of *Streptomyces coelicolor*. *Molecular Microbiology* **58**: 929-944.
- O'Connor, T. J., P. Kanellis & J. R. Nodwell, (2002) The *ramC* gene is required for morphogenesis in *Streptomyces coelicolor* and expressed in a cell type-specific manner under the direct control of RamR. *Molecular Microbiology* **45**: 45-57.
- Oh, J., J. G. Kim, E. Jeon, C. H. Yoo, J. S. Moon, S. Rhee & I. Hwang, (2007) Amyloidogenesis of type III-dependent harpins from plant pathogenic bacteria. *Journal of Biological Chemistry* **282**: 13601-13609.
- Okanishi, M., K. Suzuki & H. Umezawa, (1974) Formation and reversion of streptomycete protoplasts: cultural condition and morphological study. *Journal of General Microbiology* **80**: 389-400.
- Omer, C. A., D. Stein & S. N. Cohen, (1988) Site-specific insertion of biologically functional adventitious genes into the *Streptomyces lividans* chromosome. *Journal of Bacteriology* **170**: 2174-2184.
- Paget, M. S., L. Chamberlin, A. Atrih, S. J. Foster & M. J. Buttner, (1999) Evidence that the extracytoplasmic function sigma factor σ^E is required for normal cell wall structure in *Streptomyces coelicolor* A3(2). *Journal of Bacteriology* **181**: 204-211.
- Pastor, M. T., A. Esteras-Chopo & L. Serrano, (2007) Hacking the code of amyloid formation: the amyloid stretch hypothesis. *Prion* **1**: 9-14.
- Pope, M. K., B. D. Green & J. Westpheling, (1996) The *bld* mutants of *Streptomyces coelicolor* are defective in the regulation of carbon utilization, morphogenesis and cell-cell signalling. *Molecular Microbiology* **19**: 747-756.
- Quist, A., I. Doudevski, H. Lin, R. Azimova, D. Ng, B. Frangione, B. Kagan, J. Ghiso & R. Lal, (2005) Amyloid ion channels: a common structural link for protein-misfolding disease. *Proceedings of the National Academy of Sciences of the United States of America* **102**: 10427-10432.
- Redenbach, M., H. M. Kieser, D. Denapate, A. Eichner, J. Cullum, H. Kinashi & D. A. Hopwood, (1996) A set of ordered cosmids and a detailed genetic and physical map for the 8 Mb *Streptomyces coelicolor* A3(2) chromosome. *Molecular Microbiology* **21**: 77-96.
- Romero, D., C. Aguilar, R. Losick & R. Kolter, (2010) Amyloid fibers provide structural integrity to *Bacillus subtilis* biofilms. *Proceedings of the National Academy of Sciences of the United States of America* **107**: 2230-2234.
- Romero, D., H. Vlamakis, R. Losick & R. Kolter, (2011) An accessory protein required for anchoring and assembly of amyloid fibres in *B. subtilis* biofilms. *Molecular Microbiology* **80**: 1155-1168.

- Ross, E. D., A. Minton & R. B. Wickner, (2005) Prion domains: sequences, structures and interactions. *Nature Cell Biology* **7**: 1039-1044.
- Ryding, N. J., G. H. Kelemen, C. A. Whatling, K. Flardh, M. J. Buttner & K. F. Chater, (1998) A developmentally regulated gene encoding a repressor-like protein is essential for sporulation in *Streptomyces coelicolor* A3(2). *Molecular Microbiology* **29**: 343-357.
- Sambrook, J. & D. W. Russell, (2001) *Molecular cloning: a laboratory manual*. Cold Spring Harbor Laboratory Press, Cold Spring Harbor, N.Y.
- Sawyer, E. B., D. Claessen, M. Haas, B. Hurgobin & S. L. Gras, (2011) The assembly of individual chaplin peptides from *Streptomyces coelicolor* into functional amyloid fibrils. *PLoS One* **6**: e18839.
- Schaerlaekens, K., L. Van Mellaert, E. Lammertyn, N. Geukens & J. Anne, (2004) The importance of the Tat-dependent protein secretion pathway in *Streptomyces* as revealed by phenotypic changes in *tat* deletion mutants and genome analysis. *Microbiology* **150**: 21-31.
- Shevchik, V. E., G. Condemine & J. Robert-Baudouy, (1994) Characterization of DsbC, a periplasmic protein of *Erwinia chrysanthemi* and *Escherichia coli* with disulfide isomerase activity. *The EMBO Journal* **13**: 2007-2012.
- Soliveri, J. A., J. Gomez, W. R. Bishai & K. F. Chater, (2000) Multiple paralogous genes related to the *Streptomyces coelicolor* developmental regulatory gene *whiB* are present in *Streptomyces* and other actinomycetes. *Microbiology* **146**: 333-343.
- Stackebrandt, E. & C. R. Woese, (1981) Towards a phylogeny of the actinomycetes and related organisms. *Current Microbiology* **5**: 197-202.
- Stine, W. B., Jr., K. N. Dahlgren, G. A. Krafft & M. J. LaDu, (2003) *In vitro* characterization of conditions for amyloid-beta peptide oligomerization and fibrillogenesis. *Journal of Biological Chemistry* **278**: 11612-11622.
- Sun, Y. M., D. Y. Jin, R. M. Camire & D. W. Stafford, (2005) Vitamin K epoxide reductase significantly improves carboxylation in a cell line overexpressing factor X. *Blood* **106**: 3811-3815.
- Takano, E., M. Tao, F. Long, M. J. Bibb, L. Wang, W. Li, M. J. Buttner, Z. X. Deng & K. F. Chater, (2003) A rare leucine codon in *adpA* is implicated in the morphological defect of *bldA* mutants of *Streptomyces coelicolor*. *Molecular Microbiology* **50**: 475-486.
- Thanbichler, M. & L. Shapiro, (2008) Getting organized--how bacterial cells move proteins and DNA. *Nature Reviews Microbiology* **6**: 28-40.
- Tillotson, R. D., H. A. Wosten, M. Richter & J. M. Willey, (1998) A surface active protein involved in aerial hyphae formation in the filamentous fungus *Schizophillum commune* restores the capacity of a bald mutant of the filamentous bacterium *Streptomyces coelicolor* to erect aerial structures. *Molecular Microbiology* **30**: 595-602.
- Trovato, A., F. Seno & S. C. Tosatto, (2007) The PASTA server for protein aggregation prediction. *Protein Engineering, Design & Selection* **20**: 521-523.
- van Wezel, G. P., J. van der Meulen, S. Kawamoto, R. G. Luiten, H. K. Koerten & B. Kraal, (2000) *ssgA* is essential for sporulation of *Streptomyces coelicolor* A3(2)

- and affects hyphal development by stimulating septum formation. *Journal of Bacteriology* **182**: 5653-5662.
- Waksman, S. A., (1950) *The Actinomycetes*. Chronica Botanica Co., Waltham, Mass.
- Wallin, R., N. Wajih & S. M. Hutson, (2007) Disulfide-dependent protein folding is linked to operation of the vitamin K cycle in the endoplasmic reticulum. *Journal of Biological Chemistry* **282**: 2626-2635.
- Wang, L., Y. Yu, X. He, X. Zhou, Z. Deng, K. F. Chater & M. Tao, (2007a) Role of an FtsK-like protein in genetic stability in *Streptomyces coelicolor* A3(2). *Journal of Bacteriology* **189**: 2310-2318.
- Wang, X., N. D. Hammer & M. R. Chapman, (2008) The molecular basis of functional bacterial amyloid polymerization and nucleation. *Journal of Biological Chemistry* **283**: 21530-21539.
- Wang, X., D. R. Smith, J. W. Jones & M. R. Chapman, (2007b) *In vitro* polymerization of a functional *Escherichia coli* amyloid protein. *Journal of Biological Chemistry* **282**: 3713-3719.
- Watt, B., G. van Niel, D. M. Fowler, I. Hurbain, K. C. Luk, S. E. Stayrook, M. A. Lemmon, G. Raposo, J. Shorter, J. W. Kelly & M. S. Marks, (2009) N-terminal domains elicit formation of functional Pmel17 amyloid fibrils. *Journal of Biological Chemistry* **284**: 35543-35555.
- Wessels, J. G. H., (1994) Developmental regulation of fungal cell-wall formation. *Annual Review of Phytopathology* **32**: 413-437.
- White, J. & M. Bibb, (1997) *bldA* dependence of undecylprodigiosin production in *Streptomyces coelicolor* A3(2) involves a pathway-specific regulatory cascade. *Journal of Bacteriology* **179**: 627-633.
- Wickner, R. B., (1994) [URE3] as an altered URE2 protein: evidence for a prion analog in *Saccharomyces cerevisiae*. *Science* **264**: 566-569.
- Wildermuth, H. & D. A. Hopwood, (1970) Septation during sporulation in *Streptomyces coelicolor*. *Journal of General Microbiology* **60**: 51-59.
- Wilkins, M. R., E. Gasteiger, A. Bairoch, J. C. Sanchez, K. L. Williams, R. D. Appel & D. F. Hochstrasser, (1999) Protein identification and analysis tools in the ExPASy server. *Methods in Molecular Biology* **112**: 531-552.
- Wilkinson, B. & H. F. Gilbert, (2004) Protein disulfide isomerase. *Biochimica et Biophysica Acta* **1699**: 35-44.
- Willemse, J., J. W. Borst, E. de Waal, T. Bisseling & G. P. van Wezel, (2011) Positive control of cell division: FtsZ is recruited by SsgB during sporulation of *Streptomyces*. *Genes & Development* **25**: 89-99.
- Willey, J., R. Santamaria, J. Guijarro, M. Geistlich & R. Losick, (1991) Extracellular complementation of a developmental mutation implicates a small sporulation protein in aerial mycelium formation by *S. coelicolor*. *Cell* **65**: 641-650.
- Willey, J., J. Schwedock & R. Losick, (1993) Multiple extracellular signals govern the production of a morphogenetic protein involved in aerial mycelium formation by *Streptomyces coelicolor*. *Genes & Development* **7**: 895-903.
- Willey, J. M. & W. A. van der Donk, (2007) Lantibiotics: peptides of diverse structure and function. *Annual Review of Microbiology* **61**: 477-501.

- Willey, J. M., A. Willems, S. Kodani & J. R. Nodwell, (2006) Morphogenetic surfactants and their role in the formation of aerial hyphae in *Streptomyces coelicolor*. *Molecular Microbiology* **59**: 731-742.
- Wood, S. J., W. Chan & R. Wetzel, (1996) Seeding of Aβ fibril formation is inhibited by all three isoforms of apolipoprotein E. *Biochemistry* **35**: 12623-12628.
- Wösten, H., O. De Vries & J. Wessels, (1993) Interfacial self-assembly of a fungal hydrophobin into a hydrophobic rodlet layer. *Plant Cell* **5**: 1567-1574.
- Wösten, H. A., (2001) Hydrophobins: multipurpose proteins. *Annual Review of Microbiology* **55**: 625-646.